



This is to certify that the

dissertation entitled

Improved Compound Resolution for Chromatography
With Rapid Full Mass Spectral Detection And
A Photodissociation System For Tandem
Time-of-Flight Mass Spectrometry

presented by

Richard David McLane

has been accepted towards fulfillment of the requirements for

Ph.D. degree in <u>Analytical</u> Chemistry

Major professor

Date april 29, 1993

LIBRARY Michigan State University

PLACE IN RETURN BOX to remove this checkout from your record.

TO AVOID FINES return on or before date due.

DATE DUE	DATE DUE	DATE DUE

MSU Is An Affirmative Action/Equal Opportunity Institution

IMPROVED COMPOUND RESOLUTION FOR CHROMATOGRAPHY WITH RAPID FULL MASS SPECTRAL DETECTION AND A PHOTODISSOCIATION SYSTEM FOR TANDEM TIME-OF-FLIGHT MASS SPECTROMETRY

Ву

Richard David McLane

A DISSERTATION

Submitted to
Michigan State University
in partial fulfillment of the requirements
for the degree of

DOCTOR OF PHILOSOPHY

Department of Chemistry

1993

Christie G. Enke, Advisor

ABSTRACT

IMPROVED COMPOUND RESOLUTION FOR CHROMATOGRAPHY WITH RAPID FULL MASS SPECTRAL DETECTION AND A PHOTODISSOCIATION SYSTEM FOR TANDEM TIME-OF-FLIGHT MASS SPECTROMETRY

By

Richard David McLane

Combination of a time-of-flight mass spectrometer (TOFMS) with a storage ion electron ionization source [1] and time-array detection (TAD) [2] has produced an instrument capable of acquiring one hundred or more mass spectra each second with high sensitivity. This system overcomes the trade-off between mass spectral acquisition rate and sensitivity that exists for scanning mass spectrometers. These features are well suited for the detection of compounds as they elute from a capillary gas chromatography column.

A deconvolution approach was developed to take advantage of small temporal differences occurring across the elution profiles provided by rapid sampling of the TOFMS/TAD instrument. The retention times of unknown compounds are found by generating a mass chromatogram peak position plot from the retention times of all mass chromatograms. A unique m/z value is determined for each coeluting compound and a pure mass spectrum for each compound is extracted using a cross-correlation approach. Deconvolution approaches can be used to either locate more compounds for a given amount of chromatographic time or to reduce the amount of time required for an analysis. The former approach was compared to two-dimensional gas chromatography

with mass spectral detection (2-D GC/MS) to assess the strengths and weaknesses of each approach. The two approaches were found to be complementary. The time savings available from deconvolution was counterbalanced by the wider dynamic range afforded by the physical separation provided by 2-D GC/MS. The latter approach, called time-compressed chromatography, combines low resolution high-speed chromatography and the TOFMS/TAD system with deconvolution techniques to decrease the analysis times by a factor of ten or more.

The technology of the TOFMS instrument has been extended to tandem mass spectrometry in a tandem time-of-flight mass spectrometer. A photodissociation system was developed and used to photofragment ions at the focal plane of the ion mirror in the first time-of-flight mass analyzer. Precursor depletion efficiencies of over 90% and photodissociation efficiencies of greater than 22% have been achieved using this system.

1. Grix, R.; Kutscher, R.; Li, G.; Gruner, U.; Wollnik, H. Rapid Commun.

Mass Spectrom. 1988, 2, 83.

^{2.} Holland, J. F.; Newcombe, B.; Tecklenburg, R. E., Jr.; Davenport, M.; Allison, J.; Watson, J. T.; Enke, C. G. Rev. Sci. Instrum. 1991, 62, 69.

Copyright by
RICHARD DAVID MCLANE
1993

ACKNOWLEDGMENTS

No one ever achieves any goal in life without help from others. I am indebted to a large number of people for the help and support they have given me over the course of many years. This is especially for all of the collaborative efforts in which I was involved. The interchange of ideas and recognition of individual strengths creates excitement and achieves results.

First of all, I would like to thank my preceptor, Dr. Chris Enke, for his insight and guidance which have led to the work described in this thesis. I would also like to thank the other members of my guidance committee: Dr. Crouch, Dr. Sweeley, Dr. Babcock and Dr. Jackson for their assistance and ideas.

The individuals in the time-of-flight mass spectrometry group over the past decade provided the foundation for my research. Without them, our deconvolution approach would have only limited utility and the tandem time-of-flight instrument would not have been constructed. Dr. Raimund Grix, Dr. Ron Tecklenburg, Ben Gardner, Dr. John Allison and Dr. Jack Holland have all played roles in the development of instrumentation during my "lifetime" at MSU. I would like to thank them for many useful discussions. Dr. Ron Tecklenburg was also of tremendous help in developing my understanding of photodissociation and provided a sounding-board for many of my ideas.

Dr. George Yefchak, with many useful inputs from Dr. Jack Holland, worked with me on the development of our deconvolution approach. George's

insights and programming skills were priceless. Thanks also go to David Pinkston and Dr. Pete Rodriguez for their role in the two-dimensional gas chromatography project.

Mary Puzycki/Seeterlin and Paul Vlasak have proven to be excellent coworkers during the design and construction of the tandem time-of-flight mass spectrometer. Although we have not always agreed on things, our discussions have increased my understanding in many areas. Doug Beussman has already proven his worth to the TOF/TOF project and I thank him for it. Eric Hemenway has always been a good friend and a tremendous resource for computer/programming problems. I would like to thank him for his patience while teaching me so much. Marty Rabb, Russ Geyer, Dick Menke and Sam Jackson have always provided us with tremendous service and support in designing and building components for the TOF/TOF instrument and deserve an ovation for their efforts.

No one survives the ordeal of graduate school without a support network. I would like to thank the members of the Enke Group (past and present) for their moral support and assistance. Brett Quencer has proven to be a good and understanding friend who helped me to retain a shred of sanity via our summertime golf expeditions.

Most importantly, I would like to thank my friends and family who have always remained by my side. Dr. Mike Baim and Dr. Pam Schofield have been

good sources of encouragement over the past several years. My wife and love, Debbie, has been with me through all of the ups and downs; she has made the good times better and lessened the disappointments. My daughter, Alyson, always provides me with a source for joy. Thanks also to my mother and brother, Dan, for their constant encouragement and support.

TABLE OF CONTENTS

List of Tables	xiv
List of Figures	xv
Chapter 1 Introduction	
1.1 Introduction	1
1.2 The Problem With Conventional Mass Spectrometry	5
1.3 The Michigan State University Solution	10
1.4 Research Goals	10
References	11
Chapter 2 Introduction to Time-of-Flight Mass Spectrometry	and
Deconvolution	14
2.1 Introduction	14
2.2 Detectors for Capillary Gas Chromatography	16
2.2.1 Single Channel Detectors	17
2.2.2 Multichannel Detectors	17
2.2.3 Mass Spectral Array Detectors	19
2.3 Introduction to TOFMS for Chromatographic Detection	20
2.3.1 Limitations of TOFMS	23
2.4 The MTOF/ITR System	25
2.4.1 Development of the Ion Source	25
2.4.2 Ion Mirrors	30
2.4.3 Time-Array-detection	31
2.4.4 Characteristics of the MTOF Instrument	33
2.5 Deconvolution of GC/MS Data	34

2.5.1 Characteristics of GC/MS Data	35
2.5.2 Types of Deconvolution	36
2.6 Historical Deconvolution Approaches for Unknowns	37
2.6.1 Locating Unresolved Compounds	38
2.6.1 Extracting Pure Mass Spectra	40
2.7 Summary	42
References	43
Chapter 3 Deconvolution of GC/MS Data: Better Data Make An Old Technique Work	
3.1 Introduction	49
3.2 Approach	50
3.2.1 Location of Coeluting Compounds	51
3.2.2 Determination of the Retention Time of Each Coeluting	
Compound	55
3.2.3 Extraction of a Pure Mass Spectrum for Each	
Unresolved Compound	58
3.3 Experimental	60
3.3.1 Reagents	60
3.3.2 Gas Chromatography	61
3.3.3 Time-of-Flight Mass Spectrometer	61
3.4 Effectiveness on Gasoline Range Hydrocarbon Mixture	61
3.5 Dynamic Range Studies	67
3.6 Summary and Future Work	70
References	71

Chapter	4	Time-Comp	ressed	Gas	Chro	natograph	y/Mass	
Spectromo	etry: Fi	fty-Two Cor	npounds	in Eighty	Seco	nds	•••••	73
4.1	Introdu	ction	•••••	•••••	•••••	•••••	•••••	73
4.2	Experin	nental	•••••	•••••	•••••	•••••		75
	4.2.1	Sample Pre	paration.	••••••	•••••	•••••	•••••	75
	4.2.2	2 Gas Chrom	atography	/	•••••	•••••	•••••	75
	4.2.3	Mass Spec	trometry	••••••	•••••	•••••	•••••	77
	4.2.4	Deconvolut	ion Appro	ach	•••••	•••••		78
4.3	Results	and Discuss	sion	•••••••	•••••	•••••	•••••	78
	4.3.1	GC/MS Ana	alysis Opti	mized for	Comp	onent Sepa	aration	79
	4.3.2	2 Analysis	of the	Sample	by	Time-Comp	ressed	
	Chro	matography	• • • • • • • • • • • • • • • • • • • •	•••••			•••••	. 81
	4.3.3	3 Adequate C	hromatog	raphic Re	soluti	on	•••••	. 85
	4.3.4	Poor Chror	natograph	ic Resolu	ition o	f Compoun	ds with	
	Simi	lar Spectra	••••••	••••••	• • • • • • • • • • • • • • • • • • • •	••••••	•••••	. 87
	4.3.5	Overlap of I	More Thai	n Two Co	mpour	ıds	•••••	. 89
	4.3.6	S Quantitation	າ	••••••	••••••	•••••	••••••	. 92
	4.3.7	Limitations.	•••••	•••••	••••••		•••••	. 93
4.4	Conclus	sions	•••••		••••••	•••••	•••••	. 95
Refe	erences	3 .	•••••	•••••	••••••		•••••	. 96
Chapter	5	Comparis	on of	Two	o-Dime	ensional	Gas	
Chromato	graphy	/Mass Spec	ctrometry	with D	econ	olution o	f Gas	
Chromato	graphy	/ High-Spee	d Mass S	pectrome	etric D	ata	•••••	. 97
5.1.	Introdu	ction	•••••	•••••	•••••		•••••	. 97
521	Evnerim	nental						102

	5.2.1 Initial GC Analysis	102
	5.2.2 Two-Dimensional GC/MS	102
	5.2.3 GC/TOFMS/TAD with Data Deconvolution	103
	5.3 Results and Discussion	104
	5.3.1 Analysis of Region 1	105
	5.3.2 Analysis of Region 2	113
	5.4 Conclusions	123
	5.5 Summary	125
	References	126
Chapt	ter 6 Photodissociation in Tandem Mass Spectrometry	128
	6.1 Introduction	128
	6.2 Qualities Required For MS/MS Using TOF Instruments	128
	6.3 Photodissociation in Mass Spectrometry	130
	6.4 Time-of-Flight Instruments in MS/MS Analysis	136
	6.5 The Tandem Time-of-Flight Mass Spectrometer	139
	6.6 Theoretical Considerations	141
	6.7 Design and Construction of the TOF/TOF Instrument	144
	6.8 Overview of Other Areas	145
	6.8.1 Ion Generation and Storage	145
	6.8.2 Time-of-Flight Separation of Precursor Ions	147
	6.8.3 Gating of the Precursor lons	147
	6.8.4 Time-of-Flight Analysis of Product Ions	150
	6.9 Summary and Conclusions	151
	References	152

Chapter 7 System Control of the TOF/TOF Instrument	157		
7.1 Introduction			
7.2 Spatial-Temporal Considerations for the Interaction Region	. 158		
7.3 Laser Considerations	. 158		
7.4 System Control	. 162		
7.4.1 Delay Generator	. 164		
7.4.2 Transient Recorder	. 165		
7.4.3 Laser	. 170		
7.5 Command Flow for Data Acquisition	. 173		
7.6 System Control Software	. 175		
7.6.1 Overview of the TOF/TOF Instrument System Control			
Programs	. 176		
7.6.2 Instrumental Characteristics Requiring Special			
Attention	. 177		
7.7 Summary and Future Work	. 180		
References	. 182		
Chapter 8 Characteristics of the Ion Fragmentation Process in the			
TOF/TOF Instrument	. 183		
8.1 Introduction	. 183		
8.2 Characteristics of the Isomass Ion Packets	. 184		
8.3 Laser Timing and Focusing	. 189		
8.3.1 Laser Beam Characteristics	. 190		
8.3.2 Laser Alignment	. 190		
8.3.3 Laser Timing	. 191		
8 4 Photodissociation in the TOF/TOF Instrument	192		

8.4.1 Precursor Ion Resolution	201
8.4.2 Photodissociation Characteristics	201
8.4.3 Critical Timing Precision	205
8.5 Summary and Conclusions	209
8.6 Future Work	210
References	211
Appendix: System Control Programs for the Tandem Time-of-Flight	
Mass Spectrometer	213
A.1 TOF/TOF Instrument Control Program	214
A.1.1 Include File Called by the TOF/TOF Instrument	
Control Program	228
A.1.2 Function Panels Called by the TOF/TOF Instrument	
Control Panel	230
A.2 Program to Parse Data File Header for Acquisition Information	236
A.3 Program to Convert LeCroy Format Binary Data to ASCII	
Format	238
A.3.1 ASCII_gen Instrument Used by the Format Conversion	
Program	239
A.3.2 Include File Called by the File Format Conversion	
Program	247

LIST OF TABLES

Table 4-1. The 61 Compounds in the Test Mixture.	76
Table 6-1. Historical Background of Photoionization/Photodissociation in	
MS	132
Table 7-1. Comparison of Excimer and Nd:YAG Lasers	160
Table 7-2. Summing Times (Summed Averages per Second) for Different	
Numbers of Points at Different Frequencies	168
Table 8-1. Arrival times for m/z 156 and m/z 158 from acquisitions of one	
transient per mass spectrum using bromobenzene	208

LIST OF FIGURES

Figure 1-1. The acquisition of only a few mass spectra per second can severely
distort the shape of the chromatographic elution profile. Determining the number
of peaks in a chromatogram is difficult under these conditions
Figure 1-2. Skewing results from rapid changes in the partial pressure of the
analyte in the ion source relative to the scan rate. After a scan has been
acquired, all m/z values plotted in a mass spectrum are assigned to the same
time 9
Figure 2-1. In time-of-flight mass spectrometry, ions are formed in the ion
source, accelerated to mass-dependent velocities, separated and then
detected
Figure 2-2. The spatial location of an ion in the source and its velocity in the ion
source prior to extraction cause broadening of the arrival time distribution for an
isomass ion packet24
Figure 2-3. The MTOF/ITR system for GC/MS analysis
Figure 2-4. (A) Conceptual diagram of a Wiley-McLaren time-of-flight mass
spectrometer including the two-field ion source and the associated energy
diagram showing the various voltages felt by the ions
Figure 2-5. Diagram of the Wollnik electron impact ion source. Thermal
electrons directed into the storage area by electron pushers (Pu) create a
potential well between grids G2 and G3

Figure 2-6. Conceptual diagram of the integrating transient recorder. Transient
waveforms are captured, summed into mass spectra, converted to mass/intensity
pairs and stored
Figure 3-1. The RTIC (solid line) does not always reveal the presence of
coeluting compounds. In this case, three unresolved compounds (dotted lines)
contribute to the RTIC but cannot be located by examination of the RTIC alone.
Figure 3-2. Illustration of a mass chromatogram peak position plot (MCPPP)
showing ideal (A) and real (B) MCPPP plots for the three unresolved compounds
from Figure 3-1 54
Figure 3-3. Selection of the most unique mass for three coeluting compounds by
inspection of mass chromatogram peak morphology (A) and by the three-point
algorithm (B)
Figure 3-4. RTIC (A) and corresponding MCPPP (B) from the analysis of the 12-
component hydrocarbon mixture
Figure 3-5. Unique-mass chromatograms identified for peaks 2-9 of the
hydrocarbon mixture
Figure 3-6. Expanded view of peak 6 from the hydrocarbon mixture showing the
RTIC and unique-mass chromatograms (A). Raw mass spectra #185 (B) and
#187 (C) correspond to the apices of the unique-mass chromatograms 65
Figure 3-7. Deconvolved spectra for benzene (A) and cyclohexane (B) obtained
from peak 6 of the hydrocarbon mixture. Reference spectra are shown for
comparison (C, D)

Figure 3-8. Unique-mass chromatograms for the dynamic-range study 68
Figure 3-9. Mass spectra of tert-butylbenzene and 1,2,4-trimethylbenzene
obtained from pure samples (A,B) and from deconvolution of binary mixtures
having concentration ratios of 1:5 (C,D), 1:1 (E,F), and 50:1 (G,H)69
Figure 4-1. Reconstructed total-ion current chromatogram (RTIC) of a 61-
component mixture acquired in 30 minutes on at a rate of ten spectra per
second. Two hundred picograms of each component were separated on a 25-m
length of 0.2-mm I. D. Ultra II fused silica column having a 0.33- μ m film
thickness80
Figure 4-2. Reconstructed total-ion current chromatogram of the same mixture
acquired in 80 seconds collecting 30 spectra per second. A 3-m length of 0.1
mm I. D. DB-5 column with 0.4-μm film thickness was used
Figure 4-3. Fourteen seconds of the RTIC in Figure 2 with the times where
individual mass chromatograms maximized indicated by the mass chromatogram
peak position plot (MCPPP). The 24 compounds present in this region are
indicated by their elution order number from Table 4-1 with an arrow to indicate
their retention time. When two components exactly coelute, a (2) is placed by
the arrow83
Figure 4-4. Overlay of the MCPPP on the elution profile for partially
chromatographically resolved components86
Figure 4-5. An overlay of the MCPPP on the elution profile for two coeluting
species—tert-butylbenzene and 1.2.4-trimethylbenzene

Figure 4-6. Comparison of the deconvoluted spectra for tert-butylbenzene and
1,2,4-trimethylbenzene with their respective library spectra
Figure 4-7. Overlay of the MCPPP on the elution profile for bromoform, styrene
and o-xylene whose mass chromatograms maximize at 24.33, 24.97 and 25.40
seconds respectively91
Figure 4-8. Mass chromatogram of m/z 146 reveals that the chromatographic
resolution between the two dichlorobenzene isomers is 0.7. Because these
isomers cannot be differentiated based on their mass spectra, they must be
chromatographically resolved
Figure 5-1. Conceptual Diagram of a 2-D GC/MS System. Following an initial
GC separation is performed on the first column, a portion of the eluent is isolated
and separated on the second GC column. The separated components are
detected using a mass spectrometer
Figure 5-2. Reconstructed total-ion current chromatogram (RTIC) of the perfume
from the GC/TOFMS analysis. Responses containing multiple components are
indicated by an asterisk106
Figure 5-3. RTIC of region 1 from the GC/TOFMS analysis. The MCPPP is
superimposed on the RTIC to show the retention times of the components
ocated in this region. The shapes of characteristic mass chromatograms for
each cluster of MCPPP lines confirm the presence of two compounds in this
portion of the region107
Figure 5-4. Spectra of the two compounds located and identified in region 1 by
both techniques. Spectra A and C were obtained from the 2-D GC/MS while

spectra B and D were extracted via GC/TOFMS/TAD using mass spectral
deconvolution. Library searches of these spectra identified the two compounds
as linalool and phenyl ethyl alcohol, respectively109
Figure 5-5. Expansion of the RTIC shown in Figure 5-3 focusing on the
fluctuation in the baseline near spectrum 8725. The superimposed MCPPP
indicates the presence of at least one compound in this portion of region 1.
Outlying lines in the MCPPP are the result of noise in the mass chromatograms.
110
Figure 5-6. Spectra for the compound located in Figure 5-5. The
chromatographically resolved spectrum (A), spectrum at the retention time of the
compound (B), background-subtracted spectrum (C) and deconvoluted spectrum
(D) are shown. B is dominated by phenyl ethyl alcohol and thus gives little
information about the compound of interest. Library-searches of the other
spectra (A,C and D) all identify the compound as rose oxide112
Figure 5-7. RTIC of region 2 from the GC/TOFMS/TAD analysis with the
MCPPP superimposed to indicated the retention times of the compounds as
determined by the deconvolution algorithm114
Figure 5-8. Mass chromatograms of m/z values characteristic of each of the
three clusters of MCPPP lines. Chromatograms of m/z 147, 161 and 93
characterize the areas near spectra 25725, 25735 and 25767. The arrow points
out the shoulder in the elution profile of <i>m/z</i> 147116
Figure 5-9. Mass spectra for the three compounds located in region 2 by
GC/TOFMS/TAD include the spectrum at the time of the shoulder in the RTIC

elution profile (compound 1), the deconvoluted spectrum of the compound that
eluted at spectrum 25735 (compound 2) and the deconvoluted spectrum of the
compound that eluted at spectrum 25767 (compound 3)118
Figure 5-10. RTIC of the 2-D GC/MS analysis of region 2. The five peaks
indicate the presence of five compounds, labeled A-E, in this region120
Figure 5-11. Mass spectra of four of the five compounds located by 2-D GC/MS
(Figure 5-10). The intensity of compound B was so low that no representative
mass spectrum could be obtained. Because these compounds were proprietary,
they were not identified via library searches121
Figure 6-1. Conceptual diagram of the TOF/TOF instrument140
Figure 6-2. Ion source for the TOF/TOF instrument. This source is similar to the
Wollnik source with the exception of the use of two opposing filaments146
Figure 6-3. Graph showing the percent of ions transmitted from the gate to the
interaction region as a function of the voltage difference between the two
elements in the gate assembly149
Figure 7-1. System control for the tandem time-of-flight mass spectrometer163
Figure 7-2. Percent of transients used by the LeCroy 9450 for a 5000 point
acquisition window at triggering rates between 20 and 500 Hz169
Figure 7-3. The signal produced by the thyratron discharge. The delay time is
the time between triggering the excimer and the first response in the thyratron
discharge signal172
Figure 8-1. Portion of a bromobenzene mass spectrum acquired with detector
placed at the interaction region186

Figure 8-2. Plot of the relative intensity of m/z 18 as an aperture was closed
under normal operating conditions, to study the uniformity of the ion beam and to
examine divergence of the ion beam188
Figure 8-3. Region of bromobenzene mass spectrum showing no depletion of
m/z 156, 157, or 158. Laser emission occurred 50 ns before the arrival time of
<i>m/z</i> 156194
Figure 8-4. Laser triggered to deplete m/z 156195
Figure 8-5. Laser triggered to deplete m/z 157196
Figure 8-6. Laser triggered to deplete m/z 158197
Figure 8-7. Region containing the predicted arrival time of the m/z 77 product
ion (from m/z 156) at the detector (A) without laser pulse ion packet overlap and
(B) with overlap of the laser pulse and selected ion packet199
Figure 8-8. Photodissociation spectrum showing the appearance of the m/z 91
product ion and depletion of the <i>m/z</i> 92 parent ion200
Figure 8-9. Percent of the precursor ion remaining from the photodissociation of
bromobenzene as a function of the laser trigger delay time204
Figure 8-10. Single-shot mass spectrum of bromobenzene showing the arrival
times of m/z 156 and m/z 158. These spectra were acquired with the detector at
the end of the ion flight-path207
Figure A-1. The system control function panel for the TOF/TOF instrument230
Figure A-2. Function panel for the name of the file to be acquired231
Figure A-3. The repetition rate of the square wave trigger signal is entered into
this function panel

Figure A-4. Function panel to enter delay times for the	LeCroy 4222 delay
generator	233
Figure A-5. Function panel for entry of conditions for the Le	eCroy 9450 transient
recorder	234
Figure A-6. Function panel for screen displayed graph cond	itions235

Chapter 1

Introduction

1.1 Introduction

Nearly all analytical samples are mixtures containing more than one component. In fact, mixtures obtained from natural sources may contain hundreds or even thousands of compounds. The components of these mixtures may possess structures that are very similar and have concentrations differing by many orders of magnitude. The need to provide qualitative and quantitative information about the composition of such mixtures is one of the greatest challenges faced by analytical chemistry.

The most effective techniques for the analysis of such mixtures are multidimensional. Typically, these approaches first separate the components of the mixture and then detect the separated components. Chromatographic techniques provide temporal separation for the components of a mixture. Under ideal circumstances, each component elutes from a chromatographic column by itself. The use of a selective detection technique, such as mass spectrometry (MS) or infrared spectroscopy, can provide identification and/or structural information for each resolved compound. Thus, these detection techniques serve as component characterization tools and also produce data for

approaches are gas chromatography/ mass spectrometry (GC/MS) and tandem mass spectrometry (MS/MS).

In GC/MS, the components of thermally stable mixtures are vaporized and separated on a chromatographic column. Separation of the mixture components is determined by the relative affinities of the components for the mobile phase (carrier gas) and the stationary phase inside the column. The separated compounds are introduced into the ion source of a mass spectrometer. Ions are often formed using electron ionization. This approach uses an electron beam to ionize the sample molecules. Electron ionization (EI) is a hard ionization technique that frequently produces many fragment ions, and, thus provides significant structural information about the analyte compounds. Extensive libraries of electron ionization spectra exist and can be used to identify an unknown compound based on its fragmentation pattern. The identified compound can then be quantified using the information provided by the mass spectral detector. The effectiveness of the mass spectrometer as a detector for gas chromatography in the analysis of mixtures can be described as follows.

"The mass spectrometer provides the ultimate gas chromatographic detection system, provided that one avoids contemplation of the issue of whether a mass spectrometer unit is a gas chromatographic detector or a GC is a sampling device for a mass spectrometer." [1]

The success of GC/MS analysis of mixtures is also demonstrated by its widespread usage. Nearly every volatile and thermally stable mixture, and some that are not, has been analyzed by GC/MS. It has been used in the analysis of organic [2] and inorganic [3] compounds. GC/MS has been used in environmental analysis to determine the composition of air [4], water [5], and soil

[6] samples. It has been used in areas as diverse as the analysis of foods and beverages [7], biochemical processes [8] and even the analysis of tobacco smoke [9,10].

When GC cannot completely separate components of a mixture, mathematical deconvolution algorithms may be used to resolve these compounds. Mass spectrometers acquire hundreds of data channels during a chromatographic analysis. Deconvolution algorithms take advantage of small temporal differences between the data channels to locate and identify compounds. They can be used to analyze samples for the presence of target compounds via a reverse-library search [11] or to analyze samples whose compositions are completely unknown [12]. Deconvolution of the mass spectral data can greatly reduce the amount of time and effort required to analyze a sample by decreasing the chromatographic separation needed.

Tandem mass spectrometry can be performed to either detect individual components in a mixture without prior separation or to provide a second level of structural information about a pure component. In the latter case, the pure component may be isolated from a mixture by chromatographic separation. In direct component detection from complex mixtures, specific components are sequentially isolated using the first mass analyzer and then characterized using the second mass analysis. The most common MS/MS scan mode is product ion analysis. A chosen precursor m/z value is transmitted by the first mass analyzer while rejecting ions of all other m/z values. Dissociation of the selected precursor is then accomplished via any of a number of energizing techniques. After

precursor fragmentation, the resulting product ions are separated in the second mass analyzer and detected. Although hard ionization techniques such as EI can be used in MS/MS mixture analysis, soft ionization techniques that cause little or no fragmentation of the molecular ion simplify the separation process by reducing the number of interferences. Structural analysis of a pure compound uses the same product ion scan mode to determine the product ions that result from the ionization process. Structures can be most effectively understood for pure compounds when hard ionization techniques are used. Acquisition of the product ions for all possible precursor ions increases the amount of available structural information; setting the instrument at particular combinations of precursor and product ion masses enhances the selectivity for detecting compounds separated by GC.

A large advantage of MS/MS in the analysis of mixtures lies in the time required to complete an analysis for targeted compounds. These analyses may be accomplished in a few minutes as compared to the tens of minutes required by GC/MS analysis to achieve the same results provided that the sample remains in the source throughout the entire data acquisition. The major limitation of MS/MS analysis is the need for prior MS/MS characterization of each target analyte and the absence of information produced about any other sample components. Despite being limited to target compound analysis for most mixtures, the selectivity and speed of MS/MS make it a powerful tool.

Like GC/MS, tandem mass spectrometry has shown its effectiveness through its wide range of applicability. Analyses include aromatic hydrocarbons,

chlorocarbons, phenols, amines and carboxylic acids in sludge [13,14], terpenes, esters, diphenylpropanoids and aromatic compounds in nutmeg [15], geoporphyrins in oil [16], and peptide sequencing of tryptic digests [17]. Virtually anything that can be introduced into the ion source of a mass spectrometer has been analyzed using MS/MS techniques. Solid, liquid and gas samples have all been analyzed using MS/MS [18].

When the components in a mixture are not resolved by GC/MS or MS/MS, these two techniques can be combined as GC/MS/MS to increase the selectivity and resolving power of the separation. This approach provides the benefits of both techniques. A significant fraction of the mixture is chromatographically resolved by GC and can be detected using MS. The remaining regions containing compounds that elute from the GC column simultaneously are analyzed using MS/MS techniques. This approach is not needed as often as GC/MS, but has found applicability in the analysis of environmental [19], and food [20] samples. The resolving power and selectivity available through GC/MS/MS are best used in the analysis of complex mixtures in complex matrices.

1.2 The Problem With Conventional Mass Spectrometry

Like all multidimensional techniques, GC/MS is dependent on the qualities of the gas chromatograph and the mass spectrometer and their compatibility. Advancements made in either GC or MS have a tremendous impact on the combined technique. The development and commercialization of

capillary GC columns in the early 1980s signaled the beginning of a new era in chromatography. Peak widths were reduced from nearly 20 seconds to only a few seconds and the amount of material introduced into the mass spectrometer was reduced to picograms. This advance in the separation technology placed more stringent requirements on the mass spectrometer detector in both mass spectral generation rates and sensitivity.

Most commercially available mass spectrometers are scanning instruments. These instruments obtain a mass spectrum by sequentially acquiring information about each m/z value in the range of interest. When the scan rate of the mass spectrometer is increased to provide an adequate number of data points across a chromatographic peak, less time is spent in acquiring each m/z value and the sensitivity is reduced. Thus, a trade-off between mass spectral acquisition rate and sensitivity exists for scanning mass spectrometers. Most GC/MS analyses are presently performed acquiring only a few scans per second. These scan rates provide the sensitivity required by capillary GC.

Accurate description of the shape of the elution profile across a chromatographic peak requires at least 40 data points [21]. When the scanning mass spectrometer acquires only four to six data points across a chromatographic peak, as is the case when acquiring two scans per second across a 2-3 s peak, two types of distortions occur in the data. The first of these is shown in Figure 1-1. Chromatographic resolution is lost when the mass

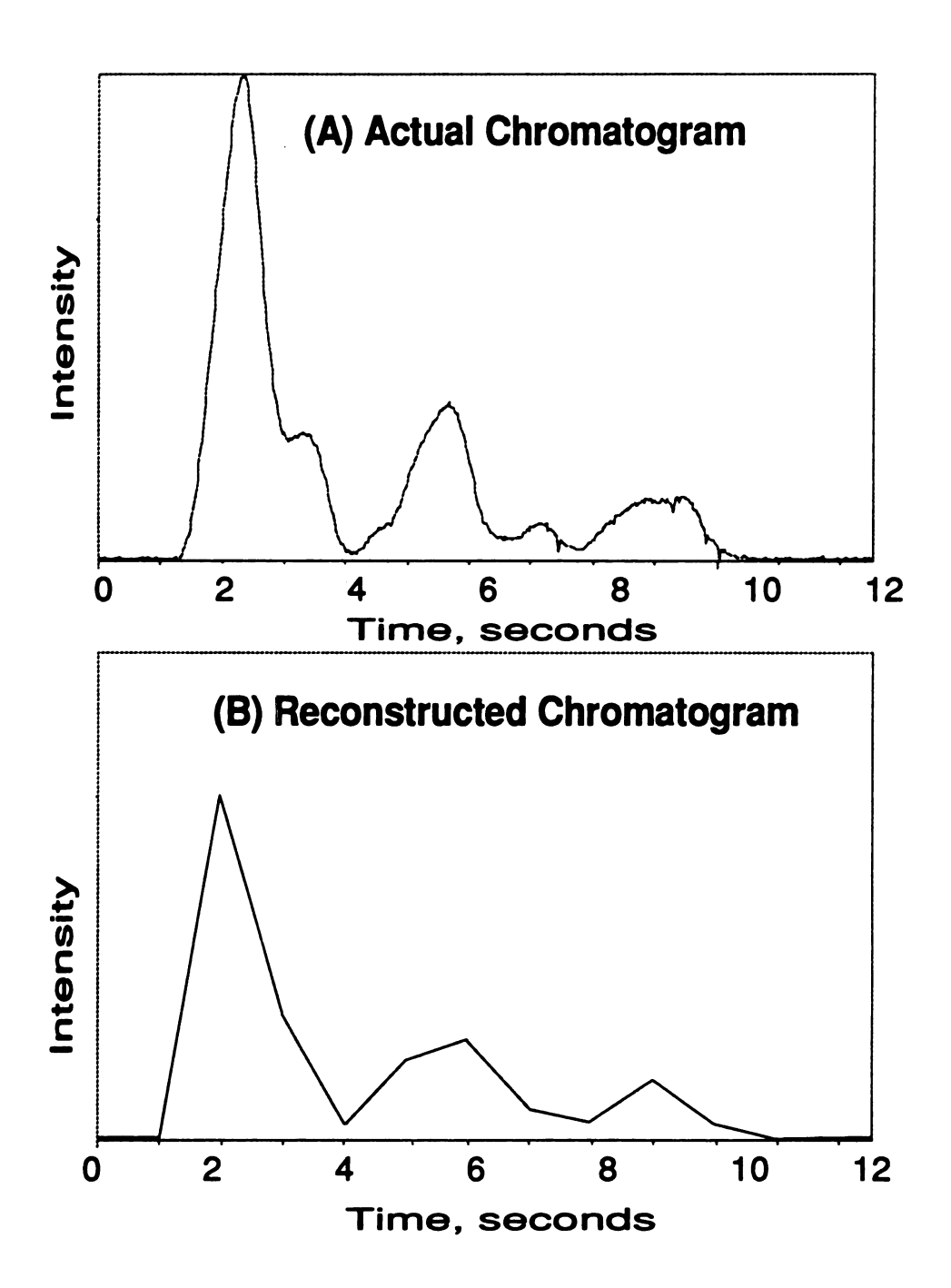


Figure 1-1. The acquisition of only a few mass spectra per second can severely distort the shape of the chromatographic elution profile. Determining the number of peaks in a chromatogram is difficult under these conditions.

spectral acquisition rate is decreased to 1 or 2 Hz. The actual reconstructed total ion current chromatogram (RTIC) of an analysis is shown in Figure 1-1A while the RTIC obtained at 1 scan per second is shown in Figure 1-1B. The slow mass spectral acquisition rate not only distorts the shape of the elution profile, compounds present in the true RTIC cannot even be detected in the acquired data. Sequential acquisition of the information about each m/z value causes the second of these distortions. Under ideal circumstances, the partial pressure of the analyte in the ion source should remain constant while the entire mass spectrum of that compound is obtained. Unfortunately, the partial pressure of an analyte eluting from a capillary GC column changes radically over the time required to perform one scan. Thus, the intensities of the m/z values are skewed by the slow scan rate. This type of distortion is illustrated in Figure 1-2. The first spectrum (I) shows the real spectrum of hypothetical compound X. The remaining spectra, II, III and IV, show the effects of skewing on a mass spectrum. Spectrum II is acquired as the concentration of the analyte was increasing in the ion source. Spectrum III was obtained across the top of the peak and Spectrum IV resulted from a decrease in the concentration of Compound X in the ion source. Since the intensities of a m/z value is an important tool in the interpretation of a mass spectrum, skewing can effect compound identification.

The low mass spectral acquisition rates and their accompanying problems can also severely limit the use of deconvolution techniques. Although skewing can be eliminated, most algorithms require much higher data sampling rates to be effective. The resolution of these algorithms is often described as 1.5 or 2

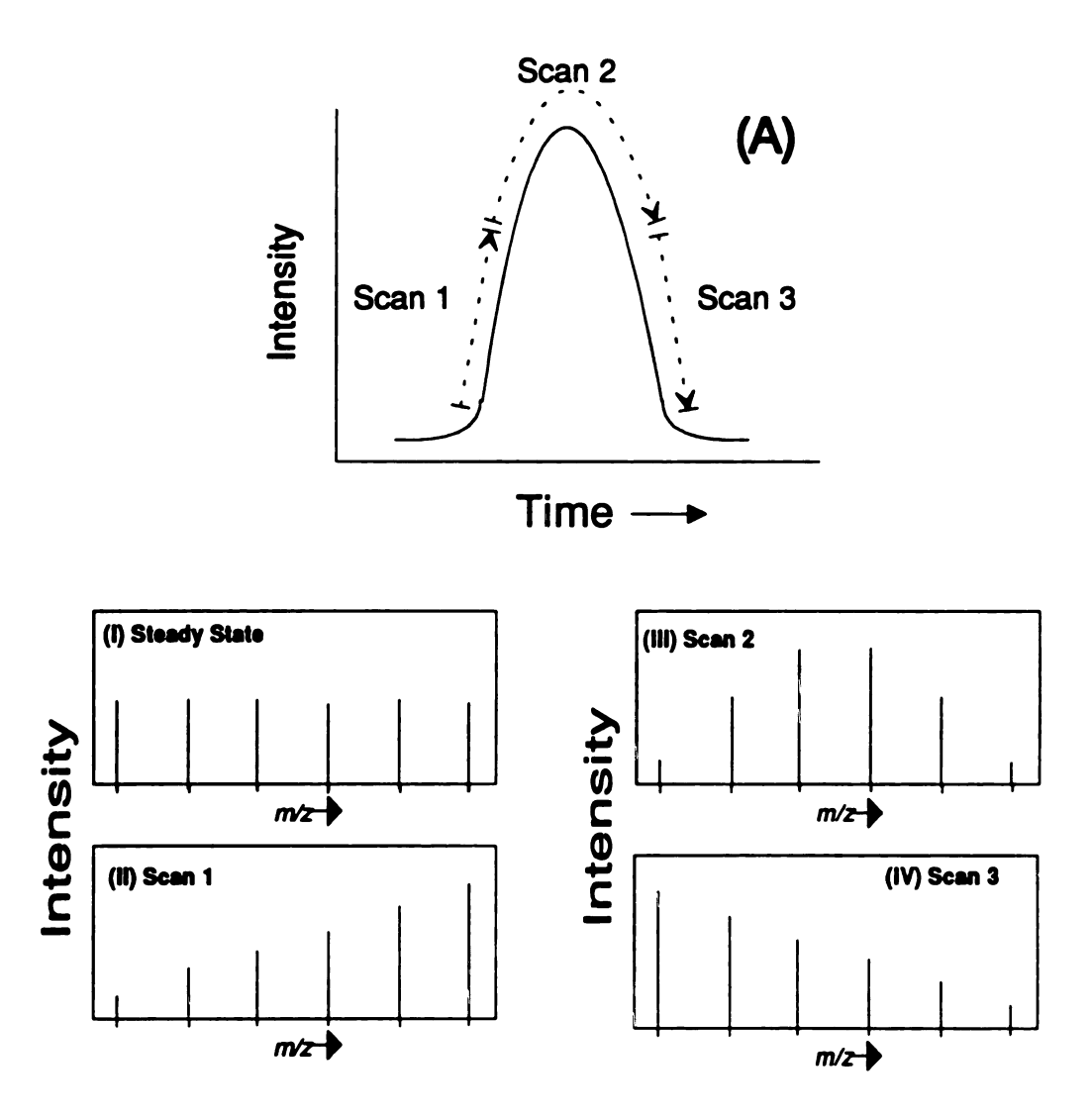


Figure 1-2. Skewing results from rapid changes in the partial pressure of the analyte in the ion source relative to the scan rate. After a scan has been acquired, all m/z values plotted in a mass spectrum are assigned to the same time.

data points. When only a few points are acquired over a chromatographic peak, these approaches are virtually useless.

1.3 The Michigan State University Solution

A time-of-flight mass spectrometric system with mass spectral acquisition rates and sensitivities required for use as a detector for capillary GC has been developed [22]. The combination of time-of-flight mass spectrometry (TOFMS) and time-array detection (TAD) permits the acquisition of 50 or more mass spectra per second and has femtogram detection limits. Capillary GC elution profiles can be accurately reconstructed on all data channels with this mass spectral detector. The mass spectra produced by this instrument are unskewed since all of the ions in the ion source are sampled at once. These qualities result in data that are well-suited for deconvolution techniques.

1.4 Research Goals

The goals of the research reported in this thesis were: (1) to exploit the capabilities afforded by TOFMS with TAD by devising a simple deconvolution approach and applying it to capillary GC/MS data and (2) to develop a major portion of an MS/MS instrument based on the TOFMS/TAD technology. Much of the research involved in achieving these goals was collaborative in nature. This thesis will focus on my contributions to each of these goals.

The remainder of this thesis is organized in the following manner. The background and some of the theoretical considerations that led to the Michigan State University TOFMS/TAD system and provides historical information about the role of deconvolution approaches for GC/MS data are described in Chapter 2. Fully using the information available from GC/MS with the MTOF/ITR detection system is the focus of Chapters 3-5. Description of a deconvolution system developed by a group at Michigan State University is the focus of Chapter 3. Time-compressed chromatography where the analysis time required for mixtures can be reduced by a factor of ten or more over the traditional GC/MS approach is described in Chapter 4. Large reductions in analysis time are achieved without sacrificing any analytical information. The deconvolution approach is compared to two-dimensional GC/MS in Chapter 5. Chapters 6 and 7 are based on the development of the TOF/TOF instrument. Pertinent background and an overview of the tandem time-of-flight MS/MS instrument are provided in Chapter 6. The development of the hardware and software necessary to supply the critical timing in the instrument and considerations about the interaction region are the focus of Chapter 7. Experimental results pertinent to my specific research goals in developing this MS/MS instrument are also included in this chapter.

References

Bunting; Thomas in Chromatographic Analysis Of The Environment,
 Second Edition Revised and Reexamined, R. L. Grob, Ed., Marcel Dekker: New York, 1983, pg. 52.

- 2. McLafferty, F. W. In *Interpretation of Mass Spectra*, Third Edition, University Science Books: Mill Valley, CA, 1980.
- 3. Schmidt, G. In *Chromatographic Methods In Inorganic Analysis*, W. Bertsch, W. G. Jennings and R. E. Kaiser, Eds., Dr. Alfred Huther Verlag: Heidelburg, 1981, Chapter 3.
- 4. Braman, R. S. In *Chromatographic Analysis of the Environment*, 2nd ed revised and expanded, R. L. Gross, ed., Marcel Dekker: New York, 1983, Chapter 3.
- 5. Giuliany, B. E. In *Chromatographic Analysis of the Environment*, 2nd ed revised and expanded, R. L. Gross, ed., Marcel Dekker: New York, 1983, Chapter 6.
- 6. Gross. R. L.; Kanatharana, P. In *Chromatographic Analysis of the Environment*, 2nd ed revised and expanded, R. L. Gross, ed., Marcel Dekker: New York, 1983, Chapter 7.
- 7. Jennings, W. G. *Gas Chromatography With Glass Capillary Column*s, Academic Press: New York, 1978, 107.
- 8. Holland, J. F.; Ledly, J. L.; Sweeley, C. C. J. Chromatogr. 1986, 397, 3.
- 9. Rapp, U.; Schroder, U.; Meier, S.; Elmhorst, M. *Chromatographia* **1975**, *8*, 474.
- 10. Jennings, W. G. Gas Chromatography With Glass Capillary Columns, Academic Press: New York, 1978, 107.

- 11. Abramson, F. P. Anal. Chem. 1975, 47, 45.
- 12. Biller, J. E.; Biemann, K. Anal. Lett. 1974, 7, 515.
- Hunt, D. F.; Shabanowitz, J.; Harvey, T. M.; Coates, M. L. *Anal. Chem.* 1985, 57, 525.
- 14. Hunt, D. F.; Shabanowitz, J.; Giordani, A. B. Anal. Chem. 1980, 52, 386.
- 15. Davis, D. V.; Cooks, R. G. J. Agric. Food Chem. 1982, 30, 495.
- Johnson, J. V.; Britton, E. V.; Yost, R. A.; Quirk, J. M. E.; Cuesta, L. L.
 Anal. Chem. 1986, 58, 1325.
- 17. Biemann, K.; Martin, S. A. Mass Spectrom. Rev. 1987, 6, 1.
- 18. Busch, K. L.; Glish G. L.; McLuckey, S. A. In *Mass Spectrometry/Mass Spectrometry: Techniques and Applications of Tandem Mass Spectrometry*, VCH Publishers: New York, 1988.
- Gale, B. C.; Fulford, J. E.; Thomson, B. A; Ngo, .A.; Tanner, S. D.;
 Davidson, W. R.; Shushan, B. I. Adv. Mass Spectrom. 1986, 10, 1467.
- 20. Trehy, M. L.; Yost, R. A.; Dorsey, J. G. Anal. Chem. 1986, 58, 14.
- 21. Chesler, S. N.; Cram, S. P. Anal. Chem. 1971, 43, 1922.
- 22. Tecklenburg, R. E., Jr.; McLane, R. D.; Grix, R.; Sweeley, C. C.; Allison, J.; Watson, J. T.; Holland, J. F.; Enke, C. G.; Gruner, U.; Gotz, H.; Wollnik, H. Proceedings of the 38th ASMS Conference on Mass Spectrometryand Allied Topics, Tucson, AZ, June 3-8, 1990.

		;

Chapter 2

Introduction to Time-of-Flight Mass Spectrometry and Deconvolution

2.1 Introduction

The development and commercialization of capillary columns for gas chromatography has made mixture analysis a reality for the masses. These highefficiency columns have been used to analyze nearly every volatile, thermally stable mixture that can be introduced onto the column. Component analysis is achieved by separating all of the mixture components using capillary GC and then detecting the separated components using one or more detectors [1]. Capillary GC has become the technique of choice for separation of mixtures because of its separation efficiency and speed [2].

Capillary GC has the ability to separate mixtures containing hundreds of components at concentrations that vary by several orders of magnitude. Unfortunately, this ability does not always translate into reality. Many mixtures, especially natural mixtures, are composed of hundreds to even thousands of components. These components often have similar chemical structures. The available chromatographic separation space is limited even for high-efficiency capillary columns. The likelihood of two or more of the components coeluting

from the GC column increases with the number of components in the mixture [3]. In 1983, Davis and Giddings [4] showed that the more-or-less randomly-spaced elution times typically found in a complex chromatogram lead to a high occurrence of overlapping peaks as well as to large regions having no peaks at all. Twenty percent or 40 of 200 components would be expected to coelute in a one hour long capillary GC analysis without accounting for the presence of isomers in a mixture [5]. Bertsch describes a separation performed on the components of tobacco smoke in which 1000 compounds were resolved in a single chromatographic run [6]. The width of most peaks was only a few seconds. Despite these optimized conditions, data from the mass spectrometer detector indicated that the average peak resulted from the elution of two components. Davis and Giddings [7] estimated the probability that a single peak contains only one compound is less than 50% for a chromatogram filled to only 35% of the peak capacity.

Analysis of such complex mixtures requires more than high-resolution chromatography, it requires a detection system capable of discriminating compounds that elute from the chromatographic column simultaneously. The detector must sample the data rapidly to accurately reconstruct the elution profile information and also must be sensitive due to the low sample capacity of capillary columns.

2.2 Detectors for Capillary Gas Chromatography

Detection of compounds separated by capillary GC may be performed using either single or multichannel detectors. Single channel detectors may have narrow ranges of selectivity or may respond to nearly every compound. Each peak produced by a single channel detector is assumed to result from a single component unless the shape of the elution profile indicates the presence of more than one component. When the chromatographic eluent is introduced to a multichannel detector or a combination of independent single-channel detectors, the information about a peak is increased tremendously. The data across the channels can be compared to determine whether a peak is from a single component or a series of compounds that are not separated by the chromatographic column. This information can be a very powerful tool for understanding the composition of a mixture.

Under ideal circumstances, a chromatographic detector would be a multichannel device that responded well to all compounds. It would have the ability to be selective by examining the information on a single or few channels or general by examining the information available across all the data channels. Compounds could then be identified using the combination of retention indices and multichannel data.

2.2.1 Single Channel Detectors

Detectors commonly used for capillary GC include the flame ionization detector (FID) [8], thermal conductivity detector (TCD) [9], electron capture detector (ECD) [10], nitrogen-phosphorous detector (NPD) [11], and mass spectrometers. While the FID and TCD respond to a wide variety of compounds, the ECD and NPD are more selective. Compound identification for single channel detectors is performed based on retention indices and knowledge of the selectivity of the detector. For instance, the response for halogenated compounds such as chloroform may be intense on the ECD while the FID response may be small. The opposite is true when an alkane elutes from the column. The ECD will not respond while the FID will produce a signal. Coupling these different selectivities serves as a simple version of a multichannel detector.

2.2.2 Multichannel Detectors

Most multichannel detectors used with capillary GC are either spectroscopic or mass spectrometric. These detectors can be operated in either of two modes. Multichannel detectors can be general and use the information on all data channels or they can be selective and use only a portion of the available information. Infrared detectors based on Fourier transform technology are commercially available for use with capillary GC. These detectors have sensitivities and acquisition rates that are compatible for use with modern

capillary columns [12]. Ultraviolet and visible detectors have found great use in high-performance liquid chromatography (HPLC). These instruments can acquire ultraviolet and visible spectra of compounds as they elute from a HPLC column. Both of these spectroscopic approaches are limited by the interdependence of the information across the available data channels resulting from the relatively broad liquid-phase spectral bands for these optical techniques. These techniques are useful but optical spectra lack the distinctiveness of mass spectra. Data from each channel in a mass spectrometer are unique and have no overlap.

Mass spectrometers acquire data about all of the ions formed from a sample in the ion source in the full scan mode. This mass spectral information can be used to determine the structure and ultimately the identity of a compound eluting from a chromatographic column. The mass spectrometer can also be operated as a selective detector using selected ion monitoring (SIM). In its ultimate form, ions of only one m/z value are detected by the mass spectrometer. This technique is often used to detect only a specific class of compounds which may be present in a complex matrix [13]. The added selectivity eliminates many possible chromatographic interferences, but bases identification of detected compounds on retention times alone. This approach has found favor with users of scanning mass spectrometers because sensitivity increases when a mass filter is set to monitor ions of only one mass. The limitations of scanning mass spectrometers have been documented in Chapter 1 of this thesis.

Array detectors can provide rapid data acquisition across all channels with high sensitivity. Consequently, they have found use as detectors for chromatography. Spectroscopic and mass spectrometric array detectors have been developed and used for these purposes. Diode array detectors are used to generate absorption spectra as a compound elutes from a HPLC column [14]. Unfortunately, these HPLC detectors have the same limitations as their sequential counterparts; the relatively broad spectral absorption bands of compounds in the liquid phase.

2.2.3 Mass Spectral Array Detectors

Although several types of array detection have been used in mass spectrometry, two have been successfully interfaced to capillary GC. These are spatial-array and time-array detectors. Both of these two approaches can acquire data rapidly and with high sensitivity.

Spatial-array detectors are electro-optical devices developed for use with magnetic sector mass spectrometers [15,16]. They take advantage of the fact that a magnetic field spatially disperses ions based on their mass. When a multichannel plate electron multiplier is connected to a photoplate and a diode array detector by optical fibers, the spatial distribution of ions can be captured. This distribution is then converted into mass and intensity information. Limitations in dynamic range, mass spectral resolution and mass range restrict the use of these detectors to low resolution analysis. From a more pragmatic

view, these detectors are expensive. Magnetic sector instruments are among the most expensive types of mass spectrometer and the addition of a detector that costs more than some mass spectrometers makes the price of such a system prohibitive for many potential applications.

Time-array detection (TAD) [1] is used in conjunction with time-of-flight mass spectrometry. Ions are pulsed out of the ion source and separated temporally in TOFMS. Ions of all masses strike the same surface but at different times. Arrival time and intensity data are captured. For each ion source pulse, these data are readily converted to the traditional mass spectrum format. Since ions from the same source extraction pulse are temporally separated, this approach can be totally continuous. Information can be captured in one part of the array and emptied out of another without affecting the data quality or acquisition rate. This is not true for a spatial-array detector. Data acquisition should be terminated while the information in the array is emptied to avoid introduction of data intensity distortion.

2.3 Introduction to TOFMS for Chromatographic Detection

The use of a time-of-flight mass spectrometer as a chromatographic detector is nearly as old as the idea of GC/MS itself. The first GC/MS system, built by Gohlke in 1959, used a time-of-flight mass spectrometer as a detector for a packed-column gas chromatography column [17]. In 1963, TOFMS was used to detect the effluent from a capillary GC column [18]. Capillary GC

columns did not become commercially available until 15 years after this work by McFadden. The major advantage of time-of-flight mass spectrometers is their ability to produce thousands of mass spectra per second using relatively simple instrumentation over a theoretically unlimited mass range. Unfortunately, early TOFMS instruments suffered from poor resolution and inefficient sample use for many years. Other types of mass spectrometers with higher resolving power came to dominate the area of packed-column GC/MS in the 1960s. This trend has continued into the present despite the problems discussed in Chapter 1 of this thesis.

Time-of-flight mass spectrometry is a fairly simple process. Ions are formed in the ion source of a mass spectrometer. They are extracted from the ion source, accelerated to a selected energy, and allowed to travel through an evacuated, field-free flight tube. The ions separate temporally into isomass ion packets based on their mass-dependent velocities. The time required for the ions to traverse the length of the flight tube is measured and used determine the mass-to-charge ratio of an ion. The signal that results from all the ions of all *m/z* values extracted from the ion source in a single pulse striking the detector is called a transient. Each transient contains complete mass spectral information. This process is illustrated in Figure 2-1. The extraction rate of the ion source is only limited by the flight time of the largest *m/z* value. As soon as all of the ions produced in one source extraction pulse have reached the detector, another extraction pulse can be applied. Extraction rates of 5000 Hz or more are often used in TOFMS instruments with 4-m flight paths.

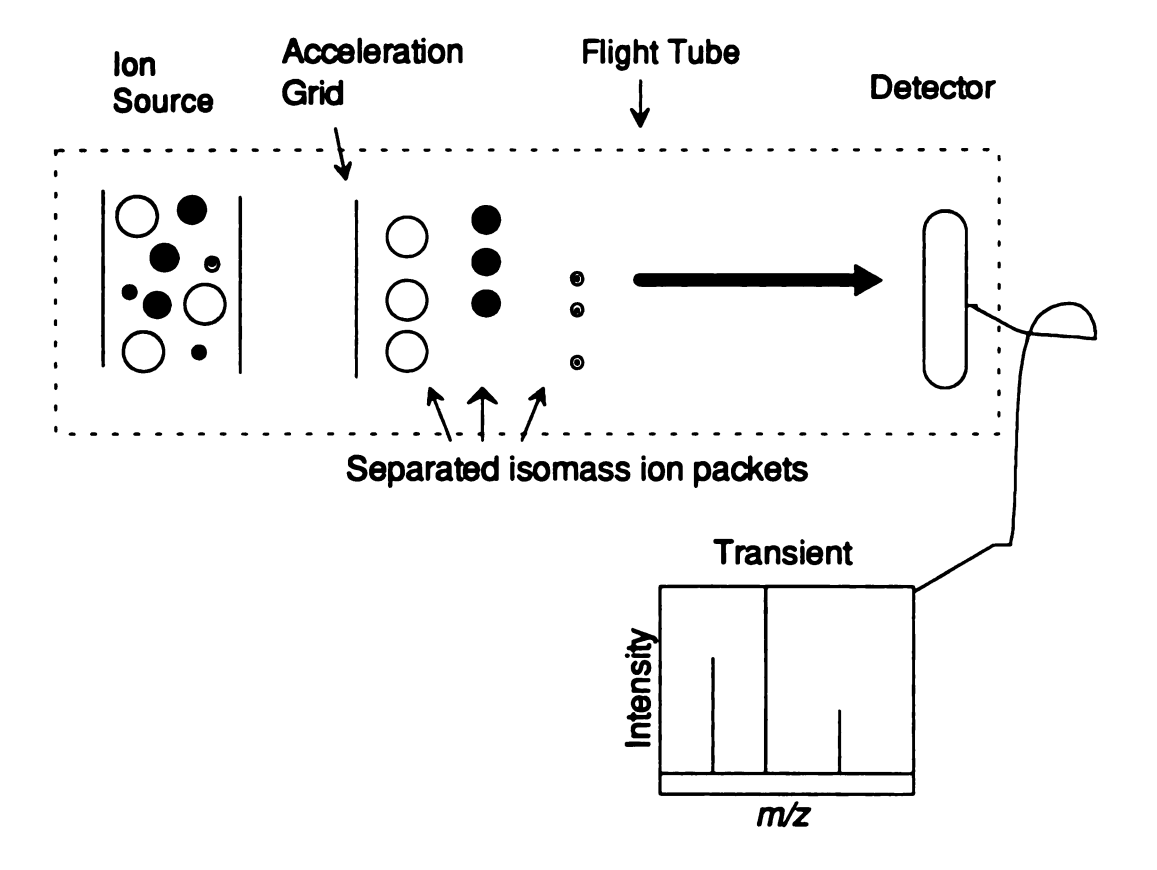


Figure 2-1. In time-of-flight mass spectrometry, ions are formed in the ion source, accelerated to mass-dependent velocities, separated and then detected.

2.3.1 Limitations of TOFMS

Under ideal circumstances, all ions of the same mass will arrive at the detector at the same time. When ions are formed from a sample introduced into the ion source as a gas or liquid, two types of effects increase the width of an isomass ion packet. These can be categorized as spatial and energy effects. Possible spatial and energy considerations affecting the arrival time distribution of an isomass ion packet at the detector are illustrated in Figure 2-2. Spatial effects are related to the position of an ion in the source when the extraction occurs. An ion may also have an initial thermal energy in any direction when it is formed in the ion source. The arrows on the ions depicted in Figure 2-2 indicate that a range of initial velocities is present in the source. lons with an initial velocity toward or away from the detector when the contents of the ion source are extracted also contribute to poor resolution. When an ion is moving away from the detector, it must first be turned around by the applied extraction field, further increasing the spread in arrival times. When the sample is desorbed from a flat surface where these effects are minimized, the resolution of time-of-flight mass spectrometers can be increased from about 1000-3000 to 10,000 or more [19].

Time-of-flight mass spectrometry is a pulsed technique. Many early instruments with electron-impact sources only ionized the sample for a short period just prior to the extraction pulse [20]. Transients were detected using boxcar integrators that collected only a small portion of the mass range at a time. Thus, only a small fraction of the sample entering the ion source was actually

Ion Source To Detector

Figure 2-2. The spatial location of an ion in the source and its velocity in the ion source prior to extraction cause broadening of the arrival time distribution for an isomass ion packet.

permitted to ionize and only a small fraction of the ions present in a transient were captured by the data system.

2.4 The MTOF/ITR System

A time-of-flight system has been developed for use as a detector for capillary GC [21]. The advantages of time-array detection have been combined with a high sensitivity mass spectrometer that uses sample efficiently and has unit resolution or better throughout the mass range of interest for capillary GC. This instrument (the MTOF), a modification of an instrument developed at the University of Giessen, uses the combination of a storage source and a non-linear ion mirror to deliver a large number of ions to the detector with high resolution [22]. All of the information generated by each pulse of the ion source is acquired by time-array detection via the integrating transient recorder (ITR). This TOFMS system is shown in Figure 2-3. The following three sections describe important components of the MTOF instrument that help overcome the sensitivity and resolution problems encountered by earlier TOFMS systems.

2.4.1 Development of the Ion Source

Wiley and McLaren [23] were the first investigators to significantly improve the resolution of TOFMS. In 1955, they developed equations to determine the flight times of ions from the source to the detector, along with the mathematical basis for the existence of a space-focus plane in a two-field ion

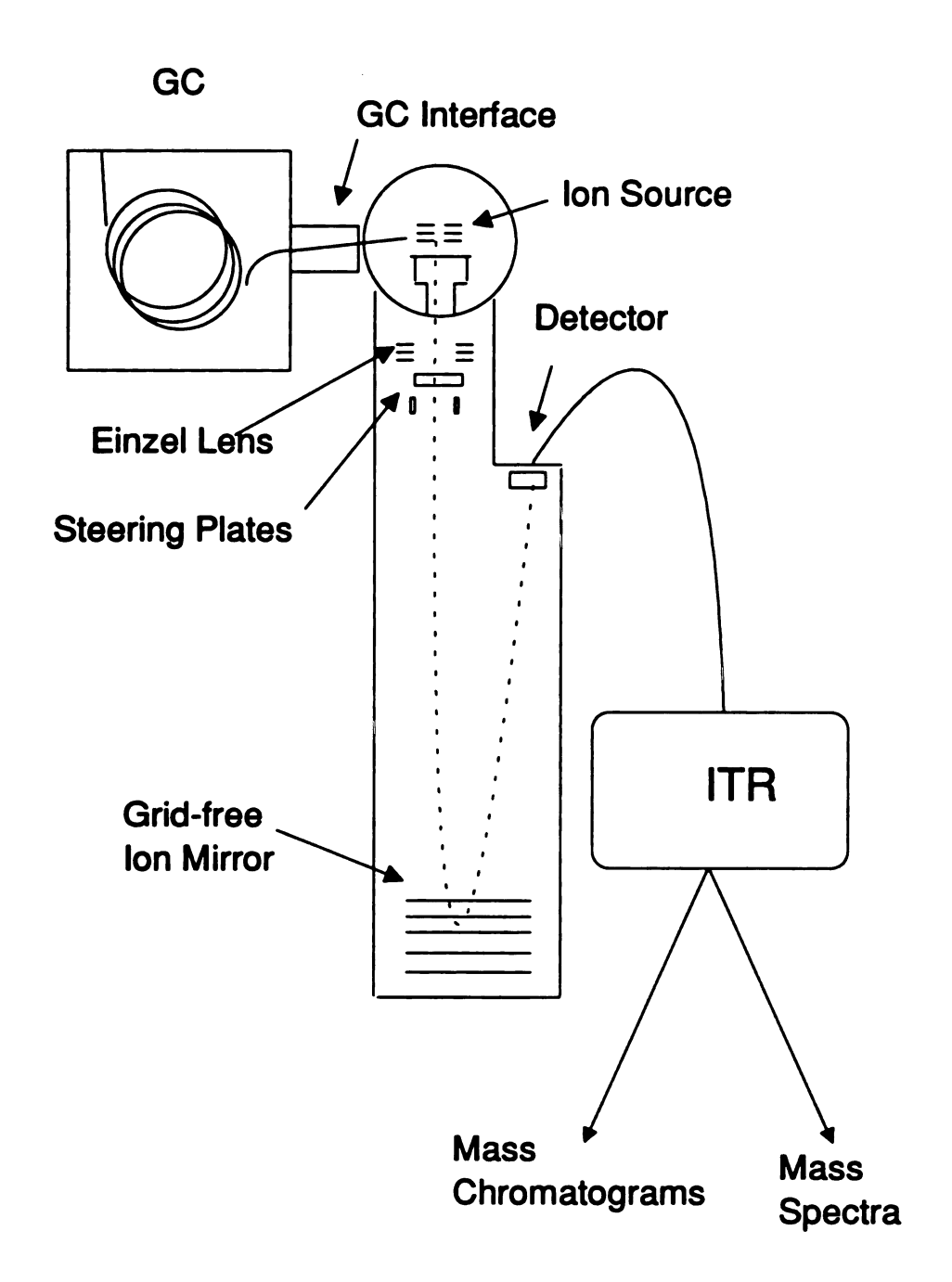
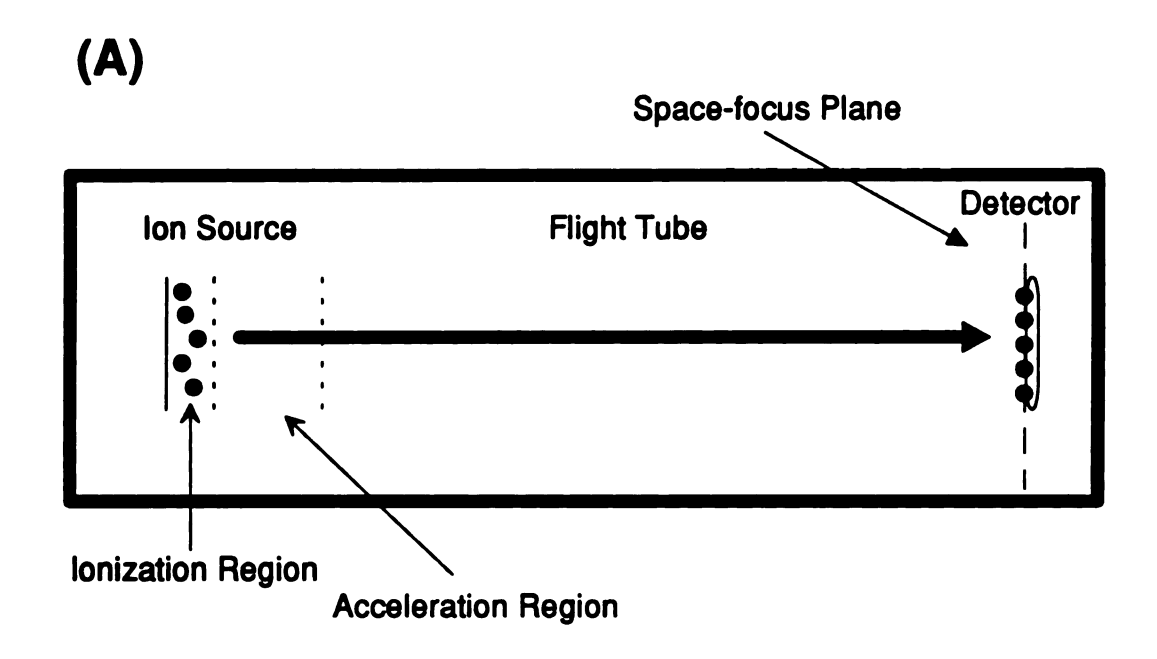


Figure 2-3. The MTOF/ITR system for GC/MS analysis.

source. Space-focusing is based on the fact that an ion closer to the front of the source is accelerated less than an ion near the back of the source. Isomass ions from the back of the source will catch up to those from the front at the space-focus plane. A conceptual diagram of an instrument containing a two-field ion source and the space focus plane is shown in Figure 2-4A. Ions are extracted from this two-field source by raising the potential on the grid at the rear of the source. The location of the space-focus plane is the same for all masses and is dependent only on the energy ratio for the fixed dimensions of the ion source.

In 1963, Studier built a continuous electron impact ionization (EI) source for time-of-flight mass spectrometers [24]. This source formed ions continuously between three grids. The ions were then stored in a potential well between the three grids. This potential well is created by the potential applied to the center of the grids in the ion source. The ions were extracted by applying a shaping waveform to the grid furthest from the detector. The ions then fall down hill out of the source and into the mass analyzer.

The idea of an El source capable of storing ions lay dormant until Wollnik and coworkers resurrected it in 1989 [25]. Their cylindrically symmetrical ion source is shown in Figure 2-5. Ions are formed and stored by a continuous electron beam between two grids (G2 and G3). Electron pushers (Pu) help to direct electrons generated by the filament through the slit between G2 and G3. Thermal electrons present between G2 and G3 aid in the accumulation of ions by creating a potential well [26]. This source accumulates a significant portion of



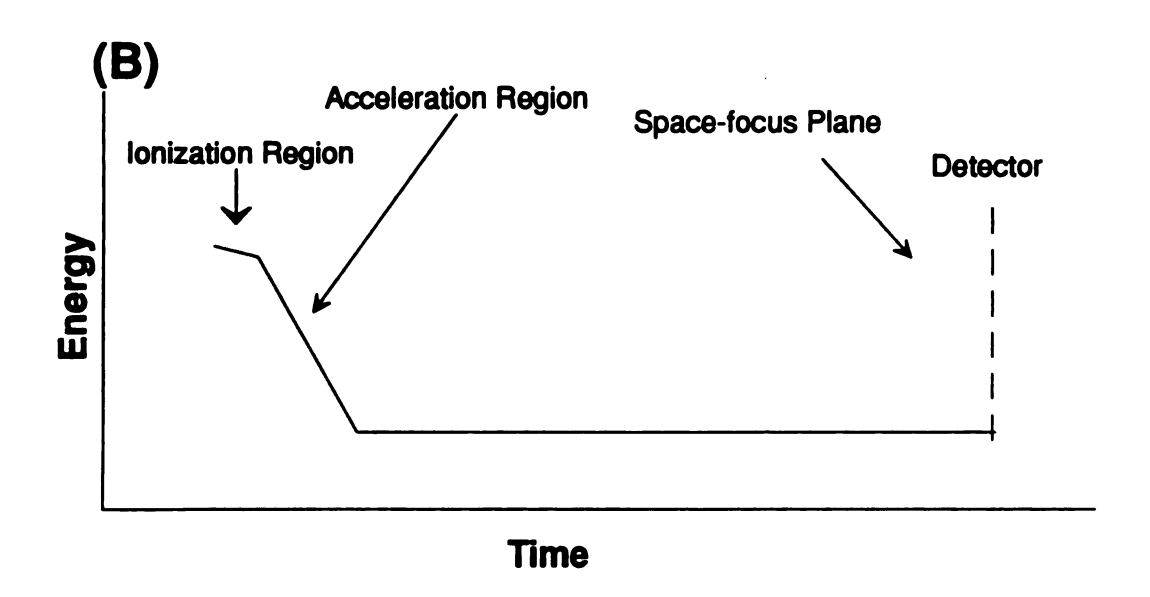


Figure 2-4. (A) Conceptual diagram of a Wiley-McLaren time-of-flight mass spectrometer including the two-field ion source and the associated energy diagram showing the various voltages felt by the ions.

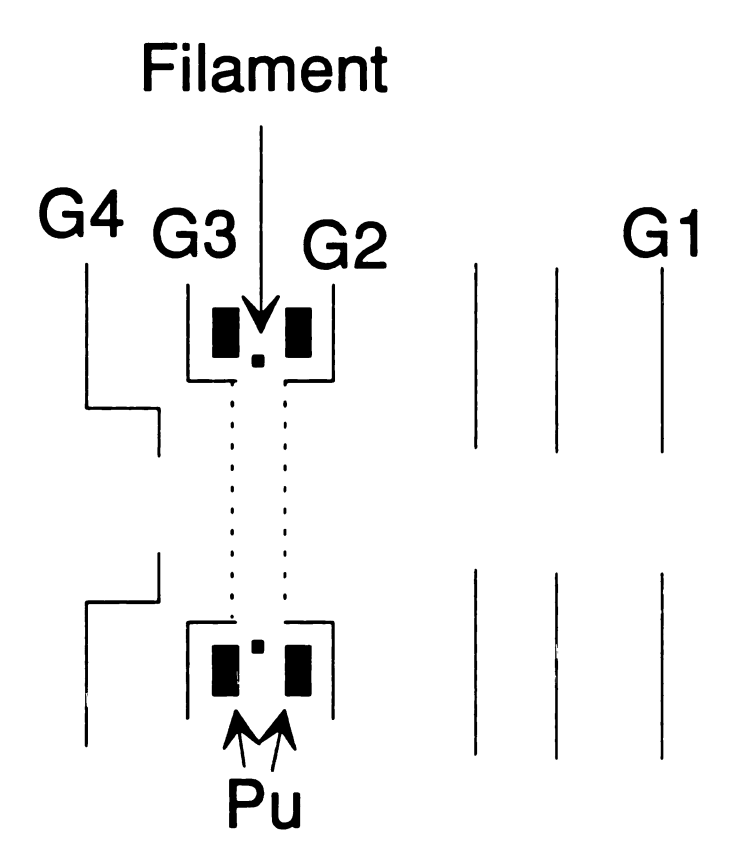


Figure 2-5. Diagram of the Wollnik electron impact ion source. Thermal electrons directed into the storage area by electron pushers (Pu) create a potential well between grids G2 and G3.

the ions formed between extraction pulses although the storage efficiency is somewhat mass and pressure dependent. Extraction is achieved by raising the potential on G3 so that the thermal energies of ions in the source are negligible when compared to the extraction voltage.

2.4.2 Ion Mirrors

An ion mirror may be used to provide either spatial or energy focusing. This mirror simply consists of a series of "washers" that create a field that causes an ion to be slowed, stopped and then reflected out of the mirror. An ion travels at the same velocity when it exits the mirror as it did upon entering it. The mirror is used to reflect the distribution of ion positions at the space-focus plane onto the detector. A mirror may have linear or non-linear electric fields. While linear-field mirrors can only correct for first order effects, mirrors with non-linear fields can provide focusing for higher-order energy effects and thus improve resolution. The resolving power of energy-focusing first and second-order mirrors has been mathematically described by loanoviciu et al. [27].

The use of mirrors in TOFMS was begun by Mamyrin and others in the 1970s [28,29]. Early experiments using electron impact ionization and a two stage mirror achieved a resolving power of over 3000 for ReBr₃ clusters with m/z 1266-1290. Mamyrin *et al.* [30] also built an instrument with a linear mirror that deflected the ions by 180° and returned them to an annular detector which surrounded the ion source. This instrument provided a resolving power of 1200

,

è

for 199 Hg 127 I+ (m/z 326) with a short flight path. Wollnik and coworkers [31] achieved a resolution of 2000 for N₂+ using an instrument similar to the original Mamyrin instrument. Thus, the use of an ion mirror raised resolution into the thousands, making time-of-flight mass spectrometers suitable for use as a chromatographic detector.

2.4.3 Time-Array-detection

The sensitivity increase from an ion source capable of storing a significant fraction of the ions generated between extraction pulses solves only one of the two problems limiting the applicability of TOFMS. The other problem was that only a small portion of the information in each transient was captured by early data acquisition systems. In a process called time-array detection, an integrating transient recorder (ITR) acquires entire transients as rapidly as they are generated [32]. A conceptual diagram of the ITR used in this research is shown in Figure 2-6. Transients are first converted from analog to digital signals by a 200 MHz Flash converter. Then a selected number (10-1000) of sequential transients are summed in one of the parallel sets of emitter-couple logic (ECL) summers. The summed transients are then moved out of the summing registers and processed into mass/intensity pairs. This mass spectral information is then stored. The ECL summers work in parallel; one is summing while the other is being emptied. No data are lost in this manner. The summed transients are called mass spectra. Although each transient contains full mass spectral information, the summing process uses the fact that transients can be generated

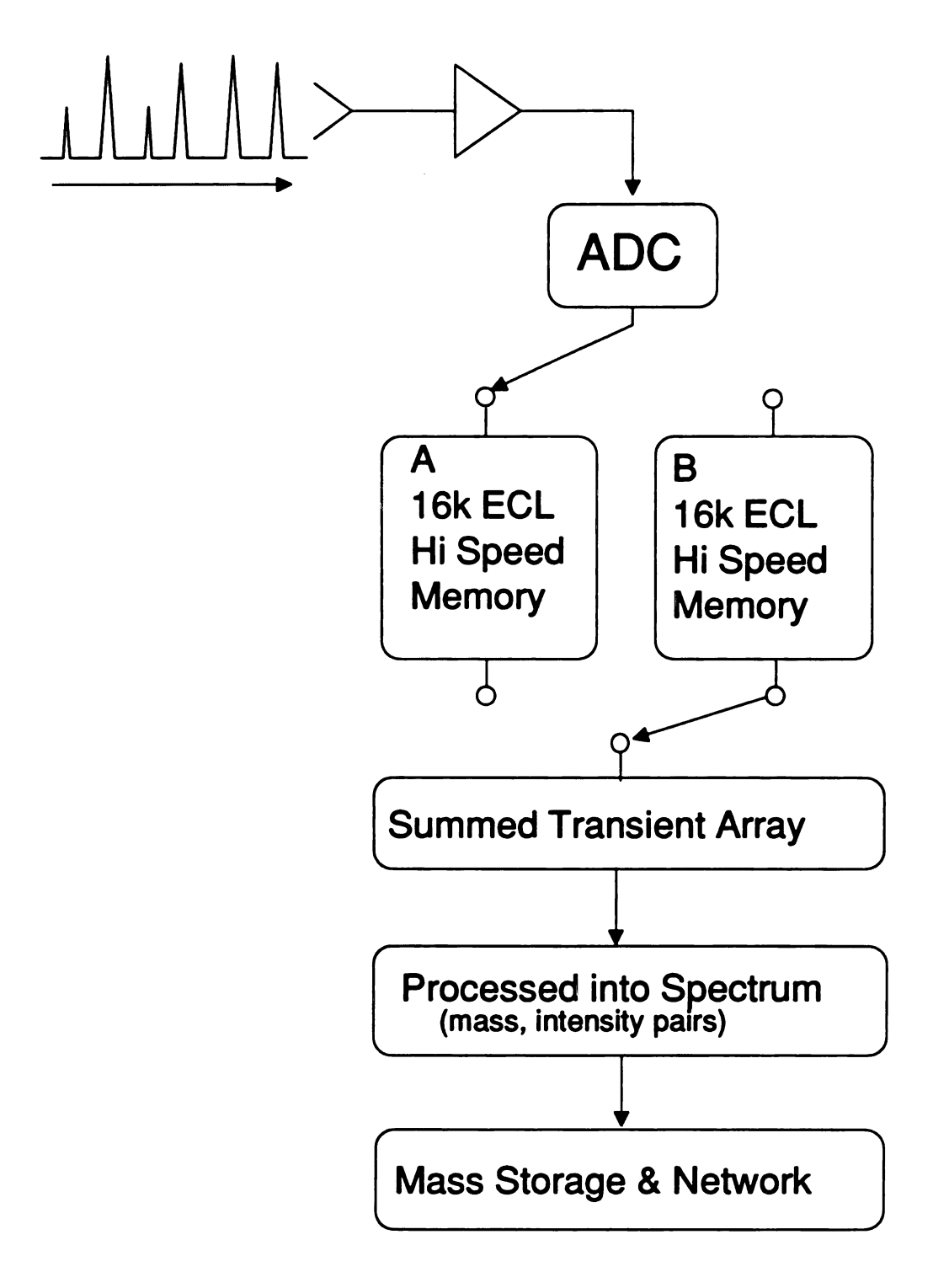


Figure 2-6. Conceptual diagram of the integrating transient recorder. Transient waveforms are captured, summed into mass spectra, converted to mass/intensity pairs and stored.

at rates exceeding the required spectrum generation rate to improve the signal-to-noise ratio. The maximum mass spectral acquisition rate is determined by the time required to transfer the mass/intensity information over the data bus to mass storage. In our system, 100 or more mass spectra can be acquired per second by the ITR without sacrificing any mass spectral information.

2.4.4 Characteristics of the MTOF instrument

lons are generated continuously and a portion of them are stored in the source. The contents of the ion source are typically sampled every 200 µs. by raising the voltage on G3 (See Figure 2-5). By the application of a high field strength, the spatial dispersion of ions in the ion source is converted into an ion energy dispersion at the space focus plane. The space focus plane of the ion source is only about 10 cm from the ion source—too short a flight-time for temporal separation of different ion masses. To accomplish mass separation, the ions drift through a 1-m flight tube to a grid-less mirror. The mirror provides mass-independent energy focusing with high ion transmission by reflecting the image at the space-focus plane onto a multichannel plate detector. The ITR then captures the information in every transient to produce mass spectra at a user selected rate. This spectral generation rate is chosen to provide the optimal combination of chromatographic resolution and sensitivity. The mirror time-of-flight instrument with time-array detection yields a system with a resolving power of 1500 (50% valley definition) and is capable of detecting 780 fg of

bromobenzene. Thus, this instrument is truly capable of performing GC/MS on the chromatographic time scale.

2.5 Deconvolution of GC/MS Data

Compounds with overlapping chromatographic elution profiles can often be distinguished using the information available across all data channels. Deconvolution approaches for GC/MS data have been developed to locate and identify coeluting compounds based on differences across the data channels. This deconvolution process can be very effective when the data on each channel are completely independent of the data on any other channel. The presence of many data channels increases the probability of locating differences across the data set.

One common feature of all mathematical algorithms is that their effectiveness is determined by the quality of the data on which they operate. Two types of problems occur in GC/MS data when relatively slow scan rates are used: the elution profile is undersampled and the resulting mass spectra are skewed [1]. When the elution profile is undersampled, its shape is not well defined and chromatographic resolution is lost. Many deconvolution approaches can resolve unknown compounds whose retention times differ by two or more sampling intervals. These algorithms have limited utility when there are a limited number of samples (often 3-6) across a three-second wide chromatographic peak. While acquiring these few mass spectra, spectral skewing occurs as the

concentration of an analyte in the ion source changes dramatically during the mass scan of the mass spectrometer. The relative intensities of the *m/z* values in each scan are distorted when the time axis of a GC/MS run is plotted as "scan number" rather than the actual time at which information about each *m/z* value is obtained. Problems with data quality, especially for the narrow elution profiles obtained with capillary GC/MS, has resulted in little development or use of deconvolution since its introduction over a decade ago. The MTOF/ITR system produces the quality data required by deconvolution algorithms. Spectra are generated at high rates and without mass scanning. Data from this instrument (TOFMS/TAD) allow the power of deconvolution approaches to be realized for capillary GC/MS.

2.5.1 Characteristics of GC/MS Data

All deconvolution algorithms for unknown samples make one assumption: the total intensity for any m/z value is assumed to be a linear combination of the responses from its contributors. This may be mathematically expressed as

$$I_i = \sum_{i=1}^n C_i E_i$$

where I_i is the intensity of the response on a given data channel, n is the number of compounds contributing to the response on the selected channel, C_i is the concentration of a compound and E_i is the efficiency for the compound forming of an ion with a m/z value on the selected channel. This is true for every m/z

value. The only information contained in the GC/MS data is the total response for all compounds of a given m/z value eluting at a chosen time.

2.5.2 Types of Deconvolution

The deconvolution approach is determined by the amount of information known about the sample and the results desired by the analyst. If the data are examined to determine the presence and concentration of a specific compound, a mass spectrum of that compound is compared to the elution profile in a reverse library-search [33-35]. This process is also called "target" analysis since the identities, retention times and mass spectra of the desired compounds are known prior to the analysis. Under these conditions, the target compound should be separated from other compounds with very similar retention behavior and mass spectra to prevent detection of interfering species. Thus, target compound analysis is most effective when the analyte and matrix are well characterized.

The opposite circumstance arises when the composition of the sample is unknown. The number of compounds present in a chromatographic peak, their retention times, identities and concentrations all need to be determined by the deconvolution approach. The ideal deconvolution approach should not only determine all of this information about coeluting compounds, it should be able resolve coeluting compounds as they elute from the column. Deconvolution of unknown samples has tremendous potential in dramatically increasing the

amount of information available from a single GC/MS run without increasing the analysis time. This area has become the focus of our deconvolution effort.

2.6 Historical Deconvolution Approaches for Unknowns

The basic steps required to deconvolute coelutions in a sample of unknown composition are: (1) determine the number of components present in each chromatographic peak, (2) determine the retention time of each coeluting compound, (3) identify the m/z values associated with each component and (4) extract a pure spectrum for each compound present. Identification and quantitation can be performed on the sample once the retention time and mass spectrum of a compound have been determined [36].

A single mathematical algorithm cannot accomplish all of these steps. Therefore, two or more algorithms are typically required to deconvolute coeluting compounds. These algorithms may be grouped by function. One class of algorithms are used to determine the number and retention times of coeluting species. Another set is used to extract mass spectra for unresolved compounds. These approaches may be related for some approaches. For example when principal component analysis is used to determine the number of compounds present in a coelution, factor analysis is often used to extract pure mass spectra.

2.6.1 Locating Unresolved Compounds

Locating and determining the retention times of coeluting compounds is typically the first step in their deconvolution. A variety of approaches have been applied to locate coeluting compounds. Some of the earliest of these extended deconvolution methods that determined the number of components present in a region by making assumptions about the shape of the elution profile from single-channel data to multichannel mass spectral data (37,38). This approach was able to find the number of coeluting compounds in simulated data but failed when applied to real data. This failure is due to the difficulty in accurately modeling the shapes of real peaks. Chromatographic peaks often contain features which are not easily modeled without any prior knowledge about their composition. Compound structures may affect peak shapes. Polar compounds often tail when analyzed on columns with non-polar stationary phases. Peak widths and shapes depend on the concentrations and amount of time a compound is retained on the chromatographic column.

One of the most common approaches used for locating coelutions is based on the observation of Biller and Biemann [39] that the intensities of ions corresponding to any given compound eluting from a chromatographic column will rise and fall synchronously with the partial pressure of the analyte in the ion source [40,41]. All mass chromatograms across the many data channels with the same temporal profiles are related to the elution of the same compound. Thus, examination of the mass chromatograms can reveal the number of compounds

eluting in a specific region and their retention times. The only difficulty associated with this approach occurs when coeluting compounds have fragment ions with the same m/z values. Shared m/z values will reach their maximum intensity at some time between the retention times of the coeluting compounds. In this case, shared m/z values must be discriminated from those which are present only in one compound. Even under best circumstances, the Biller-Biemann approach is accurate to one spectral acquisition in determining the retention time of a compound. When a compound has a retention time between two adjacent mass spectra, mass chromatograms related to only one compound may reach their maximum intensity over two sampling periods. Ghosh and Anderegg [42] used derivatives to more accurately determine the retention times of compounds. Their approach allows interpolation of the true retention time of a compound from the acquired data for each mass chromatogram.

Another more computer-intensive approach is to use factor analysis to determine the number of compounds present in a coelution [43-50]. Factor analysis can detect compounds that coelute completely if there is some distinctive feature for each coeluting compound. This includes differences in elution profile shape such as slopes of rising and falling edges. The unfortunate aspect of using factor analysis to determine the number of compounds present in a coelution is the amount of time required to process the quantity of data collected in a GC/MS run. Factor analysis approaches often rely on some assumption to reduce the processing time required to determine the number of components and their retention times. Knorr et al. [51,52] determined the

number of coeluting compounds by minimizing a function while assuming that several different numbers of compounds were chromatographically unresolved. The number of compounds present at this minimum was assumed to represent the number of coeluting species. When this approach was applied to real data, the selected functions were not always effective in determining the number of compounds, especially where large differences in relative abundance were present. These iterative approaches are limited by the time required for data analysis to post-run processing.

2.6.1 Extracting Pure Mass Spectra

Once the number of compounds present in a coelution has been determined, the next step is to extract a pure mass spectrum for each coeluting compound. The simplest approach for extraction of a pure mass spectrum relies on the presence of one data channel that is characteristic of one of the coeluting species [53-56]. Features of these unique m/z values such as retention time and the shape of the elution profile can be assumed to be characteristic of that compound. This information allows the intensities of shared m/z values to be properly assigned across all of the data channels. The spectral channel for the pure compound often has the narrowest response in the elution window of interest [57].

When factor analysis has been used to determine the number of compounds present in a coelution, least-squares [58,59], factor analysis [49,51]

or other approaches [48,50,60] have all been successfully applied to simulated and real packed-column GC/MS data. The least squares approach is dependent on a model for the elution peak shape [61]. This model must be fairly complex to permit accurate deconvolution of the overlapping components. The elution profiles of unknown compounds are difficult to portray accurately since the quality of the chromatography is dependent on the character of the analyte. Factor analysis is most easily performed when a characteristic mass can be located for each coeluting compound. Despite the increased analysis time required when no unique *m/z* value is present, factor analysis is a powerful approach for resolving coeluting compounds. Numerous curve-resolution approaches have been applied with good success [37,48,49,56]. These approaches cannot be performed in real-time but they have tremendous power when a difficult separation is being analyzed.

All of the techniques used to extract pure mass spectra for coeluting compounds have a dependence on sampling rates, the degree of chromatographic separation between the unresolved species and the relative concentrations of the compounds. As compounds elute closer together, they become more difficult to discriminate. A wide range of intensities can further complicate the situation by appearing to be noise or part of the major component's spectrum rather than another compound present at low concentration. Rapid sampling provides the best chance for resolving the coeluting species because small differences in retention time are more apparent. This does not always simplify the extraction process to obtain a pure mass

spectrum. Thus, an investigator may be able to determine that more than one compound is present in a peak but not be able to resolve them. Unfortunately, this valuable piece of information does not resolve the compounds. The resolution must be accomplished by altering the chromatographic conditions.

Despite the success of these approaches, only a few simple versions of peak finding algorithms are commercially available [62]. These Biller-Biemann based algorithms locate regions containing chromatographically unresolved compounds but do not extract pure mass spectra for the coeluting species. Thus, deconvolution has not been commonly used despite its tremendous potential for improving the compound resolution of GC/MS data.

2.7 Summary

Advancements in the field of time-of-flight mass spectrometry have resulted in a detection system capable of acquiring full MS information on the capillary GC/MS time scale. The MTOF/ITR system has the sensitivity and resolution needed to acquire MS data from a narrow-bore capillary column. These qualities provide the instrumental basis for the use of deconvolution techniques to determine the composition of unknown mixtures.

Deconvolution techniques have been applied to packed-column GC/MS data with some success but lost favor with the commercialization of capillary GC. This difficulty was a result of the trade-off between mass spectral acquisition rate

		,
		;
		:
		:

and sensitivity for scanning instruments. As a result of these problems, deconvolution techniques have been studied in less stringent environments such as HPLC with diode array detection [63,64] and analyzing HPLC fractions with Raman detection [65]. The capabilities of the MTOF/ITR system now allow the use of deconvolution techniques for data from capillary GC/MS analyses.

References

- Holland, J. F.; Enke, C. G.; Allison, J.; Stults, J. T.; Pinkston, J. D.;
 Newcomb, B.; Watson, J. T. *Anal. Chem.* 1983, 55, 997A.
- 2. Ettre, L. S. *Introduction to Open Tubular Columns*, Perkin-Elmer Corporation: Norwalk, Connecticut, 1979..
- 3. Guiochon, G.; Gonnard, M. F.; Zakaria, M.; Beaver, L. A.; Siouffi, A. M., Chromatographia 1983, 17, 121.
- 4. Davis, J. M.; Giddings, J. C. Anal. Chem 1983, 55, 418.
- 5. Rosenthal, D. Anal. Chem 1982, 54, 63.
- 6. Bertsch, W. in *Recent Advances in Capillary Gas Chromatography*, Bertsch, W., Jennings, W.G., Kaiser, R. E., Eds., Dr. Alfred Huthig Verlag: New York, 1981, Chapter 1.
- 7. Davis, J. M.; Giddings, J. C., Anal. Chem. 1983, 55, 418.
- 8. McWilliam, I. G.; Dewar, R. A. Anal. Chem. 1957, 29, 925.

- Ashbury, G. K.; Davies, A. J.; Drinkwater, J. W. Anal. Chem. 1957, 29,
 918.
- 10. Karmen, A. J. Chromatogr. Sci. 1969, 7, 541.
- 11. Lovelock, J. E. Chemtech 1981, 11, 531.
- 12. Hewlett PackardCompany, Avondale, PA 19311.
- 13. Sweeley, C. C.; Elliot, W. H.; Fries, I. Ryhage, R. *Anal. Chem.* **1966**, *38*, 1549.
- 14. Dessy, R. E.; Reynolds, W. D.; Nunn, W. G.; Titus, C. A.; Moler, G. F. J. Chromatogr. 1976, 126, 347.
- 15. Hedfjall, B.; Ryhage, R. Anal. Chem. 1979, 51, 1687.
- 16. Hedfjall, B.; Ryhage, R. Anal. Chem. 1981, 53, 1641.
- 17. Gohlke, R. S. Anal. Chem. 1959, 31, 535.
- McFadden, W. H.; Teranishi, R.; Black, D. R.; Day, J. C. *J. Food Sci.* 1963, 28, 316.
- 19. Walter, K.; Boesl, U.; Schlag, E. W. *Int. J. Mass Spectrom. Ion Processes*1986, *71*, 309.
- 20. CVC 2000, CVC Product Inc., Rochester, New York.
- 21. Tecklenburg, R. E., Jr.; McLane, R. D.; Grix, R.; Sweeley, C. C.; Allison, J.; Watson, J. T.; Holland, J. F.; Enke, C. G.; Gruner, U.; Gotz, H.;

- Wollnik, H., Presented at the 38th ASMS Conference on Mass Spectrometry and Allied Topics, Tucson, AZ, June 6, 1990.
- 22. Grix, R.; Gruner, U.; Li, G.; Stroh, H.; Wollnik, H. Int. J. Mass Spectrom. Ion Proc. 1989, 93, 323.
- 23. Wiley, W. C.; McLaren, I. H. Rev. Sci. Instrum. 1955, 36, 1150.
- 24. Studier, M. H. Rev. Sci. Instrum. 1963, 34, 1367.
- 25. Grix, R.; Gruner, U.; Li, G.; Stroh, H.; Wollnik, H. *Int. J. Mass Spectrom. Ion Proc.* 1989, *93*, 323.
- Yefchak, G. E.; Puzycki, M. A.; Allison, J.; Enke, C. G.; Grix, R.; Holland, J. F.; Li, G.; Wang, Y.; Wollnik, H., Presented at the 38th ASMS Conference on Mass Spectrometry and Allied Topics, Tucson, AZ, June 6, 1990.
- 27. Ioanoviciu, D.; Yefchak, G. E.; Enke, C. G. Int. J. Mass Spectrom. Ion Proc. 1989, 94, 281.
- 28. Karataev, V. I.; Mamyrin, B. A.; Shmikk, D. V. Sov. Phys. Tech. Phys. 1972, 37, 45.
- 29. Mamyrin, B. A.; Karataev, V. I.; Shmikk, D. V.; Zagulin, V. A. *Sov. Phys. JETP*, **1973**, *49*, 762.
- 30. Mamyrin, B. A.; Shmikk, D. V. Sov. Phys. JETP, 1979, 49, 762.

- 31. Gohl, W.; Kutscher, R.; Laue, H.; Wollnik, H. *Int. J. Mass Spectrom. Ion Phys.* **1983**, *48*, 411.
- 32. Holland, J. F.; Newcombe, B.; Tecklenburg, R. E., Jr.; Davenport, M.; Allison, J.; Watson, J. T.; Enke, C. G. Rev. Sci. Instrum. 1991, 62, 69.
- 33. Abramson, F. P. Anal. Chem. 1975, 47, 45-49.
- 34. McLafferty, F. W.; Hertel, R. H.; Villiwock, R. D. *Org. Mass Spectrom.* **1974**, *9*, 690.
- 35. Blaisdell, B. E.; Sweeley, C. C. Anal. Chim. Acta 1970, 42, 21.
- 36. Sharaf, M. A.; Kowalski, B. R. Anal. Chem. 1982, 54, 1291.
- 37. Allen, G. C.; McMeeking, R. F. *Anal. Chim. Acta Comp. Tech. Opt.* **1978**, 103, 73.
- 38. Grushka, E.; Myers, M. N.; Giddings, J. C. Anal. Chem. 1970, 42, 21.
- 39. Biller, J. E.; Biemann, K. Anal. Lett. 1974, 7, 515.
- Dromey, R. G.; Stefik, M. J.; Rindfleisch, T. C.; Duffield, *Anal. Chem.* 1976, 48, 1368.
- 41. Colby, B. N. J. Am. Soc. Mass Spectrom. 1992, 3, 558.
- 42. Ghosh, A.; Anderegg, R. J. Anal. Chem. 1989, 61, 73.
- 43. Davis, J. E.; Shephard, A.; Stanford, N.; Rogers, L. B. *Anal. Chem.* **1974**, *46*, 821.

- 44. Justice, J. B., Jr.; Isenhour, T. L. Anal. Chem. 1975, 47, 2286.
- 45. Ritter, G. L.; Lowry, S. R.; Isenhour, T. L.; Wilkins, C. L. *Anal. Chem.* **1976**, *48*, 591.
- 46. Mallinowski, E. R. Anal. Chem. 1977, 49, 612.
- 47. Mallinowski, E. R.; Howery, D. G. Factor Analysis in Chemistry, Wiley:New York 1980.
- 48. Sharaf, M. A.; Kowalski, B. R. Anal. Chem. 1981, 53, 518.
- 49. Sharaf, M. A. Anal. Chem. 1986, 58, 3084.
- 50. Vanslyke, S. J.; Wentzell, P. D. Anal. Chem. 1991, 53, 2512.
- 51. Knorr, F. J.; Futrell, J. H. Anal. Chem. 1979, 51, 1236.
- 52. Knorr, F. J.; Thorsheim, H. R.; Harris, J. M. Anal. Chem. 1981, 53, 621.
- 53. Halket, J. M. J. Chromatog. 1979, 186, 443.
- 54. Mallinowski, E. R. Anal. Chim. Acta 1982, 134, 129.
- 55. Mallinowski, E. R. Anal. Chem. 1984, 56, 778.
- 56. Windig, W; Liebman, S. A.; Wasserman, M. B.; Snyder, A. P. *Anal. Chem.*1988, 60, 1503.
- 57. Hites, R. A.; Biemann, K. Anal. Chem. 1970, 42, 855.
- 58. Allen, G. C.; McMeeking, R. F. Anal. Chim. Acta 1978, 103, 73.

- 59. Knorr, F. J.; Thorsheim, J. M.; Harris, J. M. Anal. Chem. 1981, 53, 821.
- 60. Sharaf, M. A.; Kowalski, B. R. Anal. Chem. 1982, 54, 1291.
- 61. Osten, D. W.; Kowalski, B. R. Anal. Chem. 1984, 56, 991.
- 62. Finnegan MAT SanJose, CA 95134.
- 63. Lindberg, W.; Ohman, J.; Wolde, S. Anal. Chem. 1986, 58, 299.
- 64. Gerritsen, M. J. P.; Tanis, H.; Vandeginste, B. G. M.; Kateman, G. *Anal. Chem.* **1992**, *64*, 2042.
- 65. Mallinowski, E. R.; Cox, R. A.; Haldna, U. L. Anal. Chem. 1984, 56, 778.

Chapter 3

Deconvolution of GC/MS Data: Better Data Make An Old Technique Work

3.1 Introduction

The difficulties caused by overlapping chromatographic elution profiles in which two or more distinct chemical components are present, are well known. Analyses in such situations are improved to some degree by the use of two-dimensional detectors such as mass spectrometers. These detectors reduce the temporal separation needed for the identification of components with distinctive response patterns among the detector channels. Although complete component separation is not achieved for all samples, deconvolution techniques combined with two-dimensional detection can greatly enhance the "effective" resolution of chromatographic systems. Ideally this process could be performed on GC/MS data in real time.

When the mass spectral acquisition rate and data quality are sufficient, even a simple approach will allow the deconvolution of data acquired by capillary GC/MS. The problems with commercial GC/MS systems as chromatographic detectors and our solution have been described in Chapters 1 and 2 of this thesis. The MTOF/ITR system overcomes all of the previous

.

sampling limitations that restricted the use of deconvolution techniques in the analysis of capillary GC/MS data. A relatively simple deconvolution approach that will locate and extract pure mass spectra for compounds in unknowns was developed to demonstrate the capabilities of deconvolution in GC/MS analysis when adequate mass spectral acquisition rates are used. This approach was applied to two different mixtures to demonstrate its power.

The deconvolution approach described in this chapter was developed in conjunction with Dr. George Yefchak. Our approach to peak-finding culminated from a series of discussions. George developed the cross-correlation algorithm to extract the pure mass spectra and wrote all the software necessary to apply our deconvolution approach to real data.

3.2 Approach

The goals of any deconvolution technique applied to unknown samples are to determine the number of unresolved components and their mass spectra. Mass spectrometers are often viewed as detectors for GC/MS in the same manner as flame ionization detectors or other one dimensional detectors. They are used to detect and identify the "separated" components as they elute from a GC column. Unseparated compounds are usually visible as shoulders or anomalous shapes in the elution profile. The hypothetical elution profiles for three poorly-resolved compounds shown in Figure 3-1 illustrate the weakness of this approach. The reconstructed total ion current chromatogram (RTIC) is the sum of the intensities

•

for all of the data channels at any time. Nothing in the shape of the RTIC reveals that more than two compounds elute in this profile. The three dotted lines show the three compounds that contribute to the RTIC to form the overlapped peak. Chromatographically overlapped compounds can often be located and identified using the information on the mass axis. Acquisition of GC/MS data can either be viewed as the generation of one hundred or more mass chromatograms or the acquisition of a series of mass spectra during the chromatographic run. When the information contained in these mass chromatograms is fully used by deconvolution techniques, the three compounds can in this example can easily be located and identified.

A variety of approaches have been successfully applied to GC/MS data, but most of them follow the same steps: (1) determine the number of components present in each chromatographic peak, (2) determine the retention time of each eluting compound, (3) identify the *m/z* values associated with each component and (4) extract the "true" spectrum for each compound present. A single algorithm cannot accomplish all of these steps. Therefore, combinations of two or more algorithms are typically required to deconvolute coeluting compounds.

3.2.1 Location of Coeluting Compounds

As Biller and Biemann observed [1], the intensities of ions corresponding to a given compound eluting from a chromatographic column will rise and fall

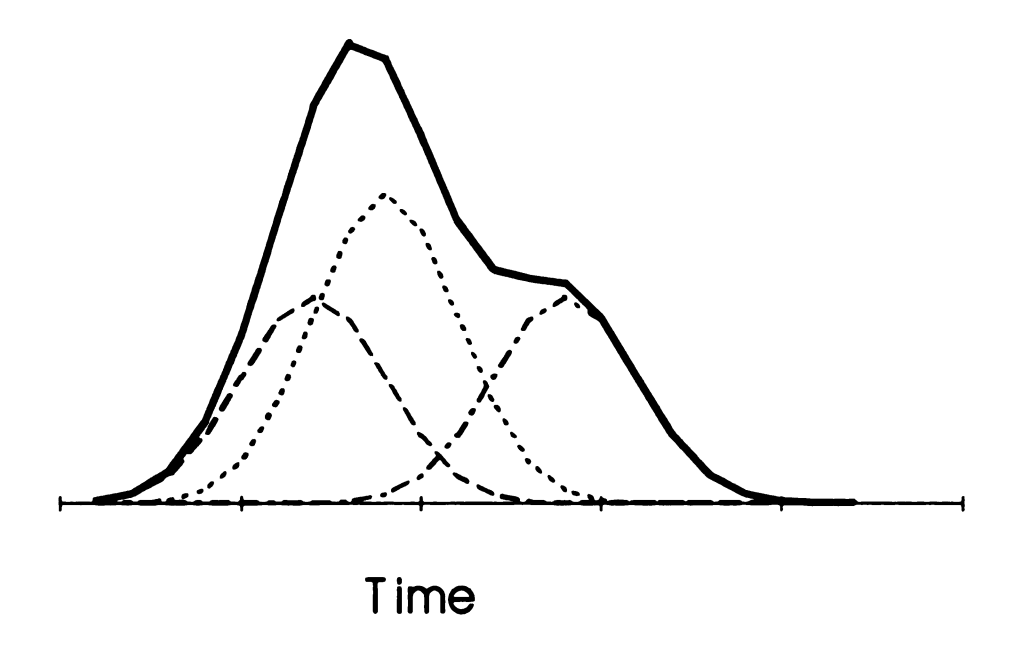


Figure 3-1. The RTIC (solid line) does not always reveal the presence of coeluting compounds. In this case, three unresolved compounds (dotted lines) contribute to the RTIC but cannot be located by examination of the RTIC alone.

	·	

synchronously as the partial pressure of that compound changes in the ion source of a mass spectrometer. If the intensities of different sets of masses have different temporal profiles, the presence of more than one compound is indicated. If all of the mass chromatograms are examined to determine the points at which they reach their maximum intensities during a peak, a mass chromatogram peak position plot (MCPPP) may be generated. Each mass chromatogram is first smoothed in the manner of Savitzky and Golay [2]. Our peak-finding algorithm then searches the smoothed mass chromatograms for any region containing intensities that nearly-monotonically increase and then decrease in the same manner. The acquisition time corresponding to the point of highest intensity within this region is taken to be the peak position of that m/z value. When this procedure is performed for every m/z value, a MCPPP may be generated to show the accumulated intensity (or some other related quantity) that maximizes during each acquired mass spectrum. This approach will effectively locate the retention time of a compound to within one spectrum generation, but does not interpolate between spectrum generation intervals.

Under ideal circumstances (Figure 3-2A), the MCPPP will show a single response for each compound. Two difficulties in generating the MCPPP usually prevent this from being true. These are illustrated in Figure 3-2B. One is the presence of noise which may shift the time of maximum intensity of individual mass chromatograms away from their true position. This difficulty results in a cluster of lines around the correct retention time. The second is the presence of m/z values shared by more than one of the coeluting compounds. The maximum

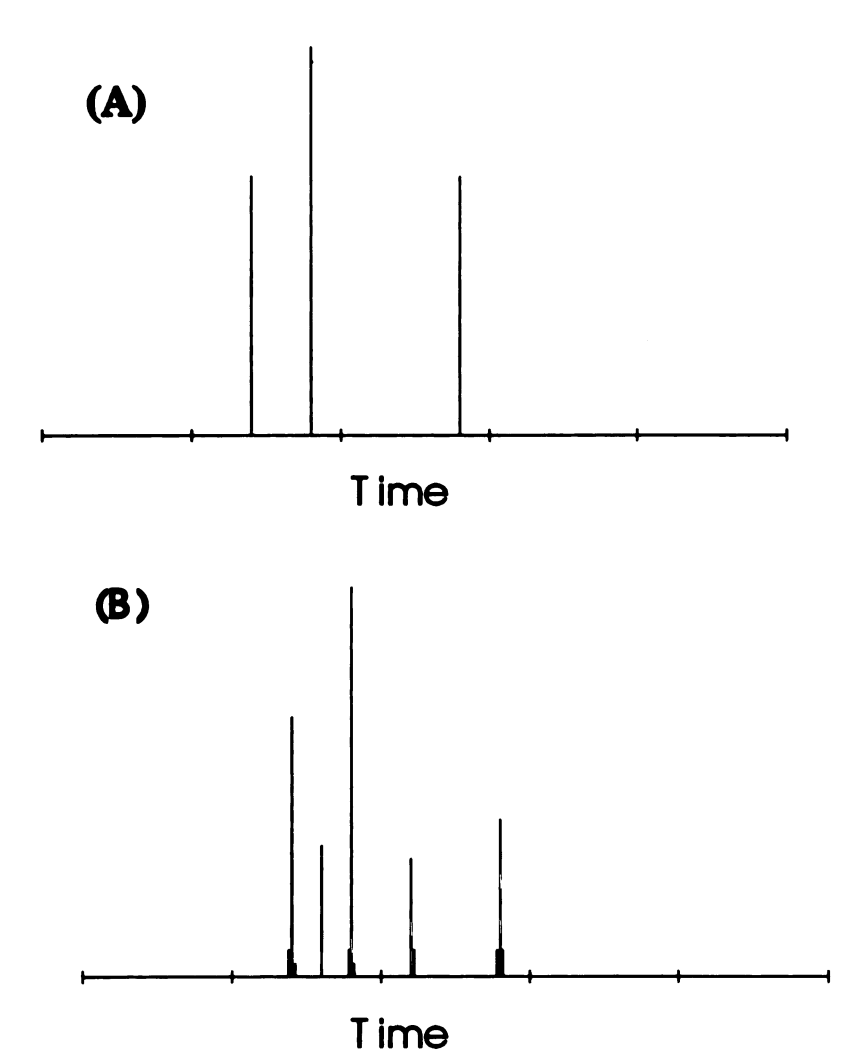


Figure 3-2. Illustration of a mass chromatogram peak position plot (MCPPP) showing ideal (A) and real (B) MCPPP plots for the three unresolved compounds from Figure 3-1.

intensity of mass chromatograms containing contributions from more than one compound occurs at some time between the retention times of the coeluting compounds. The exact position of this maximum intensity is dependent on the relative concentrations of the coeluting compounds and the relative abundance of the shared m/z value in the mass spectrum of each compound. Thus, mass chromatograms of shared m/z values may yield a series of responses in the MCPPP between the retention times of the pure compounds.

3.2.2 Determination of the Retention Time of Each Coeluting Compound

The next step in our deconvolution approach is the identification of individual mass chromatograms having responses due to only one of the compounds with overlapping elution profiles. These corresponding m/z values are termed "unique masses". The retention times for these unique m/z values are those of the pure compounds. Our simple approach is shown in Figure 3-3. Consider the task of identifying the ion that is unique for compound II. From inspection of the reconstructed mass chromatograms in Figure 3-3A, mass m_2 is clearly the correct choice; our goal for the unique-mass algorithm is to quickly determine this without visual inspection. Note that in Figure 3-3A the mass chromatograms have been normalized to unit maximum intensity. In Figure 3-3B, the normalized intensity values have been depicted for each mass only at the scans corresponding to each retention time. The intensity of the unique mass for compound II (m_2) is low at the retention times of compound I, but high at that of compound II. To find the unique ion for compound II, the algorithm computes for

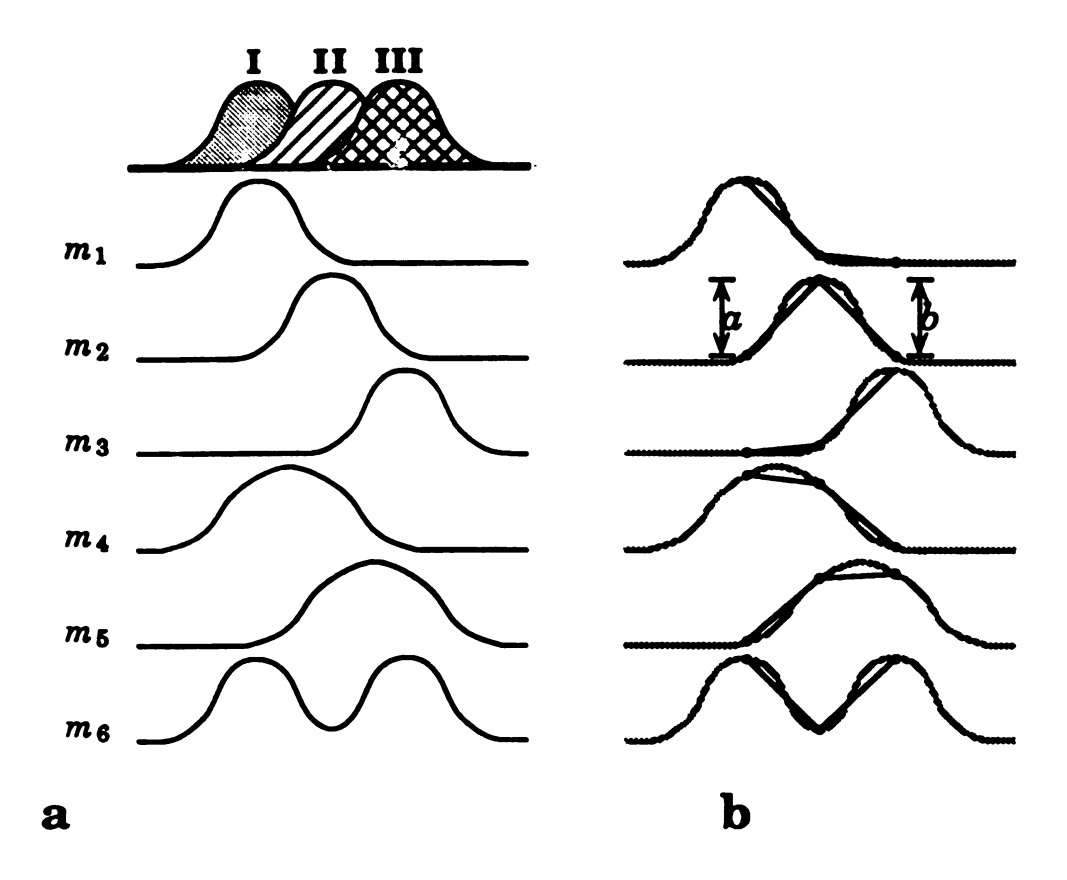


Figure 3-3. Selection of the most unique mass for three coeluting compounds by inspection of mass chromatogram peak morphology (A) and by the three-point algorithm (B).

$$H = h log I_{m,0}$$

for that mass is therefore calculated as

$$H_{m} = \left[\frac{2 l_{m,0} - (l_{m,-1} + l_{m,+1})}{\max(l_{m,-1}, l_{m,0}, l_{m,+1})} \right] \log l_{m,0}$$

where the function $\max(\cdot,\cdot,\cdot)$ yields the largest of the three raw intensities. When determining unique masses for either the first or last component in an overlapped set, intensities of zero are used for all masses in the absent (i.e., preceding or following) scan.

Peaks in the mass chromatograms identified as unique masses are confirmed by examination of the mass chromatographic profiles for the tabulated MCPPP results. Once unique masses have been located for all of the

unresolved compounds, the number of coeluting species and their retention times are known.

3.2.3 Extraction of a Pure Mass Spectrum for Each Unresolved Compound

Once the number of compounds present in a coelution has been determined, a pure mass spectrum is extracted for each coeluting compound. When a unique mass is known for each coeluting compound, intensities of shared m/z values to be properly assigned by comparison of mass chromatograms. We assume that the spectral patterns observed during the elution of overlapping peaks are linear sums of the pure-component spectra. The shape of the elution profile for each unique mass is taken to represent the true elution profile for the corresponding compound. Thus, the degree to which the temporal profile for the unique mass of a given compound is matched by mass chromatograms for the other masses should correspond, in some way, to the intensity of those masses in the desired spectrum. Cross-correlations between the normalized mass chromatograms for a unique mass with those of other masses can be used to assign intensities to all mass chromatograms associated with the elution of a compound.

To extract the pure-component spectra each mass chromatogram is first normalized to unit vector length over the region of interest according to the formula

$$N_{m,s} = \frac{R_{m,s}}{\left[\sum_{i=0}^{b} (R_{m,i})^2\right]^{1/2}}$$

where $N_{m,s}$ is the normalized intensity for mass m at scan s, $R_{m,s}$ is the raw intensity, and a and b are the first and last scan numbers, respectively, for the desired scan range. Cross-correlations between pairs of normalized mass chromatograms are calculated according the formula

$$Corr(p,q) = \sum_{i=q}^{b} N_{p,i} \cdot N_{q,i}$$

Note that, in general, $Corr(\alpha, \beta) = Corr(\beta, \alpha)$ and $Corr(\alpha, \alpha) = 1$.

The cross-correlation function is used to generate a factor which, when multiplied by the observed intensity of a given mass in a scan acquired at one of the elution times, yields an approximation of the true intensity of that mass in the spectrum of the corresponding compound. Since the mass chromatograms for unique masses from two different compounds represent independent elution profiles, the cross-correlation between these mass chromatograms represents the degree of overlap. The raw cross-correlation values will then go from zero, for completely separated peaks to unity for exactly coeluting compounds. We obtain the desired factor by linearly re-mapping the raw values so that the cross-correlation between unique masses for two adjacently-eluting compounds is mapped to zero. That is, we identify the cross-correlation between the two given unique masses as C_{low} and re-map each value according to the formula

$$Corr'(\cdot,\cdot) = \frac{Corr(\cdot,\cdot) - C_{low}}{1 - C_{low}}$$

Values for these re-mapped cross-correlations are multiplied by the corresponding raw intensities to yield the extracted spectra.

Software for the deconvolution algorithms was written in C and operated under Unix System V on a Motorola MVME147-A1 computer (Motorola, Inc.). Initial development of the algorithms was performed using the spreadsheet program Wingz (Informix Software, Inc.) on a Macintosh Ilsi computer (Apple Computer, Inc.).

3.3 Experimental

3.3.1 Reagents

The gasoline-range hydrocarbon mixture was prepared from a ThetaKit TK-102 sample set (Theta Corp.) by adding 5 μ L of each component to 5 μ L reagent-grade dodecane in a 7 mL vial. The vial was heated to 60°C, and a 0.2 μ L headspace sample was withdrawn for injection into the gas chromatograph. The compounds *tert*-butylbenzene and 1,2,4-trimethylbenzene were obtained from Chem Service, Inc. and dissolved in reagent-grade methanol. Chromatographic conditions were adjusted provide a large degree of overlap in the elution profiles for these two compounds.

,

30

v.4

100 NO 100

: - ;

3.3.2 Gas Chromatography

Chromatography and sample introduction to the mass spectrometer were accomplished with a HP-5890A (Hewlett-Packard, Inc.) gas chromatograph using a 2 m x 100 μm DB-5 column having a 0.4 μm film thickness (J&W Scientific, Inc.). The helium flow rate was adjusted to obtain optimum peak shape; resulting in a linear velocity of approximately 85 cm/s. The injector and the transfer line to the mass spectrometer were both heated to 200°C.

3.3.3 Time-of-Flight Mass Spectrometer

The MTOF instrument was operated with an electron energy of 70 eV in the ion source and an extraction frequency of 3 kHz. Mass spectra were acquired at a rates of 20 and 30 spectra per second by summing 150 and 100 transients for the respective analyses.

3.4 Effectiveness on Gasoline Range Hydrocarbon Mixture

A mixture of twelve gasoline-range hydrocarbons was prepared and partially separated over a total elution time of ten seconds by high-speed gas chromatography. The reconstructed total-ion chromatogram (RTIC), shown in Figure 3-4A, reveals only ten peaks; two coelutions (at peaks 6 and 7) are indicated, however, by the MCPPP shown in Figure 3-4B. Thus the number of components indicated by the MCPPP is correct. The algorithm used to obtain

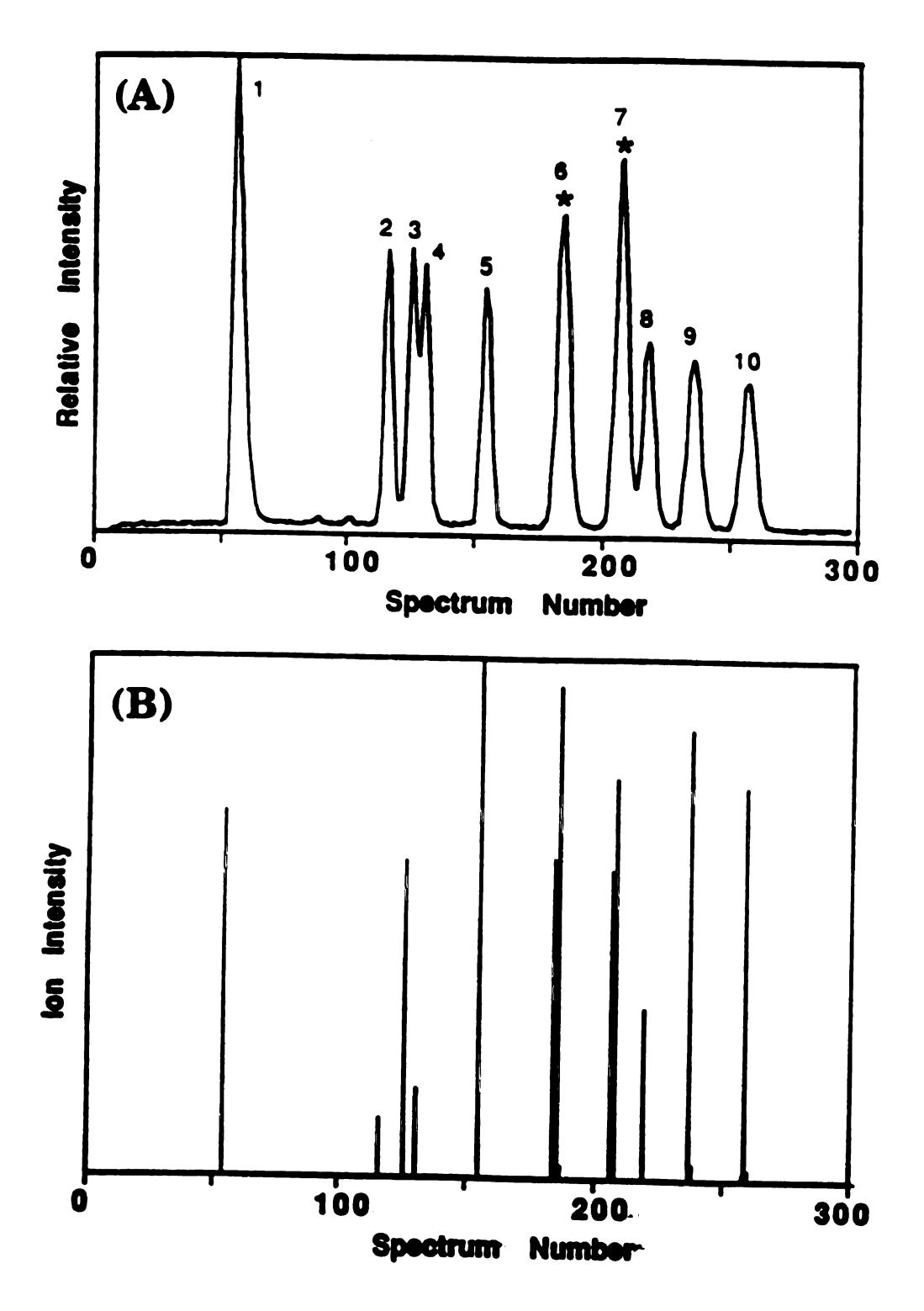


Figure 3-4. RTIC (A) and corresponding MCPPP (B) from the analysis of the 12-component hydrocarbon mixture.

this MCPPP identified any region of a mass chromatogram having at least 5 consecutively-increasing points followed by at least 5 consecutively-decreasing points as a peak. One noise spike was tolerated within both the rising and falling windows, and the data were filtered by a 3-point Savitsky-Golay smooth prior to analysis. Unique masses were determined for peaks 2–9; mass chromatograms for these are shown in Figure 3-5.

An expanded view of the RTIC for peak 6 is shown in Figure 3-6A, together with unique-mass mass chromatograms for the two overlapping components. The raw spectra obtained at the apices of the two mass chromatograms (at 9.25s and 9.35s, respectively) are shown in Figures 3-6B-C. Since the mass chromatogram maxima are separated by only two spectral acquisitions, or 0.01 s, each of these raw spectra are nearly 1:1 combinations of the actual spectra for the separate components. Spectra extracted for the peaks by deconvolution are shown in Figures 3-7A-B. Even though the elution profiles are almost completely overlapping, the algorithm yields completely acceptable spectra, as shown by comparison with the reference library spectra [3] in Figures 3-7C-D.

Although their retention times are too similar to allow their determination by scanning mass spectrometers, major differences in the mass spectra of benzene and cyclohexane allow these compounds to be easily identified. Extraction of the pure mass spectra for these compounds is simplified by their lack of shared m/z values. This study reveals the capabilities of our

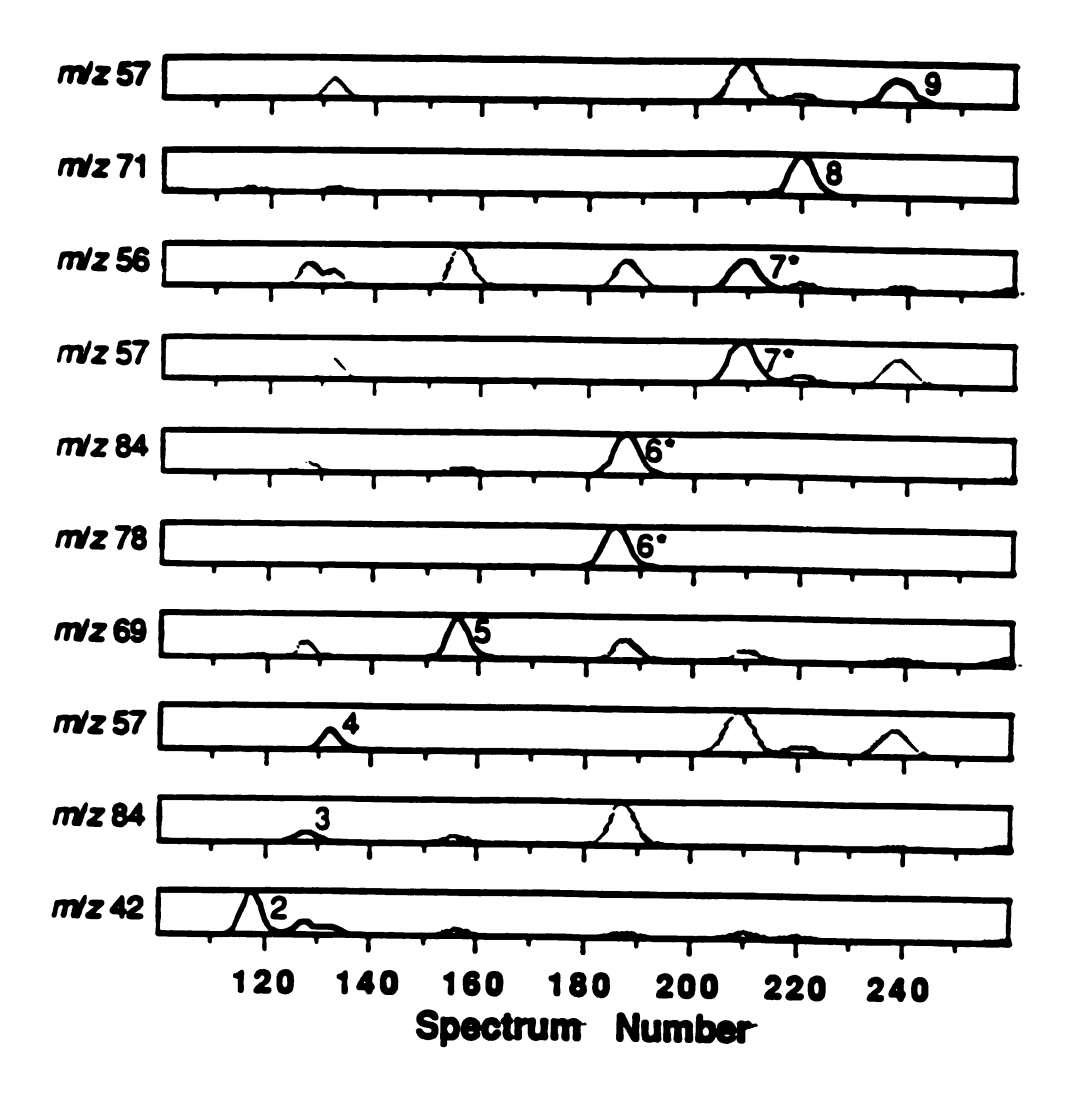


Figure 3-5. Unique-mass chromatograms identified for peaks 2-9 of the hydrocarbon mixture.

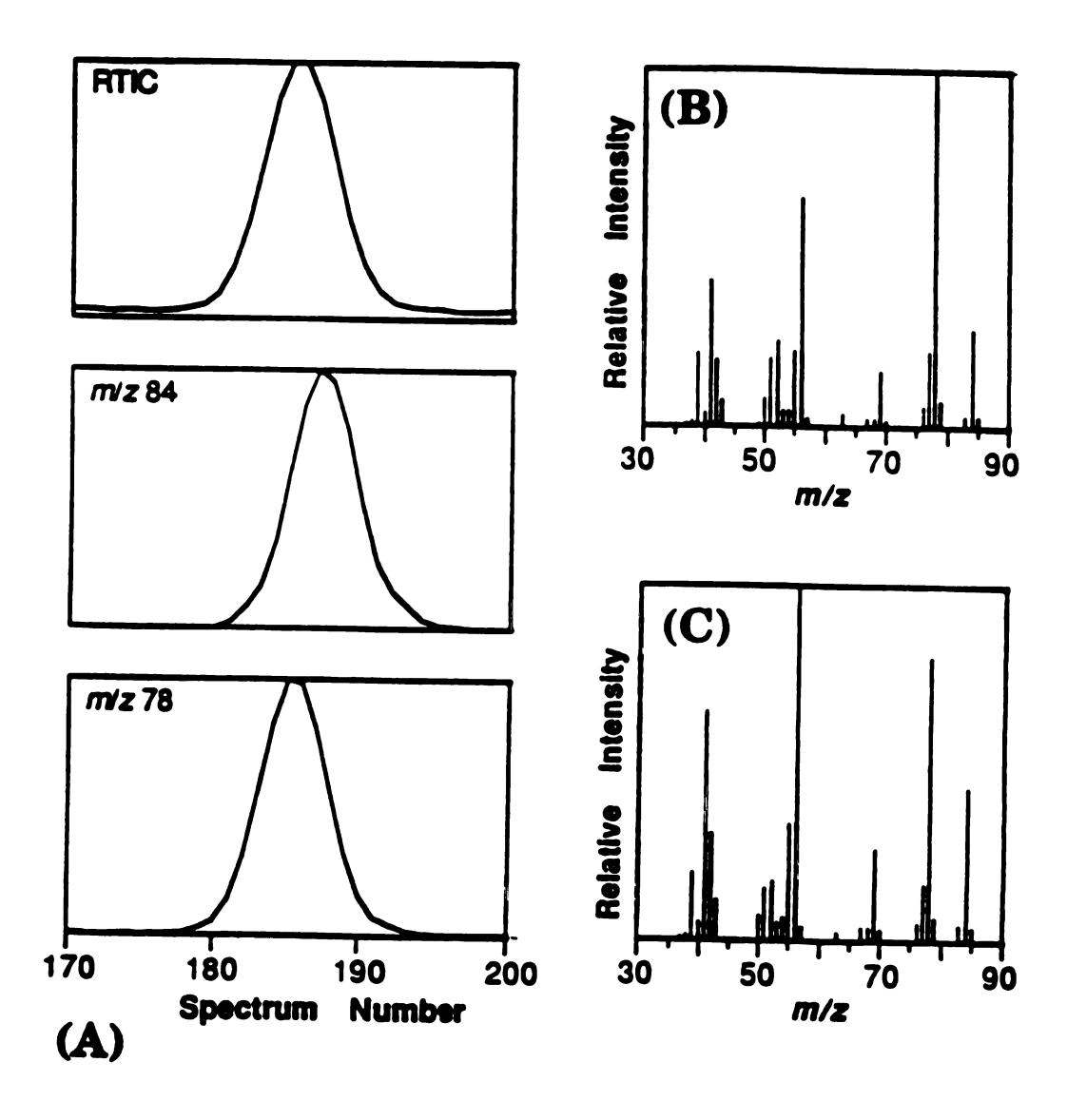


Figure 3-6. Expanded view of peak 6 from the hydrocarbon mixture showing the RTIC and unique-mass chromatograms (A). Raw mass spectra #185 (B) and #187 (C) correspond to the apices of the unique-mass chromatograms.

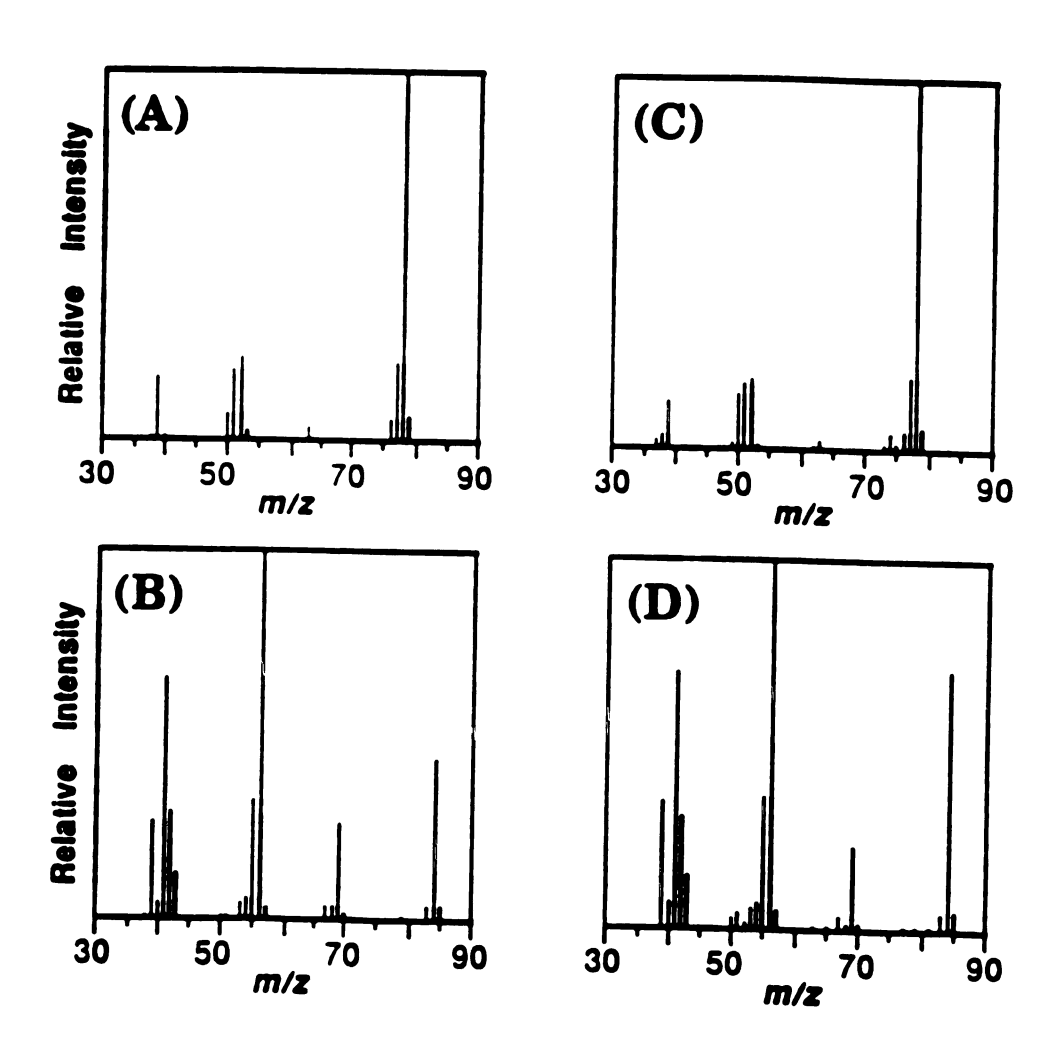


Figure 3-7. Deconvolved spectra for benzene (A) and cyclohexane (B) obtained from peak 6 of the hydrocarbon mixture. Reference spectra are shown for comparison (C, D).

deconvolution approach for locating unresolved components with distinctive spectral features at nearly equal concentrations.

3.5 Dynamic Range Studies

In order to explore the practical limits for deconvolution of minor component spectra from those of major components, a series of binary mixtures having different concentration ratios were analyzed. Mixtures of tert-butylbenzene and 1,2,4-trimethylbenzene were prepared in methanol at relative concentration ratios of 1:5, 1:1, and 50:1 and run through the GC under conditions where the two analytes nearly coelute. The mass chromatograms obtained for masses unique to these two compounds are shown in Figures 3-8A-C. Note that the peak for m/z 134 has an intensity of only about 20% in the tert-butylbenzene spectrum, but m/z 105 is the base peak of the 1,2,4-trimethylbenzene spectrum. Assuming similar ionization and fragmentation efficiencies, the unique-mass intensity ratios thus range from 1:25 to 10:1 as the concentration ratios range from 1:5 to 50:1. Spectra for the two compounds were obtained by deconvolution at each of the three concentration ratios. The resulting spectra are shown in Figures 3-9A-H together with spectra obtained from injection of the pure compounds. Acceptable spectra were obtained over the entire concentrationratio range, except for the loss of the m/z 119 ion in the 50-fold dilution of 1,2,4trimethylbenzene.

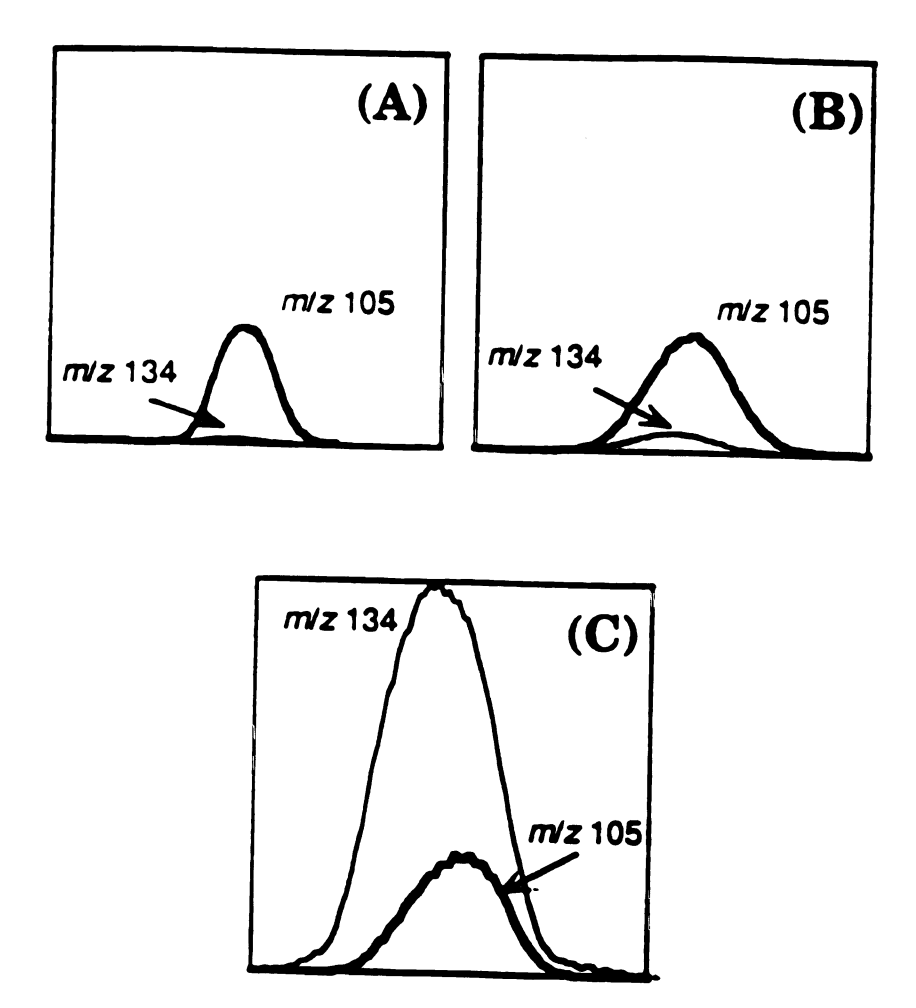


Figure 3-8. Unique-mass chromatograms for the dynamic-range study.

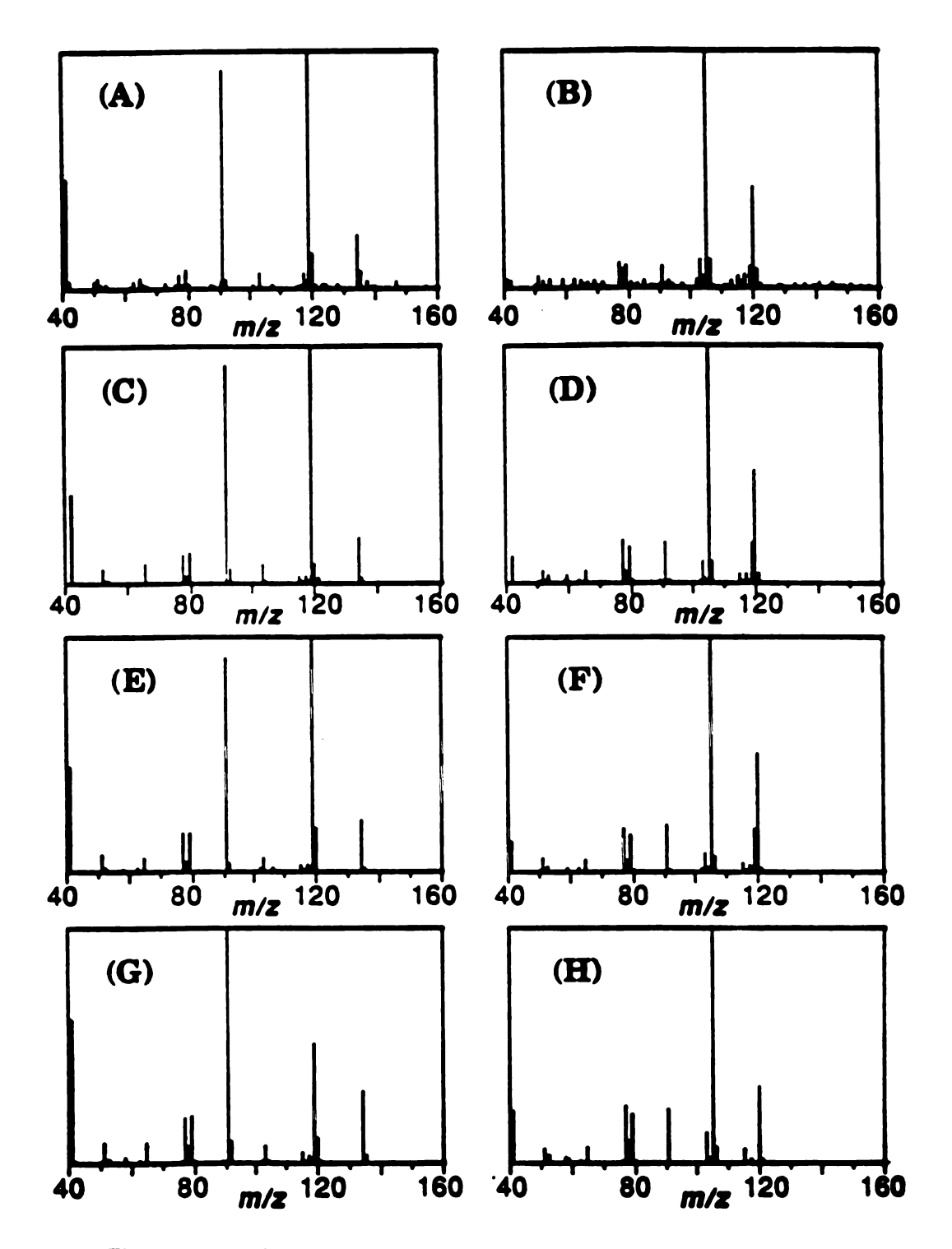


Figure 3-9. Mass spectra of *tert*-butylbenzene and 1,2,4-trimethylbenzene obtained from pure samples (A,B) and from deconvolution of binary mixtures having concentration ratios of 1:5 (C,D), 1:1 (E,F), and 50:1 (G,H).

This study was a rigorous test of the deconvolution approach. The algorithms had to not only locate unresolved species and allocate the intensities of many shared m/z values over a significant range of concentrations. The use of real experimental data shows the capabilities of the deconvolution approach in relatively difficult circumstances.

3.6 Summary and Future Work

Mass spectral deconvolution of chromatographically unresolved components has been attempted by many researchers following the seminal paper of Biller and Biemann. Despite these studies, however, automated spectral deconvolution in GC/MS has not become routine. The promising results shown here result not from any fundamental breakthrough in deconvolution algorithms but rather by the abundance and fidelity of data provided by TOFMS/TAD. Although this approach does not represent the pinnacle of deconvolution, it shows the power of deconvolution approaches and their potential role in chromatography/MS analysis.

Although this deconvolution approach is powerful, it also has several areas that should be improved to make real-time deconvolution a reality. The first of these is the method used for MCPPP generation. The Biller-Biemann approach is effective, but has resolution of ± 1 scan. A derivative approach such as that used by Anderegg [4] can improve the compound resolution to a fraction of a scan. The derivative approach is also more amenable to use with digital

			'
			į
			,
			•
			;
			:
	·		:

signal processors (DSPs) than the present approach. This would permit generation of the MCPPP in real-time. MCPPP interpretation is the most difficult step in the deconvolution of unknowns. Each MCPPP response must initially be presumed to result from a different compound. A variety of factors can be examined to determine the best means of locating shared and pure m/z values. These include the peak widths and shapes of mass chromatograms. Another limitation of this approach is the use of the cross-correlations to generate factors which are, in turn, used to generate the mass spectrum of pure compounds. This cross-correlation approach is a simple trick whose mathematical basis is questionable. The success of this mass spectral extraction technique lies partially in the algorithms used for library-searches. The presence of a m/z value in a mass spectrum is considered more important than its intensity by many library-search algorithms [5]. Thus, properly assigning a m/z value to the mass spectrum of a compound is more important than having the correct intensity. Other mass spectral extraction approaches such as factor analysis should be investigated to improve the accuracy of the "pure" mass spectra generated by the deconvolution approach.

References

- 1. Biller, J. E.; Biemann, K. Anal. Lett. 1974, 7, 515-528.
- 2 Savitzky, A.; Golay, M. Anal. Chem. 1964, 36, 1627-1639.
- 3 NIST/EPA/MSDC Mass Spectral Database, PC Version 3.0, National Institute of Standards and Technology, Gaithersburg, Maryland.

- 4. Ghosh, A.; Anderegg, R. J. Anal. Chem. 1989, 61, 73.
- 5. Crawford, L. R.; Morrison, J. D. Anal. Chem. 1968, 40, 1464.

Chapter 4

Time-Compressed Gas Chromatography/Mass Spectrometry: Fifty-Two Compounds in Eighty Seconds

4.1 Introduction

The basis of high resolution gas chromatography/mass spectrometry is the chromatographic separation of components in a mixture. The speed of analysis is determined by the time required for the optimum chromatographic separation; the mass spectrometer functions simply as a detector. In practice, the ability to accurately identify unknown components, having overlapped elution profiles, by means of deconvolution techniques actually decreases the need for optimum chromatographic separation if many mass spectra are acquired across the elution profile of a compound. As long as a component possesses at least one distinctive data channel in its mass spectrum, it may be identified and accurately quantified. Chromatographic analysis times can often be greatly reduced while still providing enough separation to meet this criterion. We call this approach time-compressed chromatography. Time-compression of GC/MS data is attained by combining "high-speed chromatography" with high mass spectral acquisition rates. The use of deconvolution techniques requires

differences on only one of the several hundred available data channels to discern the presence of even an unknown component.

The greatest reductions in analysis time are achieved by eliminating excess chromatographic resolution via a shorter length of column and/or faster carrier gas linear velocity. Taking advantage of the vacuum outlet of the column, the chromatographic conditions can be adjusted to provide the best separation per unit of time [1,2]. Because shorter columns produce narrower elution profiles [3], rapid mass spectral acquisition rates are needed to provide a minimum of ten data points across the elution profile of each component. The contribution of inlet variance which becomes greater when operating at high linear velocities can be decreased by using specialized injection techniques to further reduce peak widths [4-7].

For this study, we chose to treat the mixture as an unknown and use no specialized techniques for reducing injection variance. Thus, we separated the sample using low-resolution high-speed chromatography with rapid mass spectral detection. Deconvolution techniques were then employed to resolve compounds that were not separated by the chromatography. Further decreases in analysis time should be attained if the sample is analyzed using target compound analysis and better sample introduction methods. As demonstrated here, analysis times can be reduced by an order of magnitude or more without a reduction in the quantity or quality of information provided even for this worse case scenario.

4.2 Experimental

4.2.1 Sample Preparation.

A 61-component mixture of volatile organic compounds (Ultra Scientific) was used in all of these analyses. The concentration of each component (see Table 4-1) in the methanol solvent was 200 µg/mL. Although this sample was designed to be used as a standard for a purge-and-trap method (EPA Method 524.2), the sample was injected directly into the gas chromatograph.

4.2.2 Gas Chromatography.

A 5890A gas chromatograph (Hewlett-Packard, Inc.) equipped with a 5% phenyl dimethyl silicone capillary column was used for all analyses. Two columns of different physical dimensions were used in these experiments. In either case the column was interfaced directly into the ion source of the mass spectrometer. The injector and transfer line temperatures were always held at 200°C. The split ratio of the gas chromatograph and injection volume were adjusted so that about 100 pg of each component were placed onto the chromatographic column.

The 30-minute analysis was performed using a 25 $m \times 0.2$ mm i.d. Ultra II column with a 0.33- μm film (Hewlett-Packard, Inc.). The linear velocity of the helium carrier gas was 26 cm/s. Oven conditions were optimized to

Table 4-1. The 61 Compounds in the Test Mixture.

- 1. Dichlorodifluoromethane
- 2. Chloromethane
- 3. Trichlorofluoromethane
- 4. 1.1-Dichloroethene
- 5. Vinyl Chloride
- 6. Bromomethane
- 7. Chloroethane
- 8. Dichloromethane
- 9. 1,1-Dichloroethane
- 10. cis-1,1-Dichloroethene
- 11. trans-1,1-Dichloroethene
- 12. Bromochloromethane
- 13. 2,2-Dichloropropane
- 14. Chloroform
- 15. 1,1,1-Trichloroethane
- 16. 1,2-Dichloroethane
- 17. 1,1-Dichloropropene
- 18. Carbon Tetrachloride
- 19. Benzene
- 20. 1,2-Dichloropropane
- 21. 1,3-Dichloropropane
- 22. Trichloroethene
- 23. Dibromomethane
- 24. Bromodichloromethane
- 25. cis-1,3-Dichloropropene
- 26. trans-1,3-Dichloropropene
- 27. Toluene
- 28. 1,1,2-Trichloroethane
- 29. Ethylbenzene
- 30. Chlorodibromomethane
- 31. 1.2-Dibromomethane

- 32. Tetrachloroethene
- 33. Chlorobenzene
- 34. 1,1,1,2-Tetrachloroethane
- 35. m-Xylene
- 36. p-Xylene
- 37. Bromoform
- 38. Styrene
- 39. o-Xvlene
- 40. 1,1,2,2-Tetrachloroethane
- 41. 1,2,3-Trichloropropane
- 42. Isopropylbenzene
- 43. Bromobenzene
- 44, 2-Chlorotoluene
- 45. n-Propylbenzene
- 46. 4-Chlorotoluene
- 47. 1,3,5-Trimethylbenzene
- 48. tert-Butylbenzene
- 49. 1,2,4-Trimethylbenzene
- 50. 1,3-Dichlorobenzene
- 51. 1,2-Dichlorobenzene
- 52. sec-Butylbenzene
- 53. 4-Isopropyltoluene
- 54. 1,4-Dichlorobenzene
- 55. n-Butylbenzene
- 56. 1,2-Dibromo-3-Chloropropane
- 57. 1,2,4-Trichlorobenzene
- 58. Napthalene
- 59. 1,3,5-Trichlorobenzene
- 60. Hexachlorobutadiene
- 61. 1,2,3-Trichlorobenzene

chromatographically resolve as many of the 61 components as possible using the chosen stationary phase. In this case, the oven temperature was initially held at 10°C for 3 minutes and then programmed to 130°C at 4°C/minute.

The 80-second analysis was performed using a 3 m \times 0.1 mm i.d. DB-5 column with a film thickness of 0.4 μ m (J&W Scientific, Inc.). Oven conditions for these analyses were optimized to provide the maximum chromatographic resolution in the run without increasing the analysis time. The linear velocity of the helium carrier gas was set to 88 *cm/s* and the oven temperature was ramped from 60°C to 130°C at 50°C/minute.

4.2.3 Mass Spectrometry

The time-of-flight mass spectrometer used for this work has been described in Chapter 2 of this thesis. Analyte ions are accumulated in the source during the period between ejection pulses. Every 333 µs, the ions are pulsed out of the source. The ions are accelerated into the field-free flight tube, reflected by the mirror, and detected by a dual multichannel plate detector. Time-array detection is performed using an integrating transient recorder [8]. For this analysis, 300 and 100 consecutive transients were summed to produce 10 and 30 spectra per second for the initial and time-compressed analyses, respectively.

4.2.4 Deconvolution Approach

The deconvolution algorithm used in this analysis is described in Chapter 3 of this thesis. A mass chromatogram peak position plot (MCPPP) was generated by determining the retention time for each mass chromatogram. The information contained in the MCPPP and individual mass chromatograms was used to determine the number of components present in the region of interest. A characteristic m/z value, shared by no other compound, was used to determine the mass spectrum of each coeluting compound via the cross-correlation approach.

4.3 Results and Discussion

We chose to test the concept of time-compressed chromatography and the capability of our instrumentation to perform it with a commonly used commercial test mixture of 61 volatile compounds (Table 4-1). The mixture of volatile organic compounds contains over twenty pairs of isomers with similar or identical mass spectra. Many of the compounds in this mixture, including several sets of these isomers, are difficult to resolve chromatographically. This mixture was analyzed with and without time-compression to determine the minimum attainable analysis time and to determine the limitations imposed by the presence of so many isomers.

4.3.1 GC/MS Analysis Optimized for Component Separation

The mixture was first analyzed under typical high-resolution GC/MS conditions to provide a basis for comparison. The linear velocity of the carrier gas and the temperature program were adjusted to yield optimum chromatographic separation of the components in the mixture. A data acquisition rate of 10 spectra per second was used to obtain at least ten mass spectra for each eluting component. The results of this 30-minute analysis are shown in the reconstructed total-ion current (RTIC) chromatogram contained in Figure 4-1. The high data acquisition rate better defines the elution profiles and allows more accuracy in determining component retention times and areas than is attainable using the slower data acquisition rates available on commercial mass spectrometers.

Even under these conditions, not all of the components in the mixture are chromatographically resolved. Methanol, present as a solvent in the mixture, prevents the identification of components 1-7 in Table 4-1. Several other components have overlapping elution profiles (compounds 9-10,11-12,18-19, 21-22, 33-34, 35-36 and 38-39 in Table 4-1). Some of these coeluting species may be resolved by unique ion identification aided by spectral subtraction since the spectrum obtained from any point in the elution profile is unskewed (for example, compounds 31 and 32 in Table 4-1). Other coeluting compounds, such as the xylenes (compounds 35, 36 and 39 in Table 4-1), are isomers and

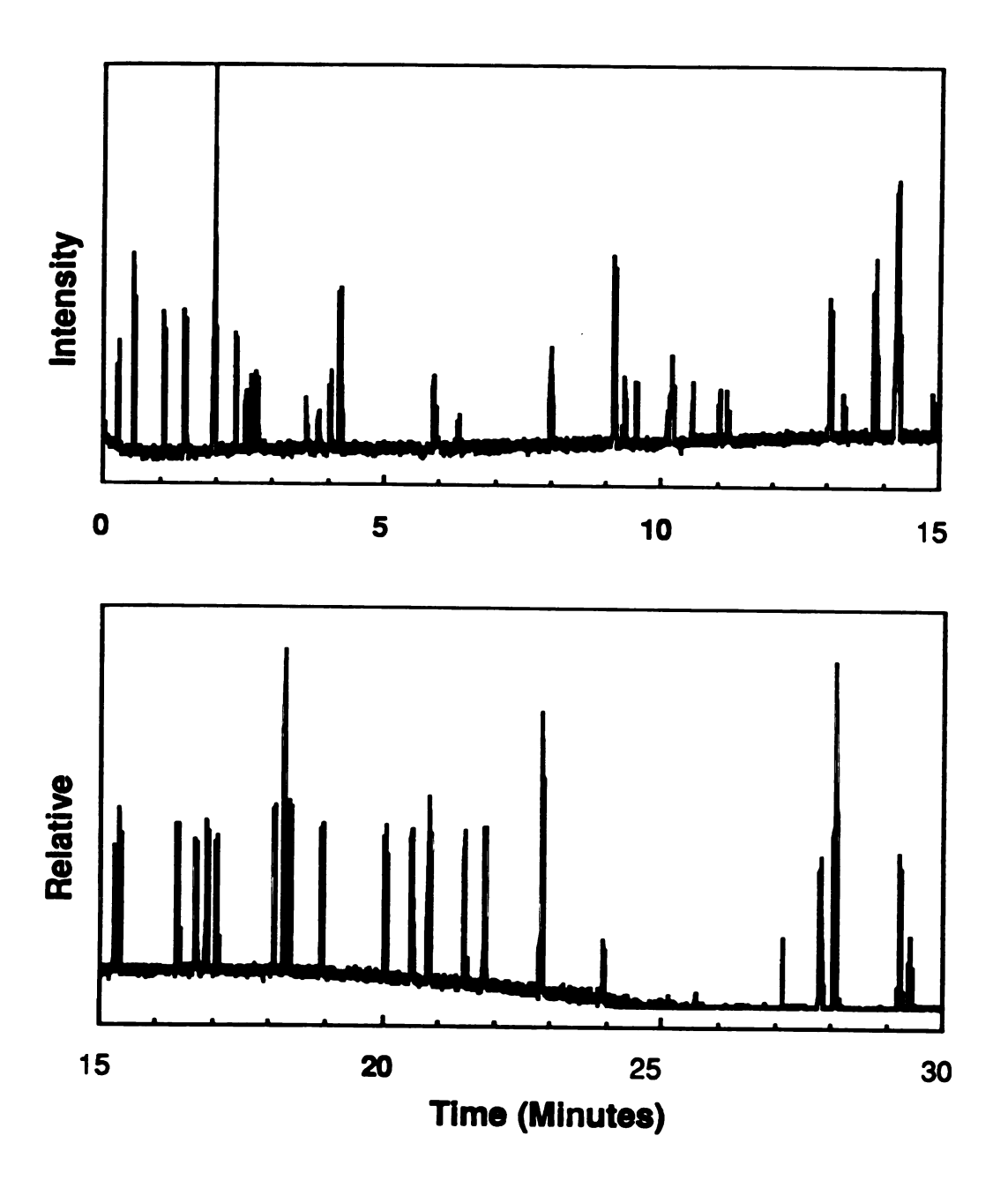


Figure 4-1. Reconstructed total-ion current chromatogram (RTIC) of a 61-component mixture acquired in 30 minutes on at a rate of ten spectra per second. Two hundred picograms of each component were separated on a 25-m length of 0.2-mm I. D. Ultra II fused silica column having a 0.33- μm film thickness.

possess similar mass spectra. These compounds must be chromatographically resolved to be successfully identified.

4.3.2 Analysis of the Sample by Time-Compressed Chromatography

The time required for the chromatographic separation was reduced by using a short length of column and a rapid GC temperature-program. The RTIC chromatogram obtained when the 30-minute run was reduced to 80 seconds is shown in Figure 4-2. Thirty spectra were acquired each second to ensure the acquisition of at least 10 mass spectra while each component elutes from the column. The resolving power for this analysis is comparable to that of a packed-column GC.

The nature of the data obtained and the method of analysis employed is illustrated by the 14-second segment of the 80-second run is shown in Figure 4 - 3. The retention times of individual components are determined from the overlaid Mass Chromatogram Maximum Peak Position Plot (MCPPP) [11]. This plot shows the sum of the peak intensities for m/z values that maximize during each acquired spectrum. Since the MCPPP is simply a plot of the retention times of all of the mass chromatograms, each MCPPP line indicates the possible elution of a component. Examination of the MCPPP reveals multiple responses rather than a single response for each eluting compound. These responses result from the effects of noise and the presence of peaks at m/z values that are common to the mass spectra of two or more compounds with overlapping elution

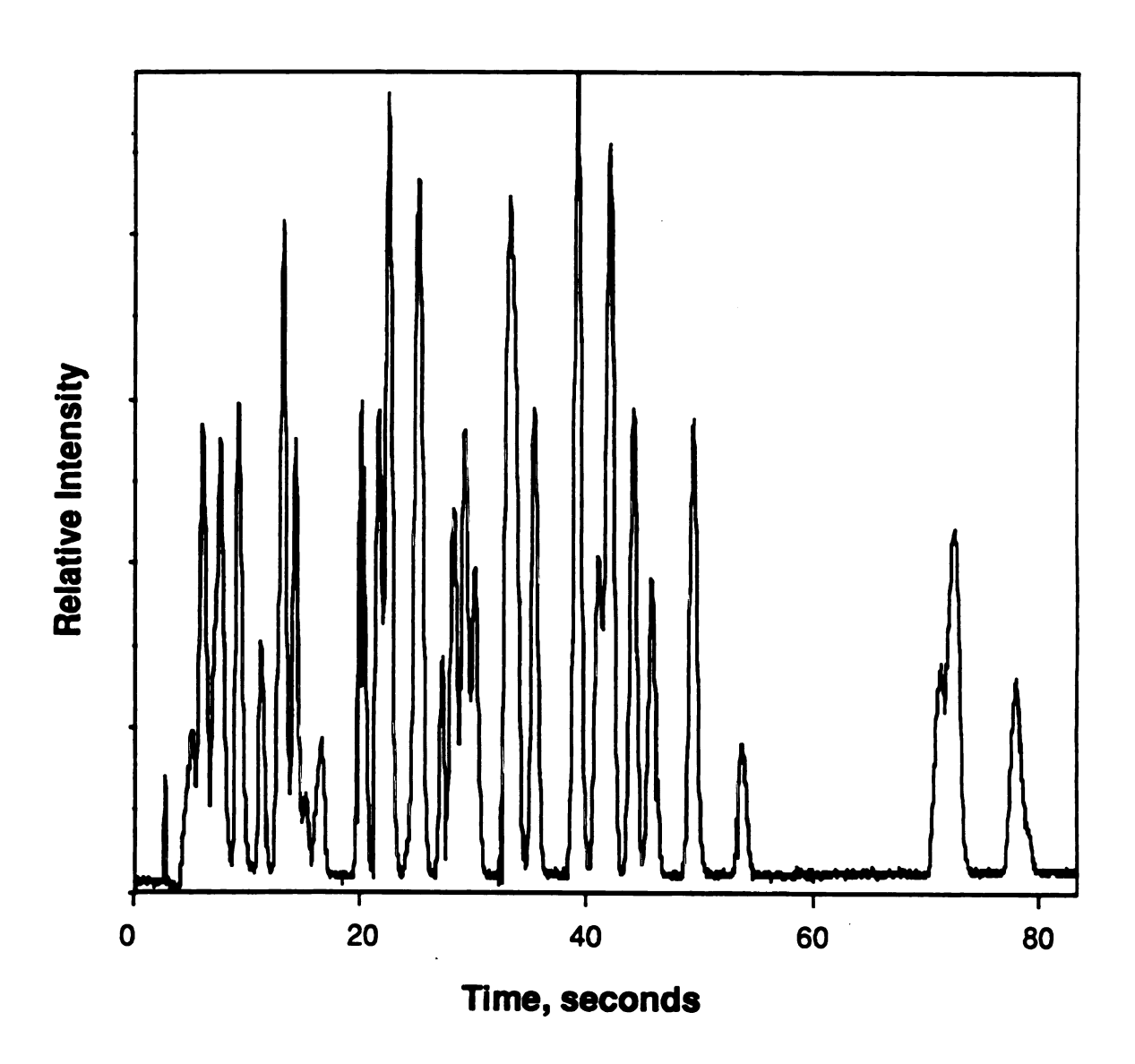


Figure 4-2. Reconstructed total-ion current chromatogram of the same mixture acquired in 80 seconds collecting 30 spectra per second. A 3-m length of 0.1 mm I. D. DB-5 column with 0.4- μ m film thickness was used.

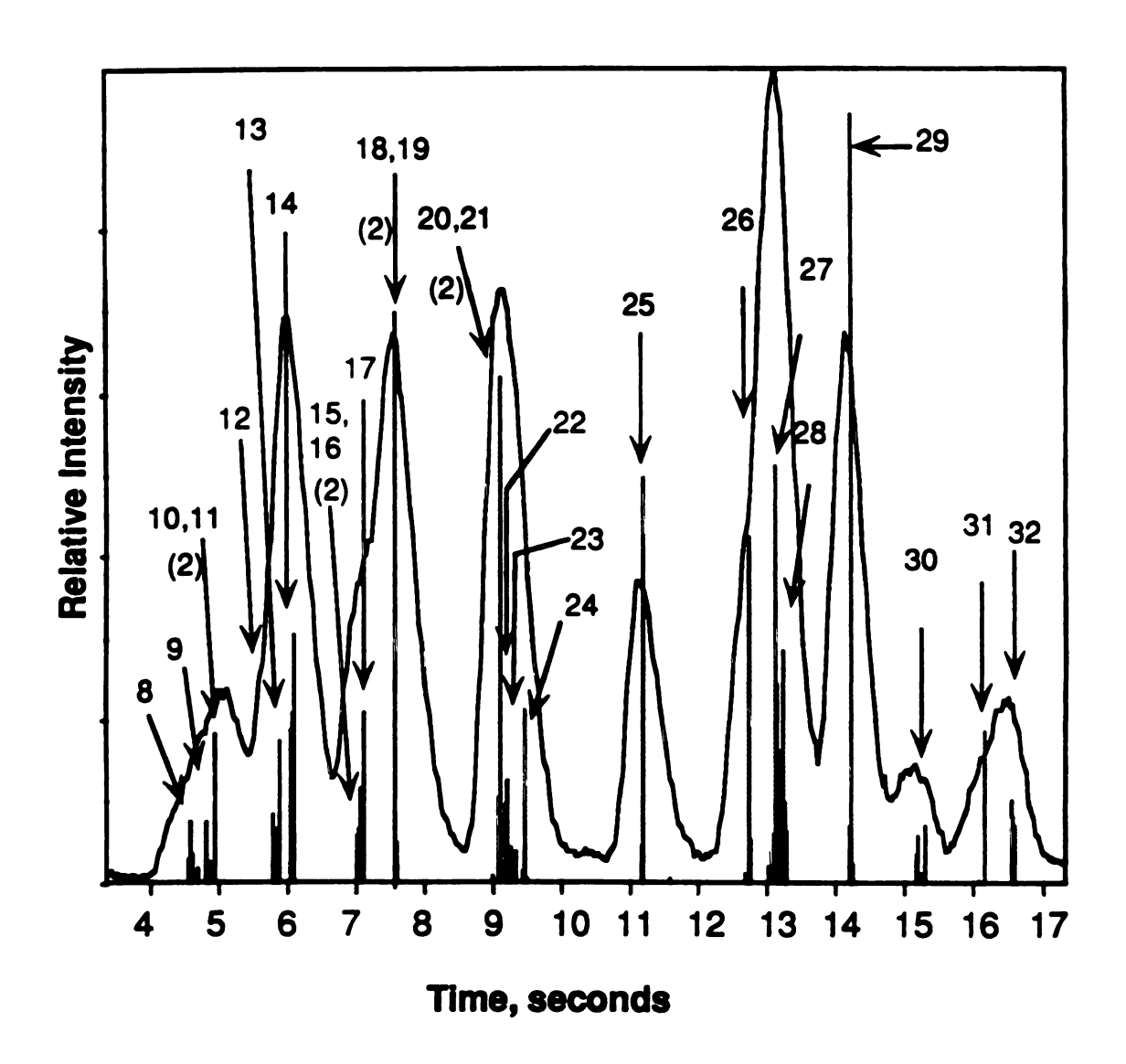


Figure 4-3. Fourteen seconds of the RTIC in Figure 2 with the times where individual mass chromatograms maximized indicated by the mass chromatogram peak position plot (MCPPP). The 24 compounds present in this region are indicated by their elution order number from Table 4-1 with an arrow to indicate their retention time. Where two compounds exactly coelute, a (2) is placed by the arrow.

profiles. Noise effects manifest themselves by splitting the response for a single compound over more than one "scan" or via small responses that do not correlate with the retention time of any compound. These can be located by examining mass chromatograms at the appropriate retention times. When coeluting compounds contain ions with the same m/z value, the shared m/z values will have a retention time that is between that of the coeluting compounds. The actual retention time of each shared mass is determined by the relative concentrations of the coeluting compounds and the intensity of the response for a given shared m/z value in each compound. Once the correct mass chromatograms have been examined, the MCPPP interpretation was corrected for these artifacts. The actual retention times of the mixture's components were known. Their mass spectra were determined using mass spectral deconvolution strategies. The 24 compounds that elute in the 14-second region shown in Figure 4-3 are numbers 8-32 in Table 4-1.

In all, 52 of the 61 components in the mixture were identified. Compounds 1-7 were not observed because they coeluted with the solvent. If the mixture was analyzed using the purge-and-trap technique specified by the EPA protocol, these components would be easily identified since there are significant differences in their mass spectra. Four pairs of compounds, benzene/carbon tetrachloride, 2-chlorotoluene/4-chlorotoluene, 1,2-dichloropropane/1,3-dichloropropane and ethylbenzene/xylene eluted simultaneously, which prevented their distinction by direct deconvolution; our approach requires the presence of a unique m/z value for each coeluting compound. The spectra

obtained during their elution were those of a mixture of the two compounds. The latter three pairs of coeluting compounds must be chromatographically resolved due to the similarity of their mass spectra. Spectral matching software and principal component analysis can, in some cases, unravel simple mixtures from their mixed spectra [9]. This task is, of course, greatly simplified if the list of compounds expected or sought is limited [targeted analysis). While identifying 52 of the 61 compounds, a number of distinct and interesting situations were encountered. These are discussed separately in the following sections.

4.3.3 Adequate Chromatographic Resolution

The first and simplest case occurs when the GC separation chromatographically resolves one component from all others in the sample. This is illustrated in the 4.67-second segment of the 80-second analysis shown in Figure 4-4. Since 1,1,2,2-tetrachloroethane, 1,2,3-trichloropropane, isopropylbenzene and bromobenzene are resolved chromatographically, the data do not require deconvolution. For these compounds, there was no difference between a single spectrum acquired at any point in the elution profile and a spectrum obtained via deconvolution. All spectra were readily recognized when compared with library spectra.

The overlaid MCPPP in Figure 4-4 shows the retention time of each component and reveals that there are no other components present in this region. Spurious MCPPP responses (adjacent to the major responses) resulted

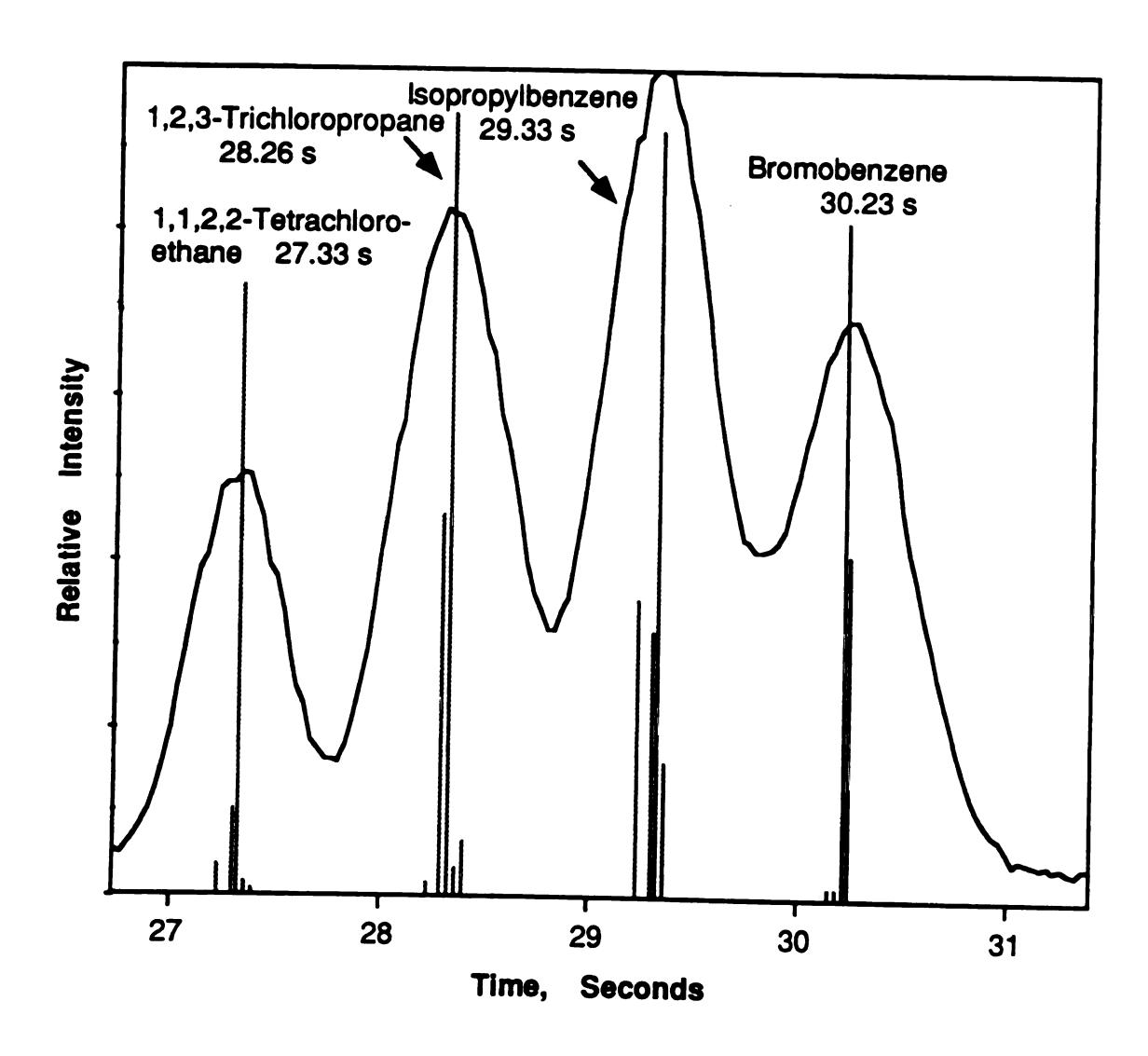


Figure 4-4. Overlay of the MCPPP on the elution profile for partially chromatographically resolved components.

from the method used to obtain the peak positions in the individual mass chromatograms, noise in the mass chromatographic data and instrument anomalies. Component peaks that maximize at times between consecutive spectra often result in individual mass chromatograms that maximize at the spectrum either before or after the actual elution maxima. Examination of the appropriate mass chromatograms reveals these effects. An intensity change in the RTIC of the isopropylbenzene response resulting from a data point lacking intensity values for a portion of the mass range was responsible for the most intense, spurious MCPPP response at 29.2 s in Figure 4-4.

4.3.4 Poor Chromatographic Resolution of Compounds with Similar Spectra

A second and more complex situation exists with the coelution of two components with similar retention times and mass spectra. The RTIC chromatogram of the 2.3-second region where *tert*-butylbenzene and 1,2,4-trimethylbenzene elute is shown in Figure 4-5. These two compounds, possessing similar mass spectra, have retention times that differ by only 0.13 seconds. These retention times are so close that nothing in the shape of the RTIC elution profile would indicate that this band represents more than one component. However, each compound has an intense mass spectral peak at an m/z value not shared by the other. The molecular ion of tert-butylbenzene (m/z 134) and the [M-15]+ fragment of 1,2,4-trimethylbenzene (m/z 105) are unique to the mass spectrum of each compound. Although the MCPPP is complicated by

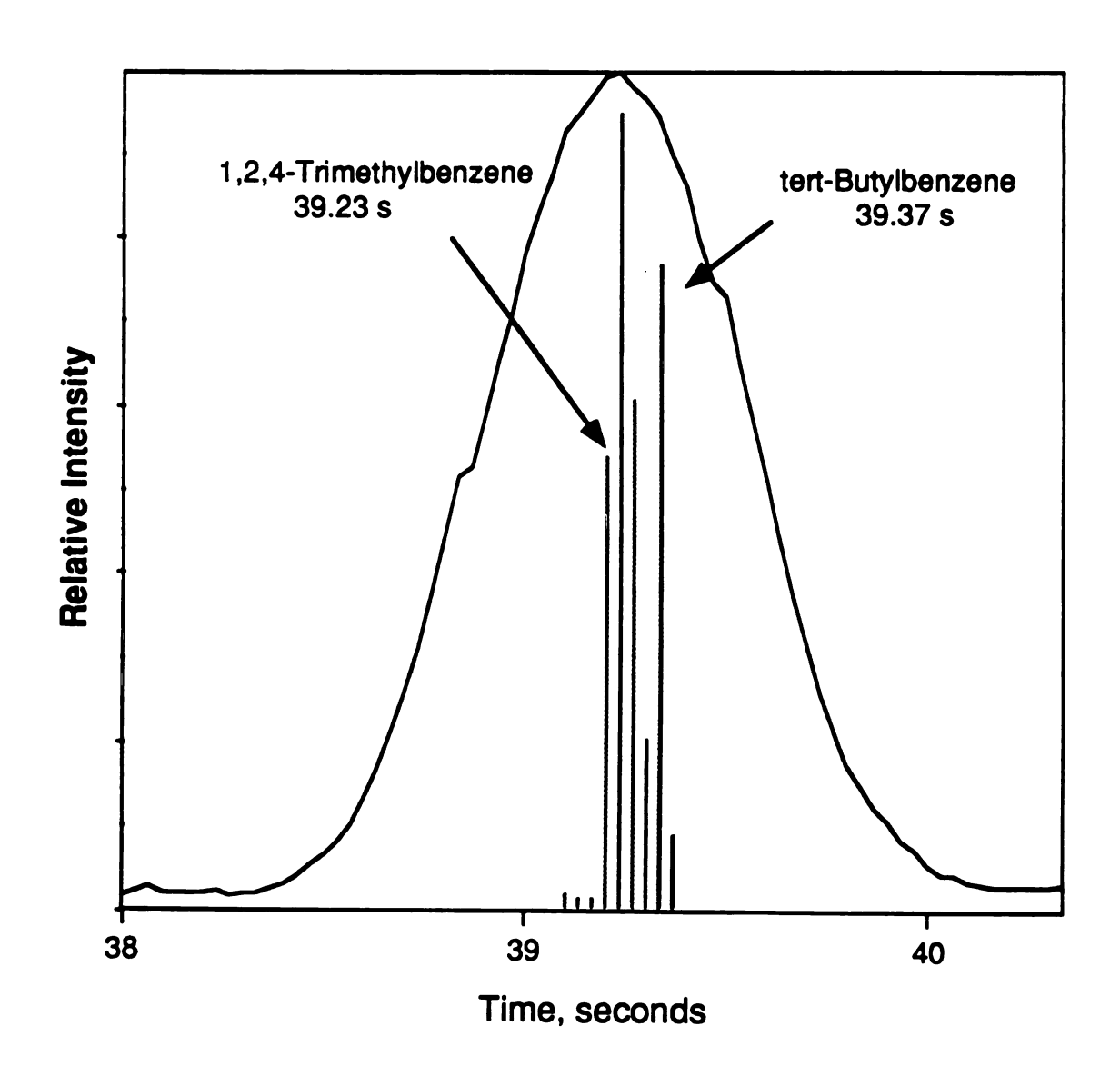


Figure 4-5. An overlay of the MCPPP on the elution profile for two coeluting species—tert-butylbenzene and 1,2,4-trimethylbenzene.

the many shared m/z values and the effects of noise, the time difference at which the mass chromatograms of m/z 134 and m/z 105 maximized was greater than experimental error, suggesting the presence of multiple components with similar mass spectra. This is confirmed by comparing the library spectra in Figure 4-6. The two mass spectra share many similarities. Among these are the presence of many fragments resulting from the aromatic ring and the loss of a methyl group.

Although the spectra obtained by deconvolution of the overlapped peaks compare favorably to the library spectra (Figure 4-6), the effects of noise on the deconvolution algorithm are apparent in the loss of several low intensity peaks. Using slightly different chromatographic conditions, this same pair of components was resolved and a pure matchable spectrum of each component was obtained when the retention times of the two compounds were only two spectra apart (0.07 seconds). These two compounds were identified and could be quantitated in the presence of each other with a chromatographic resolution of less than 0.2 as compared to the 0.7 normally required to quantify on the basis of height when using non-selective detectors with GC [10].

4.3.5 Overlap of More Than Two Compounds.

Although the majority of the observed elution bands are composed of one or two components, a few regions contain three components. In the 2.67-second region shown in Figure 4-7, bromoform appears as a slight shoulder on the

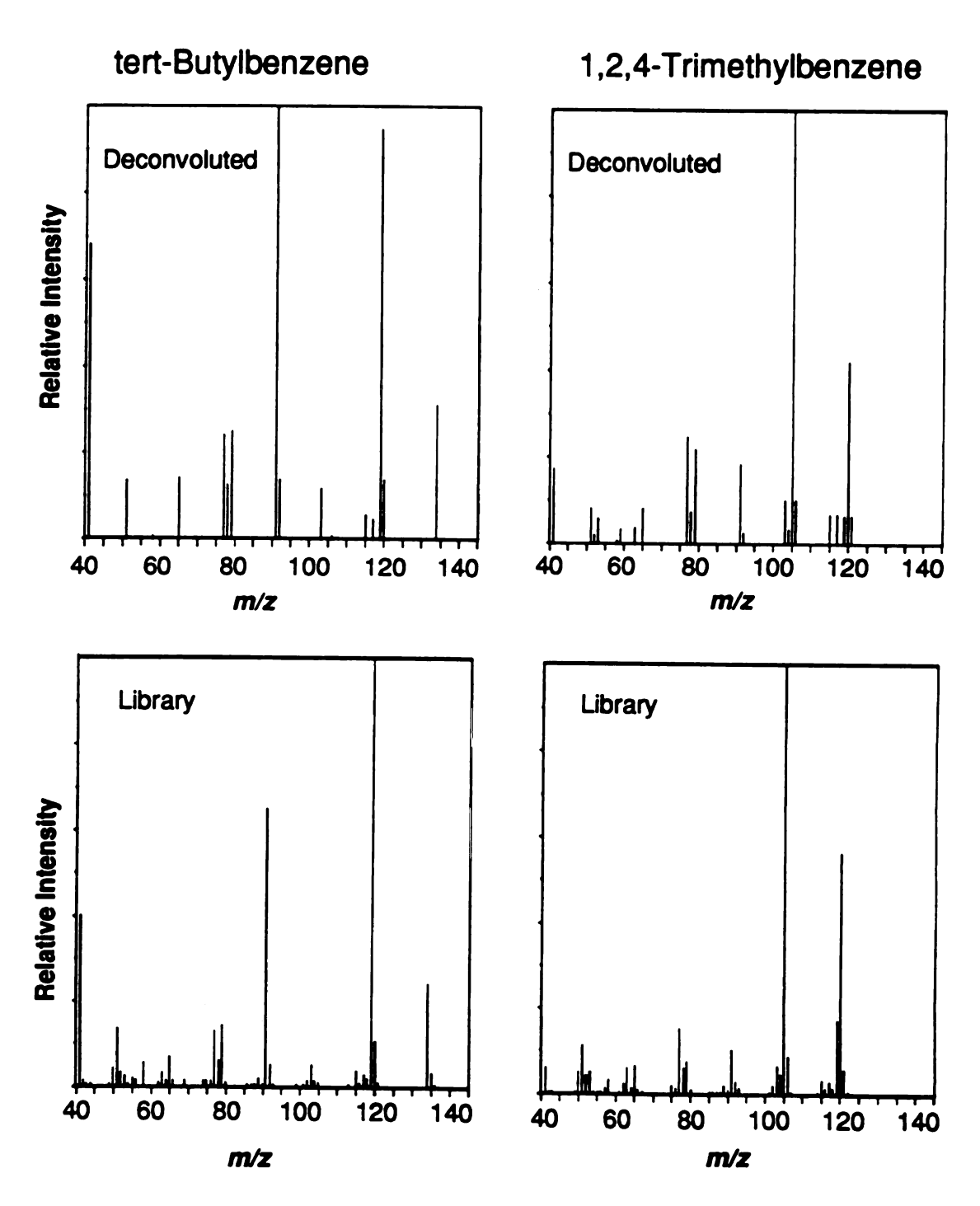


Figure 4-6. Comparison of the deconvoluted spectra for *tert*-butylbenzene and 1,2,4-trimethylbenzene with their respective library spectra.

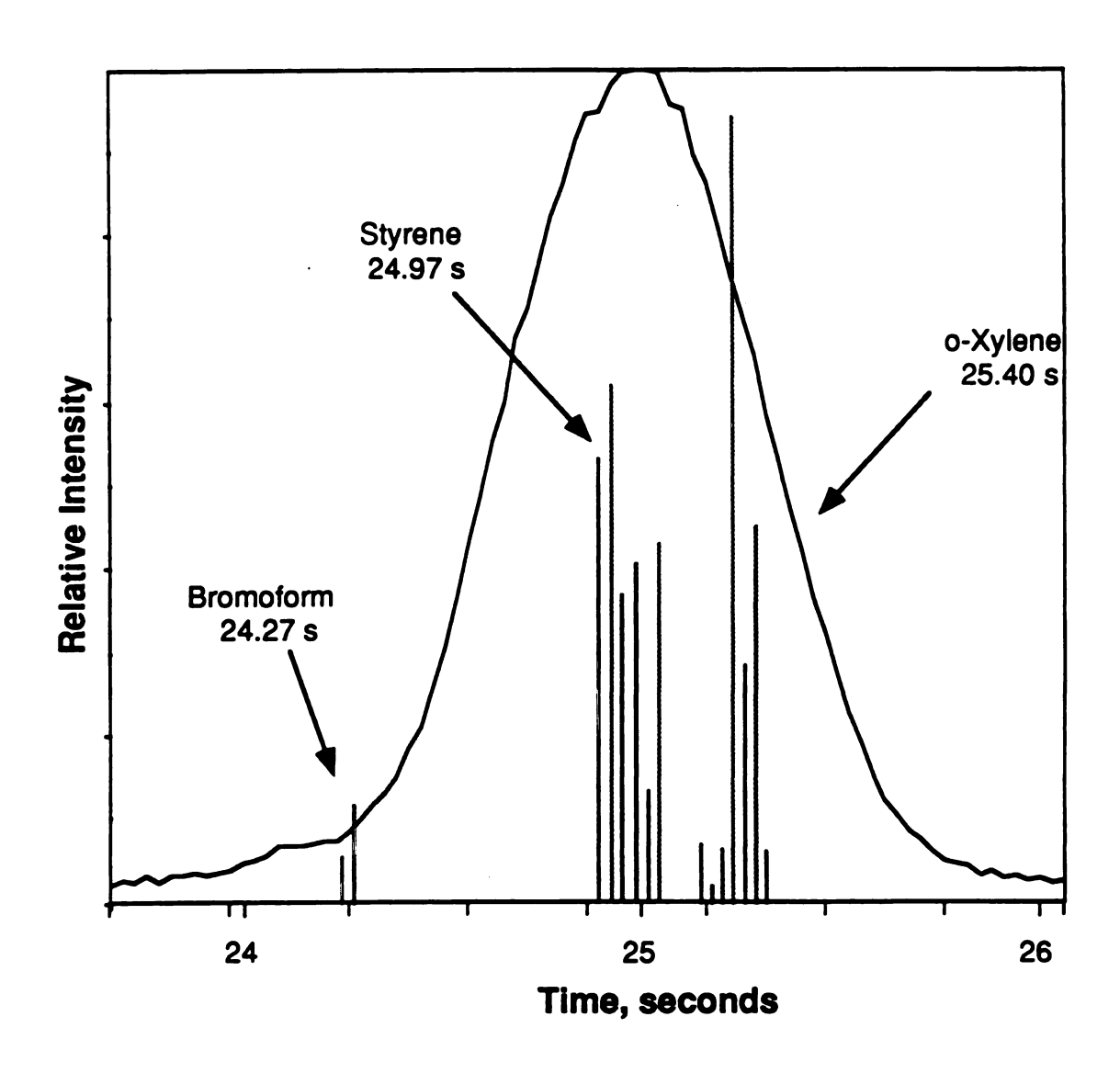


Figure 4-7. Overlay of the MCPPP on the elution profile for bromoform, styrene and o-xylene whose mass chromatograms maximize at 24.33, 24.97 and 25.40 seconds respectively.

leading edge of the elution profile. Despite the low-intensity response, the MCPPP clearly indicates the presence of a component. The remaining compounds in this region, styrene and o-xylene, are easily differentiated on the basis of their mass spectra. Although the deconvolution is capable of resolving more than three components, three was the most encountered in this analysis.

4.3.6 Quantitation

Once a compound has been identified by high resolution GC/MS, it can be quantified in either of two ways. If the compound is chromatographically baseline-resolved from all other compounds, quantitation can be based on the RTIC profile. If the sample is not completely resolved from other species, the mass chromatogram for a unique molecular or fragment ion is typically the basis for quantitation. When time-compressed chromatography is performed, one of the steps in the generation of the MCPPP is the determination of those m/z values that are not shared among the coelutants. The intensities from the mass chromatograms for all those m/z values unique to a given compound can then be summed to more accurately determine a response related to that compound. Quantitation may then be performed by comparing the unknown response with that of an internal or external standard.

4.3.7 Limitations

Time-compressed GC/MS possesses most of the same instrumental limitations as normal GC/MS. The maximum mass spectral acquisition rate allowed by the mass spectrometer and data system is a major limiting factor. Deconvolution, when using our cross-correlation approach, requires that the elution profiles of two coeluting species do not maximize at the same spectrum number. Therefore, a greater mass spectral acquisition rate coupled with faster chromatography (narrower elution profiles) can further reduce the required analysis time. In our case, for a mass range of m/z 40-200, (due to current ITR limitations) the greatest acquisition rate available for 80 seconds is 30 spectra per second. Thus, we could resolve closely eluting compounds with retention time differences of 0.07 seconds or more. Another hardware limitation is the maximum rate at which the oven of a gas chromatograph can increase temperature. Although isothermal GC analysis is capable of providing a much faster separation, a complex mixture, particularly one whose components possess a wide range of volatilities, may be separated more efficiently when a temperature program is used.

Our approach to deconvolution of mass spectra also places limitations on the attainable speed of analysis. As the degree of similarity in the mass spectra of two compounds increases, the chromatographic resolution also must be increased. The resolution achieved for the separation of two dichlorobenzenes is shown in Figure 4-8. The chromatographic resolution between these two isomers

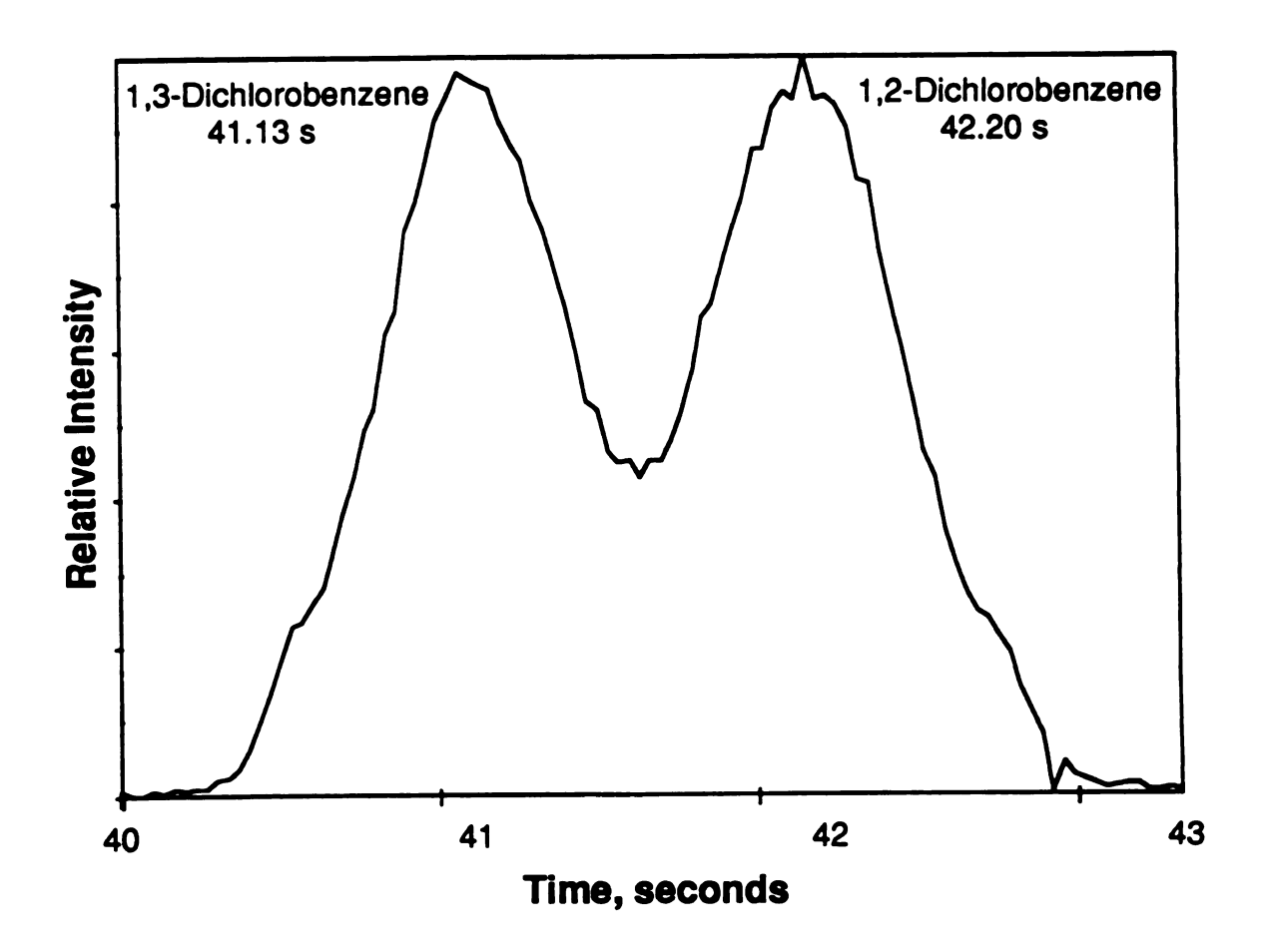


Figure 4-8. Mass chromatogram of m/z 146 reveals that the chromatographic resolution between the two dichlorobenzene isomers is 0.7. Because these isomers cannot be differentiated based on their mass spectra, they must be chromatographically resolved.

; ;

Q.

is 0.7—adequate for identification and quantitation on the basis of peak height [20]. In this example time-compression cannot be significantly extended beyond this point without loss of resolving power.

4.4 Conclusions

Time-compressed chromatography is a powerful tool for greatly reducing the time required for analysis of complex mixtures. The combination of fast data acquisition of unskewed mass spectra and spectral deconvolution allows for dramatic reductions in analysis time using a normal capillary gas chromatograph. The major limitations on the analysis time reduction factor obtainable are the maximum mass spectral acquisition rate at the required detection limits and the necessary chromatographic resolution of mass spectra that contain no unshared m/z values.

In most of the above data analysis and discussion, we have assumed that the complex mixture was of completely unknown composition. However, the aim of many analytical procedures is the quantitation of targeted compounds in samples with a generally predictable list of components. In these situations, time-compression could potentially reduce the required analysis times by even larger factors. With an accurate library of mass spectra and approximate retention times of the sought compounds, overlapping components can be resolved by reverse-search methods and even exactly coeluting components quantitated by principal component analysis.

References

- 1. Giddings, J. C. Anal. Chem. 1962, 34, 314-319.
- Cramers, C.A.; Schutjes, C. P. M.; Leclercq, P. A. J. Chromatogr. 1981, 203, 207-216.
- 3. Yost, R. A.; Fetterolf, D. D.; Hass, J. R.; Harvan, D. J.; Weston, A. F.; Skotnicki, P. A.; Simon, N. A. *Anal. Chem.* **1984**, *56*, 2223-2228.
- 4. Gaspar, G.; Arpino, P.; Guiochon, G. J. Chrom. Sci. 1977, 15, 256-
- 5. Wade, R. L.; Cram, S. P. Anal. Chem. 1972, 44, 131.
- 6. Schutjes, C. P. M.; Cramers, C. A.; Vidal-Madjar, C.; Guiochon, G. in Proc. Fifth Intl. Symposium on on Capillary Chromatography, Rijks, J.; ed., Elsevier: Amsterdam, 1983, 304.
- Desty, D. H.; Goldup, Swanton, W. T. in Gas Chromaography, Brenner,
 N.; Gallen, J. E.; Weiss, M. D.; eds., Academic Press: New York, 1962,
 105.
- 8. Holland, J. F.; Newcombe, B.; Tecklenburg, R. E., Jr.; Davenport, M.; Watson, J. T.; Enke, C. G. Rev. Sci. Instrum. 1991, 62, 69-76.
- 9. Sharaf, M. A.; Kowalski, B. R. *Anal. Chem.* **1982**, *54*, 1291-1296.
- 10. Snyder, L. R. J. Chrom. Sci. 1972, 10, 200-212.

;

3

Chapter 5

Comparison of Two-Dimensional Gas Chromatography/Mass Spectrometry with Deconvolution of Gas Chromatography/ HighSpeed Mass Spectrometric Data

5.1. Introduction

Resolving the components of complex mixtures is a difficult challenge for high-resolution gas chromatography/mass spectrometry (GC/MS). These mixtures may contain hundreds of components whose concentrations may differ by several orders of magnitude. Since the separation space in a chromatogram is limited, the likelihood of two or more of the components coeluting from the GC column increases with the number of components in the mixture [1]. Davis and Giddings [2] estimated the probability that a single peak contains only one compound is less than 50% for a chromatogram filled to only 35% of the peak capacity.

One approach to resolving coeluting components is two-dimensional gas chromatography with mass spectral detection (2-D GC/MS). A conceptual diagram of a 2-D GC/MS instrument is shown in Figure 5-1. In a procedure called heart-cutting, regions of the chromatogram containing coeluting species

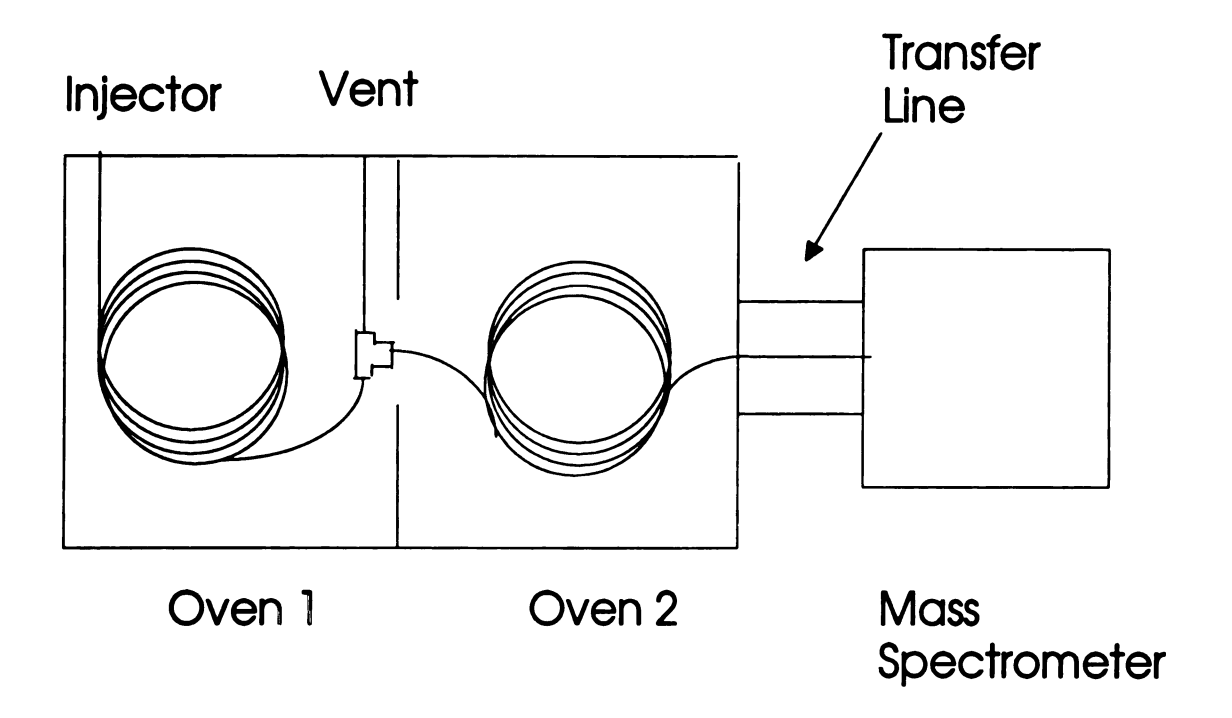


Figure 5-1. Conceptual Diagram of a 2-D GC/MS System. Following an initial GC separation performed on the first column, a portion of the eluent is isolated and separated on the second GC column. The separated components are detected using a mass spectrometer.

		;
		į
		ž.

are isolated and then separated on a second chromatographic column with a different selectivity from that of the original column. The separated components are detected using a mass spectrometer. While this approach can effectively resolve many coeluting species, it is relatively time-consuming. Regions that potentially contain chromatographically unresolved components must first be somehow identified. The regions selected for further separation are, in subsequent runs, sequentially isolated onto the second column. The second column is placed in its own oven and operated under a separate set of conditions. Because the second stage of GC analysis can only be performed on one selected heartcut region at a time, multiple chromatographic runs are generally required to examine all of the selected regions that are suspected of containing coeluting species.

Heartcutting relies on a pressure controlled valve which either directs the eluent onto the second GC column or vents it. The process of venting the column eluent is often performed via a detector such as a flame ionization detector. A mass spectrometer or any other type of GC detector can be used to examine the results of the initial GC separation.

Column selection is the basis of any chromatographic separation and is especially important in 2-D GC. Two sets of factors determine column choice. The choice of stationary phase is based on the nature of the sample to be analyzed. A non-polar stationary phase is often used for the preliminary separation while the final separation is performed on a more polar column. This

combination of selectivities increases the resolving power of the chromatography to a far greater extent than would the coupling of two columns with similar polarities. The second set of considerations relate to the concentrations of components in the mixture to be analyzed. 2-D GC is often used to isolate trace components that coelute with compounds present at higher concentrations. Thus, a thick-film column with its large sample capacity is often selected for the preliminary separation while the final separation is performed on a thin-film column. The first column has a large sample capacity, but less resolving power than a thin film column. The final column is selected to provide the best possible resolving power for the material isolated by the heart-cut.

An alternative approach is to analyze the sample using gas chromatography/high-speed mass spectrometry and then to examine the data from the regions that contain coeluting compounds by data deconvolution. Rapid acquisition of mass spectral information across the elution profile allows accurate reconstruction of the elution profile for each m/z value. Mathematical deconvolution algorithms, such as the approach described in Chapter 2 of this thesis, can effectively use the small temporal differences present in the mass chromatograms to determine the number of compounds present in a peak and provide a mass spectrum for each compound in an unknown mixture.

Although deconvolution algorithms have been around since the 1960's [3], these algorithms have not been in general use for several reasons.

Algorithms used to deconvolute unknown samples function most effectively when

the elution profile of each mass chromatogram is known accurately. This requires 20 or more data points across each chromatographic peak. The narrow peaks produced by capillary columns (a few seconds in width) thus require mass spectral acquisition rates of 5 to 25 spectra per second. One system capable of simultaneous acquisition of all masses is the combination of time-of-flight mass spectrometry with time-array detection (TOFMS/TAD) which can generate 25 or more mass spectra per second with subpicogram detection limits [3].

Analysis of unknown mixtures by either 2-D GC/MS or deconvolution of GC/high-speed MS data requires the same series of steps. First, regions containing chromatographically unresolved compounds must be identified. The number of components present in each coelution is then determined. Finally, a pure mass spectrum of each unresolved compound is obtained to allow identification of that compound. These capabilities were compared for the two techniques using a test perfume sample whose composition was unknown to the analysts. The sample for this collaborative effort was selected in conjunction with David Pinkston of The Procter and Gamble Company (P&G). Pedro Rodriguez and other collaborators at P&G performed the 2-D GC/MS analysis, while the TOFMS/TAD/Deconvolution analysis was performed by me.

5.2 Experimental

5.2.1 Initial GC Analysis

The sample was screened by gas chromatography (Hewlett-Packard, Inc., Model 5880A.) on a 30-m methyl silicone column (J&W Scientific). The linear velocity of the helium carrier gas was set to 30 cm sec⁻¹ for the 0.32-mm i.d. column which was coated with a 1.0 μm film. One microliter of the neat mixture was injected at a split ratio of *ca.* 100:1. The oven was initially held at 40°C for two minutes. It was then ramped to 250°C at 5°C min⁻¹, and the final temperature was held for 15 minutes. The column effluent was split with half going to a flame ionization detector and half to a sniff-port. The temperature of the injector and detectors was 250°C.

5.2.2 Two-Dimensional GC/MS

Two columns, a 30-m x 0.32-mm i.d. Rt_X-1 column with a 3.0-μm film and a 60-m x 0.32-mm i.d. Stabilwax column with a 0.5-μm film (Restek) were installed in the first and second ovens of a 2-D gas chromatograph (ES Industries, Siemens SiChromat, Model 2-8). The injector temperature was set to 250°C. The linear velocity of the first column was adjusted to 17 cm sec⁻¹ while the second column had a linear velocity of 38 cm sec⁻¹. Following injection of 1.0 μL of the neat oil at a split ratio of *ca.* 100:1, the first column was held at 50°C for 4 minutes and then ramped to 250°C at 5°C per minute. When a cut was

initiated, the temperature of the second oven was held at 70°C for 2 minutes and then programmed to 220°C at 10°C per minute. The second column was then held at 220°C until all of the components in the cut eluted from the column. The column effluent was split equally between three detectors: a flame ionization detector, a mass-selective detector (Hewlett-Packard, Inc. Model 5790A) and a matrix-isolation FTIR detector (4). The quadrupole mass spectrometer was scanned from m/z 14-300 at 1.5 scans per second. For the purposes of this paper we considered only the range between m/z 40-200. These conditions provided 4-5 mass spectra over chromatographic peaks that were approximately six seconds wide at the baseline.

5.2.3 GC/TOFMS/TAD with Data Deconvolution

A 25-m x 0.20-mm i.d. HP-5 column with a 0.33- μ m film (Hewlett-Packard, Inc.) was installed in a gas chromatograph (Hewlett-Packard, Inc., Model 5890A). This instrument was operated under the same conditions that were used in the initial analysis of the sample with the following exceptions. The sample was analyzed twice. The split ratio was adjusted to 30:1 for the first run and 250:1 for the second, while 0.1 μ L of the neat oil was injected for each analysis.

The time-of-flight mass spectrometer used for this work was the MTOF instrument described in Chapter 2 of this thesis. Ions, continuously formed and stored in the ion source via electron ionization, were extracted every 200 µs. Two hundred successive transients were summed by an integrating transient

recorder (ITR) [5] to produce 25 spectra per second for this analysis. These conditions resulted in the generation of about 50 spectra across chromatographic peaks that were approximately two seconds wide at the baseline.

The deconvolution algorithm used in this analysis is described in Chapter 3 of this thesis. A mass chromatogram peak position plot (MCPPP) was generated by determining the retention time for each mass chromatogram. The information contained in the MCPPP and individual mass chromatograms was used to determine the number of components present in the region of interest. A characteristic m/z value, shared by no other compound, was used to determine the mass spectrum of each coeluting compound via the cross-correlation approach.

5.3 Results and Discussion

We chose a perfume sample with which to compare the resolving powers of 2-D GC/MS and GC/TOFMS/TAD with deconvolution. Perfumes are typically prepared by combining natural extracts and distillation fractions. Consequently, they often contain a large number of compounds with similar structures and chromatographic behavior. Many chromatographic regions were expected to contain coeluting compounds when the unknown sample was screened under standard chromatographic conditions. The results of this analysis are shown in the reconstructed total-ion current chromatogram (RTIC) from the

GC/TOFMS/TAD data contained in Figure 5-2. Although this chromatogram appears to be relatively simple in comparison to those obtained for many complex mixtures, several of the peaks in the RTIC actually result from the coelution of two or more compounds. Two of these regions were selected for further study based upon the sniff-port data. These regions are indicated in Figure 5-2. Two-dimensional GC/MS and GC/high-speed MS with deconvolution were used to examine each of these regions.

5.3.1 Analysis of Region 1

The first of the two regions to be analyzed was the area eluting at about 13 minutes (first starred peak in Figure 5-2). An expanded view of this region is shown in Figure 5-3, the RTIC from the GC/TOFMS/TAD analysis. The shoulder on the leading edge of the RTIC (near spectrum 8075) indicates that at least two components elute in this region. Because the detector was saturated for some *m/z* values when using the 30:1 split ratio, these data were obtained using the 250:1 split. The MCPPP is superimposed on the RTIC in this figure to show the retention times of any compounds in this region. The shape of the elution profile and MCPPP lines indicated that two partially resolved components were present in this response. Mass chromatograms of two *m/z* values characteristic of the clusters of MCPPP responses are also shown in Figure 5-3. The retention times and peak shapes of these two masses account for the shape of the RTIC. Sniffport analysis of this same region also located two components.

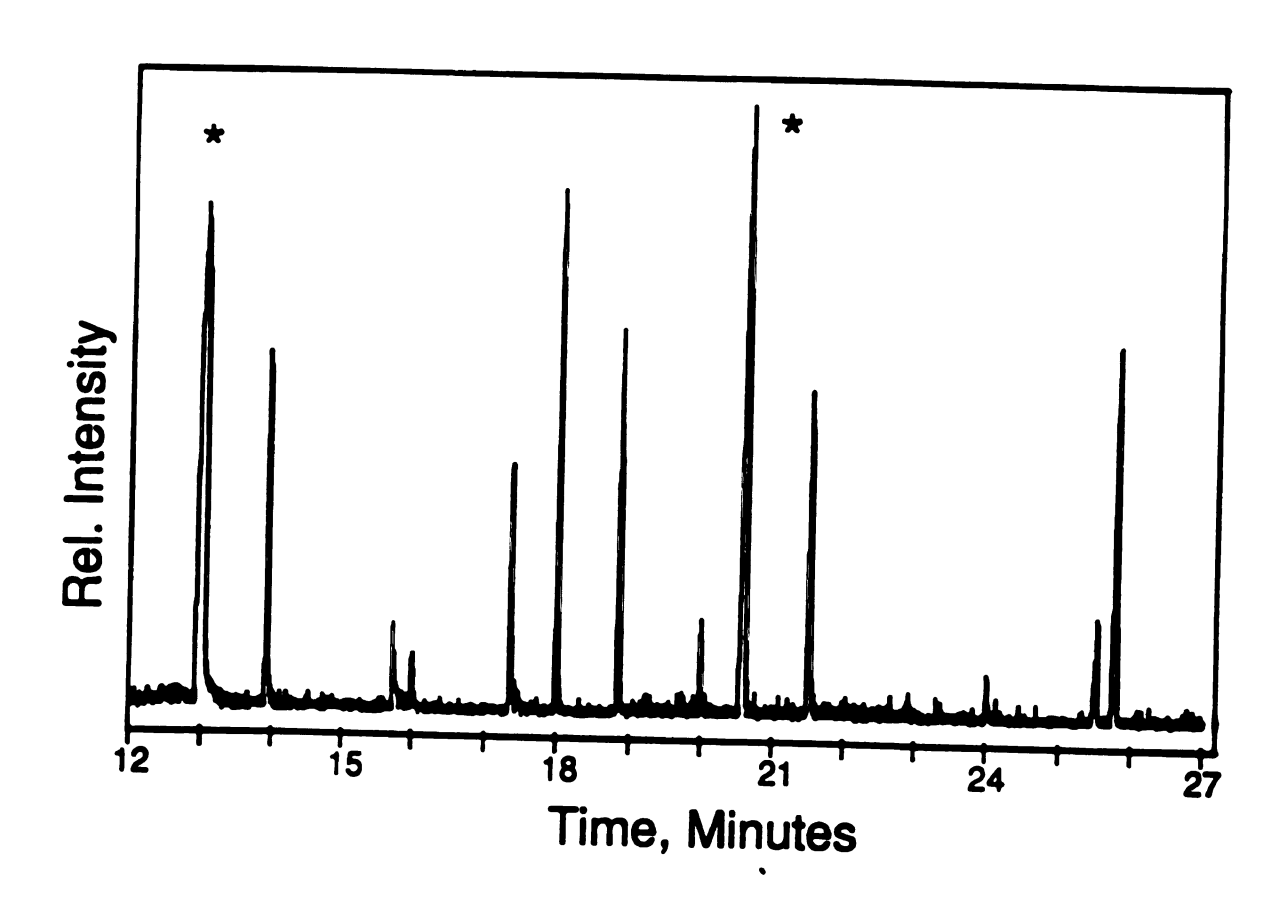


Figure 5-2. Reconstructed total-ion current chromatogram (RTIC) of the perfume from the GC/TOFMS analysis. Responses containing multiple components are indicated by an asterisk.

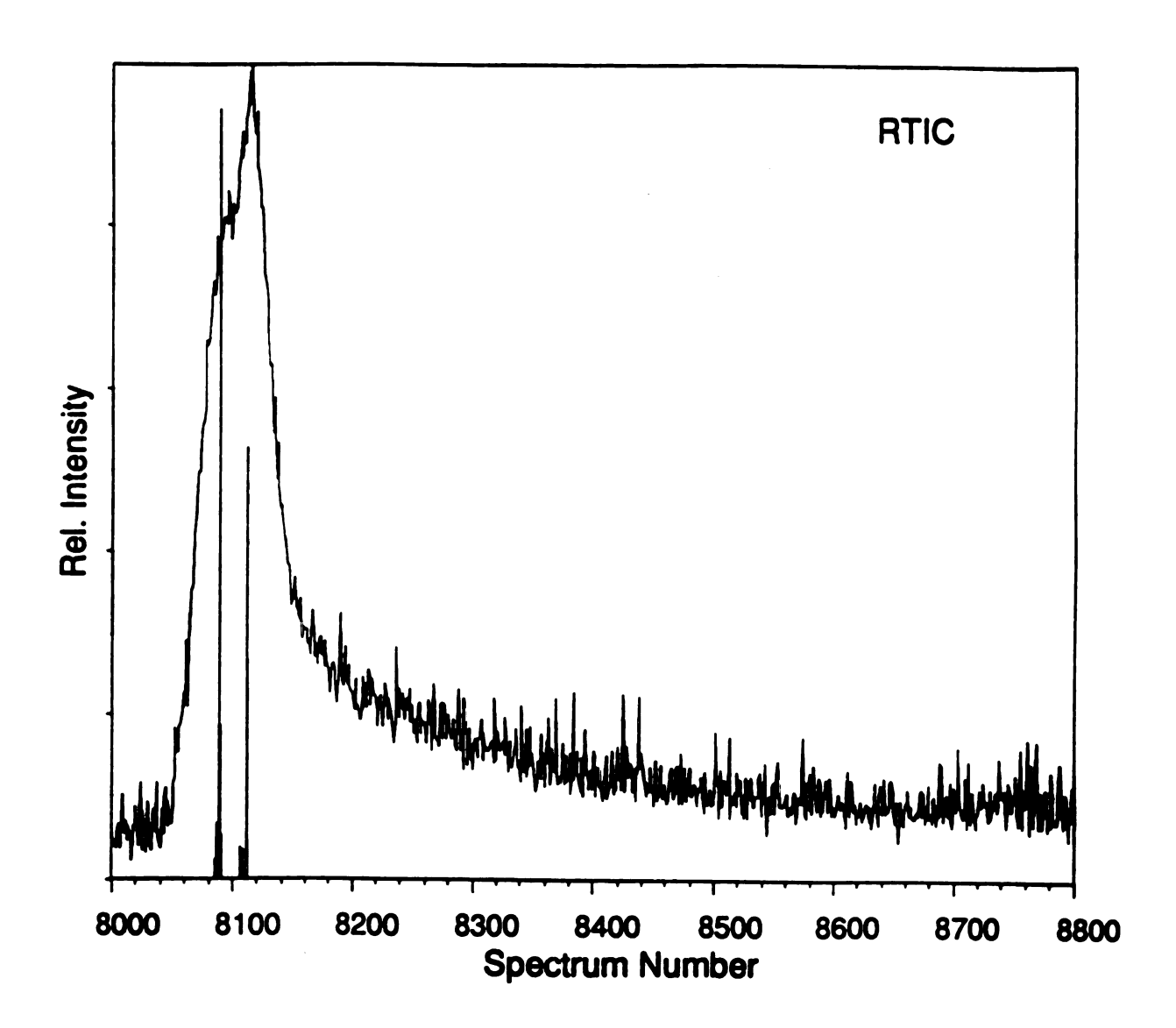


Figure 5-3. RTIC of region 1 from the GC/TOFMS analysis. The MCPPP is superimposed on the RTIC to show the retention times of the components located in this region. The shapes of characteristic mass chromatograms for each cluster of MCPPP lines confirm the presence of two compounds in this portion of the region.

Because the chromatographic separation of these two components was significant, 2-D GC/MS was not necessary to obtain a clean spectrum of each compound. Although spectra obtained from the GC/MS data are library-searchable, the physical separation provided by 2-D GC/MS yields spectra containing less chemical noise. Spectra from the 2-D GC/MS data are shown in Figure 5-4 (A and C). Deconvolution of the GC/high-speed MS data was not required for this region. However, it could be employed to produce the same clean spectra that were available from the 2-D GC/MS analysis, as shown in Figure 5-4 (B and D). The deconvolution approach eliminates noise from the spectra, but may also have difficulty in discriminating low intensity response from the background. The only other notable difference between the two sets of spectra is the slight change in relative intensities of some m/z values. These variations in relative intensity were too small to affect their identification. Library searches of the spectra using a NIST database identified, with good agreement, the compounds as linalool and phenyl ethyl alcohol, respectively.

One of the major challenges for either of these techniques is to determine the presence of minor components in the mixture. The small fluctuation in the baseline near spectrum 8725 is the focus of Figure 5-5. The MCPPP has been overlaid on the RTIC to show the retention times of individual mass chromatograms. The small cluster of MCPPP lines at about spectrum 8725 indicated that at least one compound with low intensity was eluting at this time. The two outlying responses at spectrum 8708 and 8769, upon inspection, were assigned to noise, being anomalous jumps in the intensity of an apparently

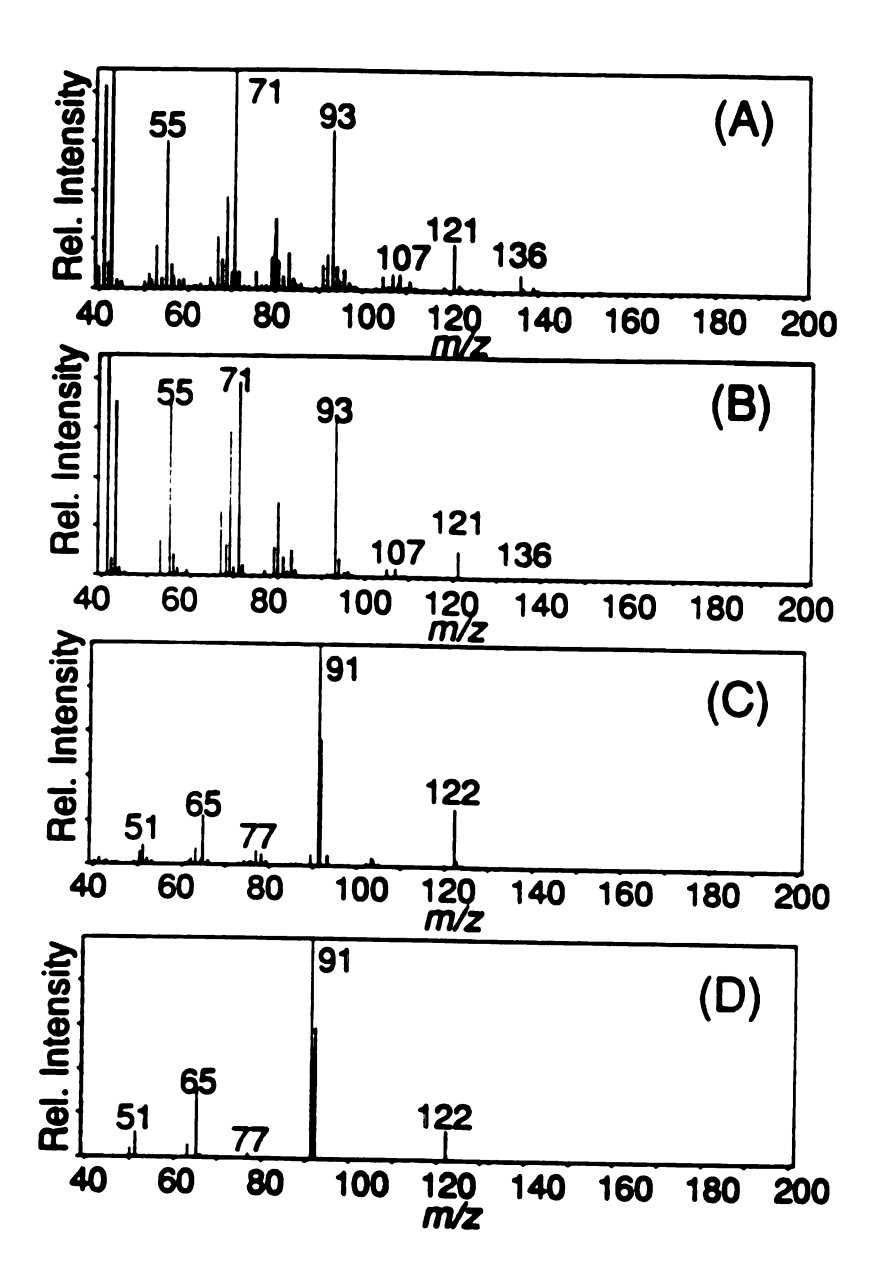


Figure 5-4. Spectra of the two compounds located and identified in region 1 by both techniques. Spectra A and C were obtained from the 2-D GC/MS while spectra B and D were extracted via GC/TOFMS/TAD using mass spectral deconvolution. Library searches of these spectra identified the two compounds as linalool and phenyl ethyl alcohol, respectively.

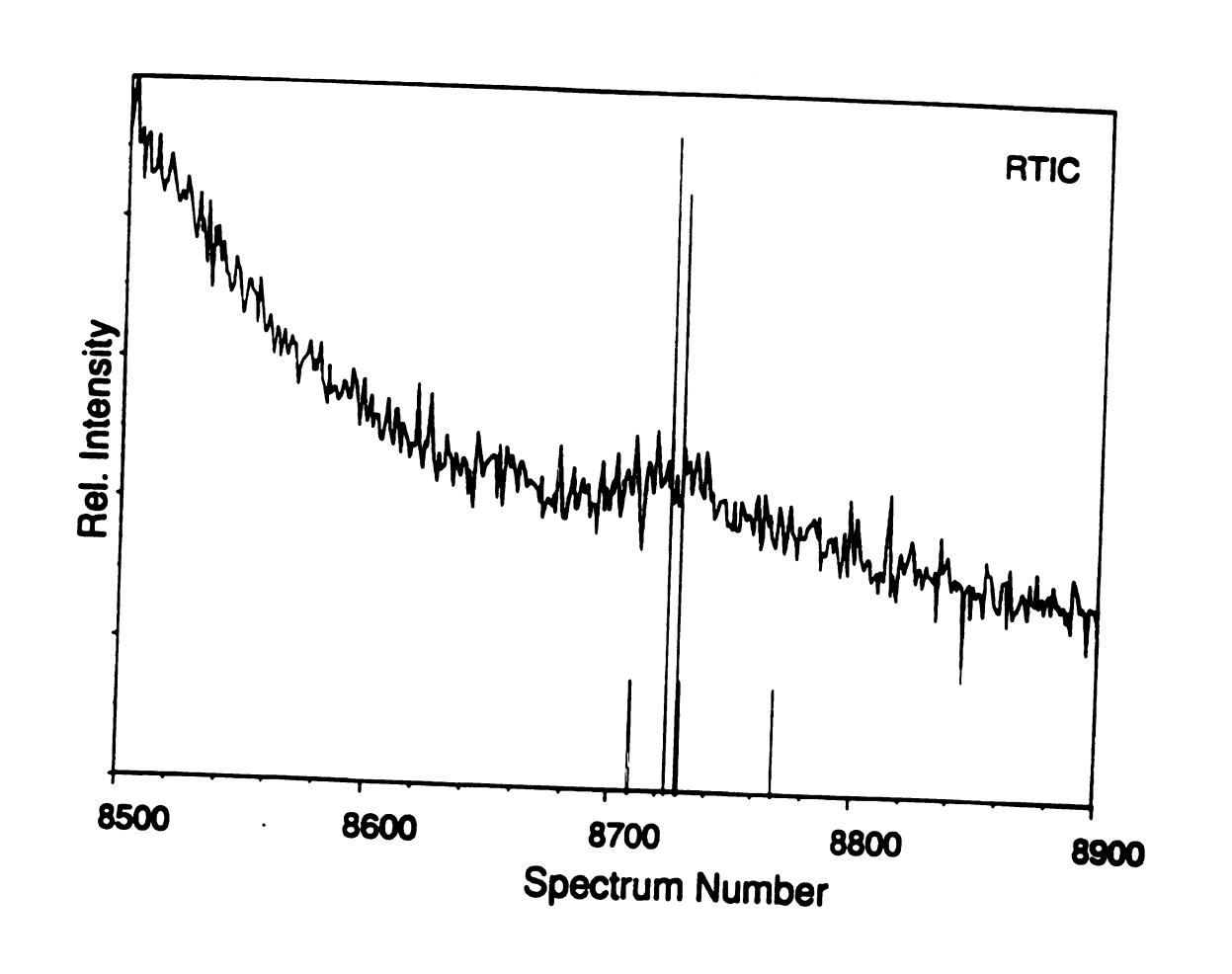


Figure 5-5. Expansion of the RTIC shown in Figure 5-3 focusing on the fluctuation in the baseline near spectrum 8725. The superimposed MCPPP-indicates the presence of at least one compound in this portion of region 1. Outlying lines in the MCPPP are the result of noise in the mass chromatograms.

unrelated *m/z* value. The remaining peaks resulted from a single compound where noise at the low-intensity levels interfered with exact peak position assignment. Thus, only one compound was present in this region.

Once a compound has been located, a clean mass spectrum is sought for compound identification. Figure 5-6 shows a series of mass spectra obtained for the compound that elutes at about spectrum 8725 in the GC/high-speed MS analysis. The first spectrum (A) was obtained from the 2-D GC/MS data. The large signal-to-background ratio for the 2-D GC/MS analysis results from the combination of increased sample concentration in the GC/high-speed MS analysis and chromatographic resolution of this compound from all other components (i.e. reducing the chemical noise). Thus, this spectrum is an accurate spectrum of the compound of interest. The remaining three spectra were all obtained from the GC/high-speed MS data. Spectrum B shows the mass spectrum at the retention time indicated by the MCPPP. The base peak in this spectrum is m/z 91 which is not even present in the spectrum A. Since this lowintensity compound eluted on the tail of phenyl ethyl alcohol, whose base peak is m/z 91, the spectrum at the retention time of the compound is dominated by the intense background and is not really representative of the compound of interest. Subtraction of an average background from the average signal across the peak yielded spectrum C. This spectrum contains most of the same m/z values as are found in spectrum A. However, the presence of several responses at masses greater than m/z 154 shows that a significant amount of noise remains when this approach is used. The final spectrum (D) was produced using

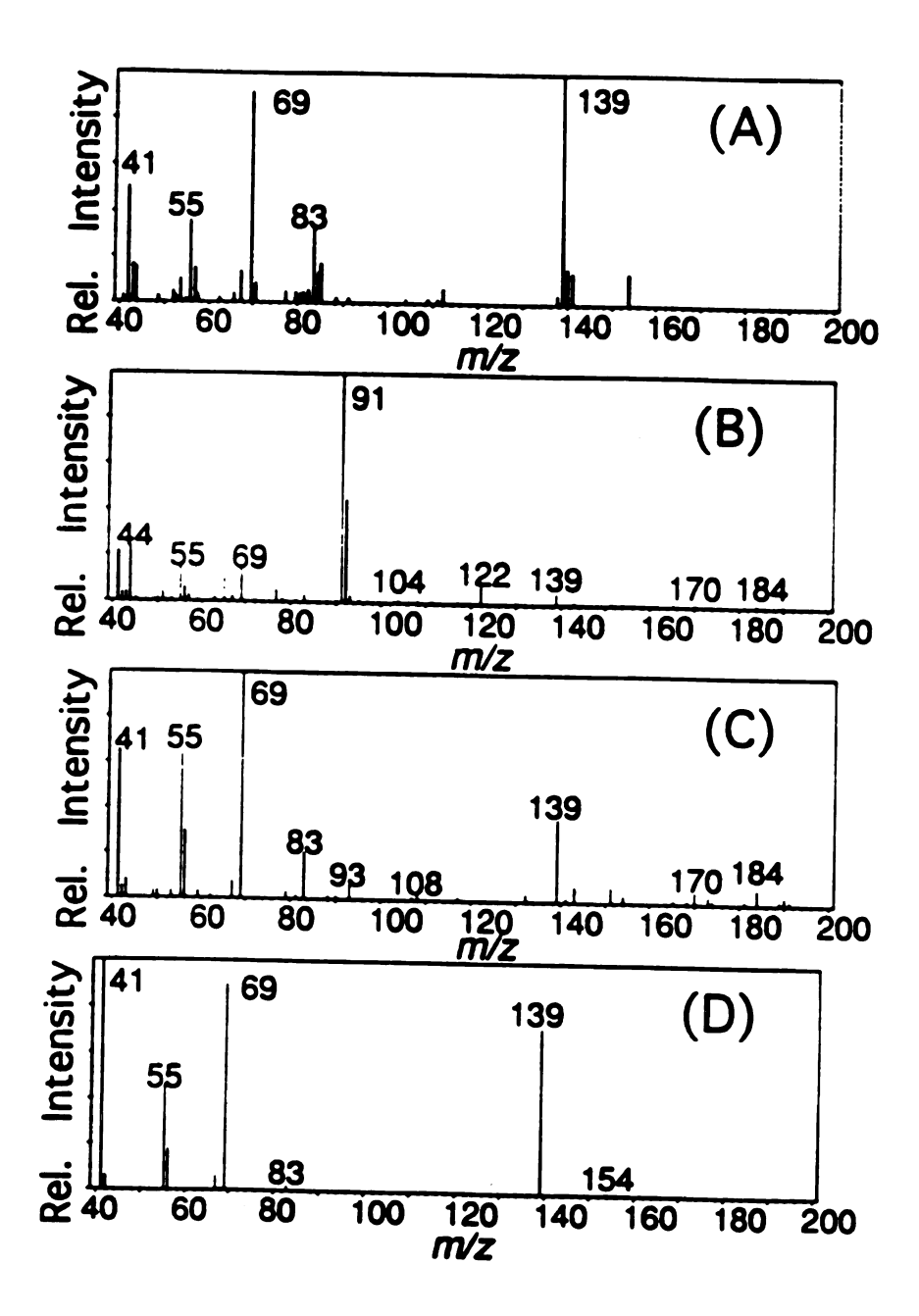


Figure 5-6. Spectra for the compound located in Figure 5-5. The chromatographically resolved spectrum (A), spectrum at the retention time of the compound (B), background-subtracted spectrum (C) and deconvoluted spectrum (D) are shown. B is dominated by phenyl ethyl alcohol and thus gives little information about the compound of interest. Library-searches of the other spectra (A, C and D) all identify the compound as rose oxide.

the deconvolution algorithm. This spectrum contains every m/z value that has a relative intensity greater than 20% in spectrum A, without the noise observed in spectrum C. The m/z values with relative intensities less than 20% were not extracted by the cross-correlation algorithm due to their similarity to the baseline. Library searches of the NIST database for spectra A, C and D all selected rose oxide as the first choice for this compound.

5.3.2 Analysis of Region 2

The second of the two regions selected for detailed study eluted at about 20 minutes into the chromatogram contained in Figure 5-2 (second starred region). The most notable feature of this region was the asymmetric shape of the elution profile as shown in the RTIC of the GC/high-speed MS data in Figure 5-7. One explanation for the fronting observed in this response is column overload. However, other responses of similar intensity would also be expected to show fronting. The peaks occurring at about 18 minutes and in region 1 are of similar intensity and still symmetrical. Close examination of the RTIC reveals a small shoulder on the leading edge of the elution profile (spectrum 25590). Based on these features, more than one compound was suspected of eluting in this region.

GC/TOFMS/TAD with Deconvolution Analysis. The data obtained by the GC/TOFMS/TAD analysis are shown in Figure 5-7. The MCPPP is overlaid on the RTIC to indicate the retention times of compounds detected by the deconvolution algorithm. These lines cluster into three groups. They are

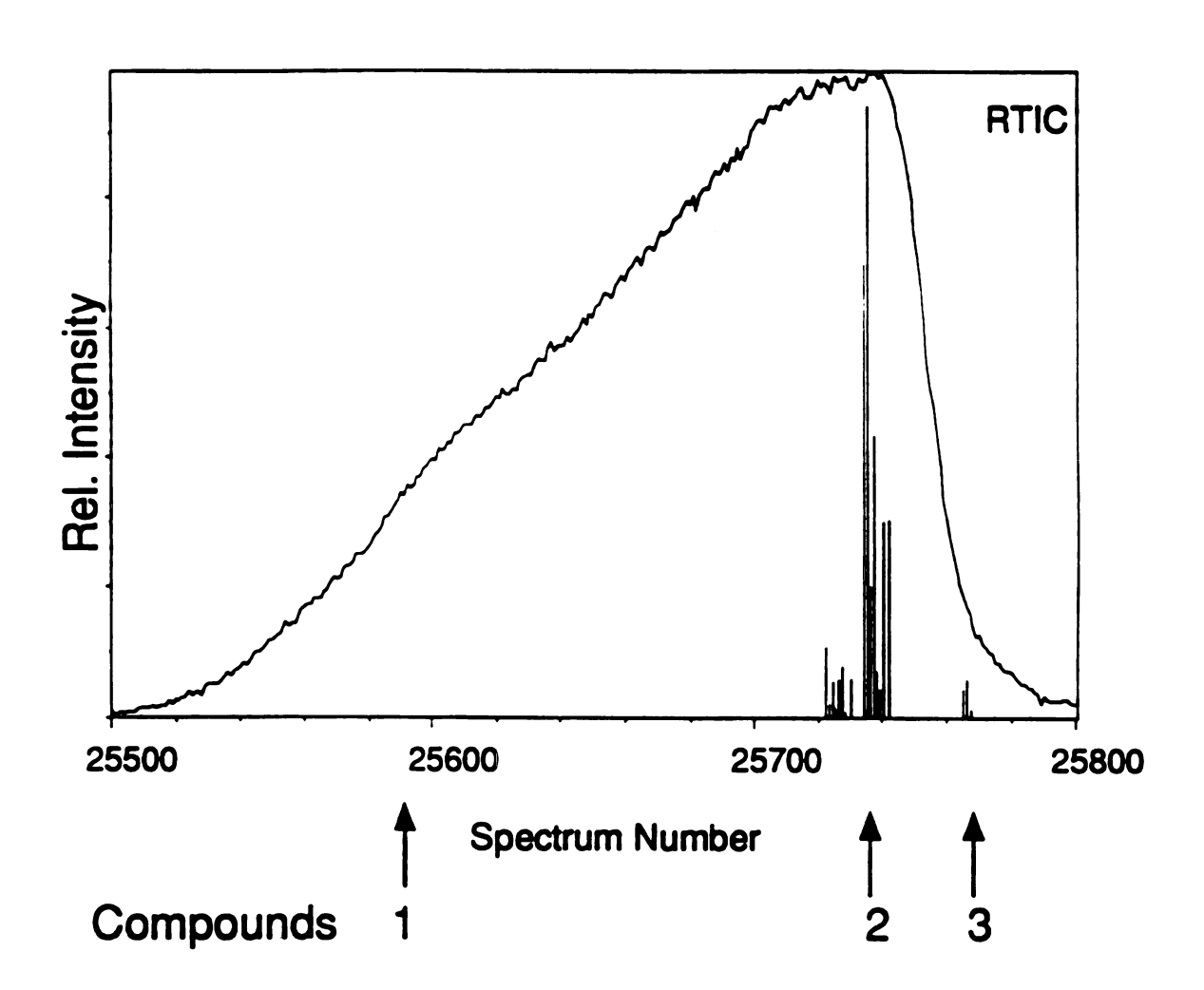


Figure 5-7. RTIC of region 2 from the GC/TOFMS/TAD analysis with the MCPPP superimposed to indicated the retention times of the compounds as determined by the deconvolution algorithm.

centered at spectra 25725, 25735 and 25767. Three groups of MCPPP lines might be interpreted as indicative of three compounds, but even three compounds eluting at the times suggested by the clusters do not explain the shape of the elution profile. However, if two or more compounds that share all m/z values (such as isomers) coeluted in region 2, the MCPPP would have responses only at the times when the broad, individual mass chromatograms reach their maximum intensity. When the component eluting last in this region has the largest intensity, the MCPPP lines will indicate the retention time of this compound and not give any retention information about any other isomers. Mass chromatograms representing each of the three clusters are shown in Figure 5-8. We selected m/z 147, 161 and 93 to represent the clusters of MCPPP responses at spectra 25725, 25735 and 25767, respectively. (The elution profiles of these mass chromatograms illustrate the presence of more than one compound better than other m/z values even though they have more intense responses.) The elution profiles of m/z 147 and 161 are very similar in shape. They both exhibit the fronting observed in the RTIC of region 2. The shoulder at spectrum 25590 in the RTIC is apparent only in the responses characterized by m/z 147 (indicated by the arrow in Figure 5-7). As expected from the combination of elution profile and lack of a MCPPP response, the intensity of m/z 147 increases until about spectrum 25725. The series of MCPPP responses near spectrum 25735 occurs at the retention time of the most abundant of these compounds. while the series of MCPPP lines around spectrum 25725 probably results from shared m/z values whose relative intensities are larger for a compound other than the most abundant one. Thus, at least two compounds that share all

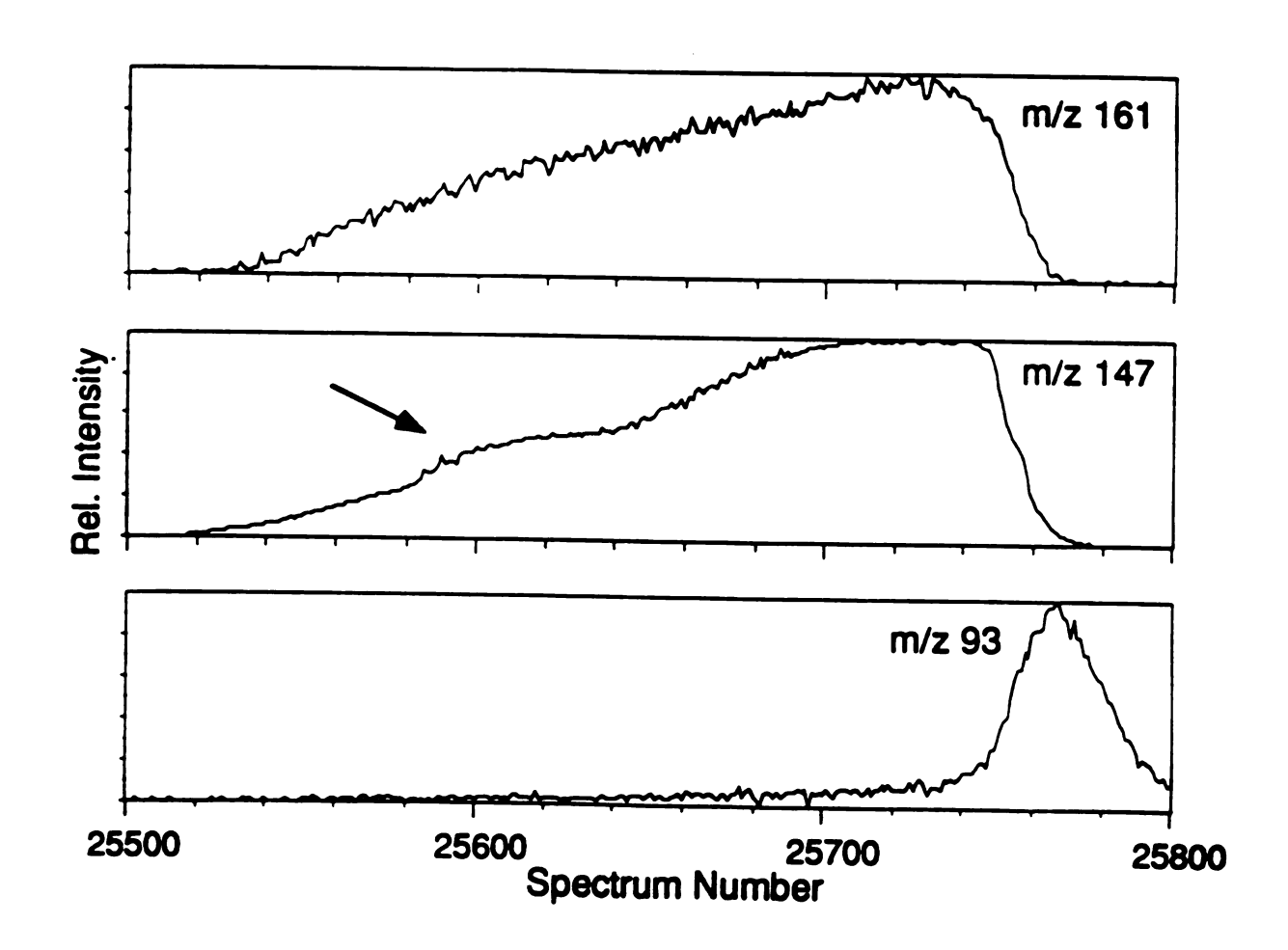


Figure 5-8. Mass chromatograms of m/z values characteristic of each of the three clusters of MCPPP lines. Chromatograms of m/z 147, 161 and 93 characterize the areas near spectra 25725, 25735 and 25767. The arrow points out the shoulder in the elution profile of m/z 147.

abundant m/z values are present in this region. Additional isomers may be present in this region, but the MCPPP and chromatographic information were not adequate to locate and identify them. Changes in the chromatographic conditions could provide the resolution required for their location and identification.

The third set of MCPPP responses are very different from those of the isomers. The lack of response around spectrum 25767 by the other mass chromatograms indicates that the compound eluting at this time differs greatly in structure from other compounds in this region. The narrow peak width and symmetrical shape of the mass chromatogram for m/z 93 indicated the presence of a single component. The tight cluster of MCPPP responses at this time confirms this conclusion.

Mass spectra of the three compounds in region 2 obtained by deconvolution of GC/TOFMS/TAD data are shown in Figure 5-9. The spectrum of the first of the two isomers was obtained from a spectrum that occurred at the time of the shoulder in the elution profile because our deconvolution algorithm requires a m/z value unique to each coeluting compound. The two remaining mass spectra were generated using the deconvolution algorithm. The mass spectra of the two isomers differ only in relative intensity for all significant m/z values. This supports the MCPPP results and explains the shape of the elution profile of the RTIC and mass chromatograms in region 2.

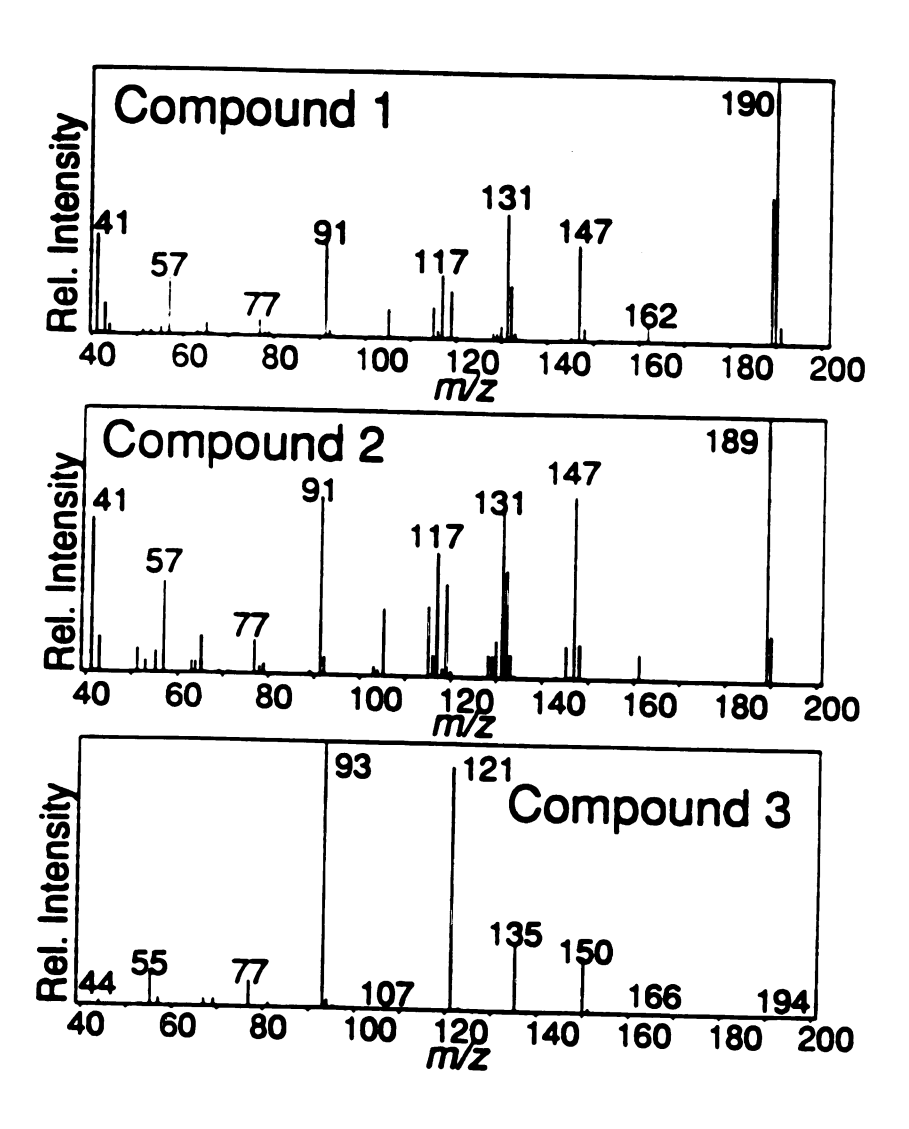


Figure 5-9. Mass spectra for the three compounds located in region 2 by GC/TOFMS/TAD include the spectrum at the time of the shoulder in the RTIC elution profile (compound 1), the deconvoluted spectrum of the compound that eluted at spectrum 25735 (compound 2) and the deconvoluted spectrum of the compound that eluted at spectrum 25767 (compound 3).

2-D GC/MS Analysis The RTIC shown in Figure 5-10 was obtained when region 2 was isolated onto a second GC column and the components separated. Since the goal of 2-D GC/MS is to resolve all of the components chromatographically, each peak should represent a single compound. Five peaks, labeled A-E, were found in this region. Compounds A, D and E were baseline resolved from all other components and, thus, could be easily distinguished from other components. Compounds B and C were not completely chromatographically resolved, but the shape of the elution profile revealed the presence of at least two components in this peak.

Mass spectra obtained from region 2 by 2-D GC/MS are shown in Figure 5-11. While no identifiable mass spectrum was obtained for compound B due to the extremely small response at all m/z values and interference from compound C, the mass spectral data at the elution time of compound B contain the same key masses as compound D (i.e. m/z 135, 150, 163 and 191). The background-subtracted spectra of the other four components are clean and distinctive. Scrutiny of the mass chromatograms across the asymmetrical elution profile of compound E revealed no changes in the relative intensities of any m/z values.

Region 2: Summary and Conclusions Substantial differences exist in the results produced by the two techniques in region 2. The most striking of these differences is that the deconvolution approach located only three compounds in region 2 while the chromatographic approach found five compounds. Examination of the mass spectra in Figures 5-9 and 5-11 shows

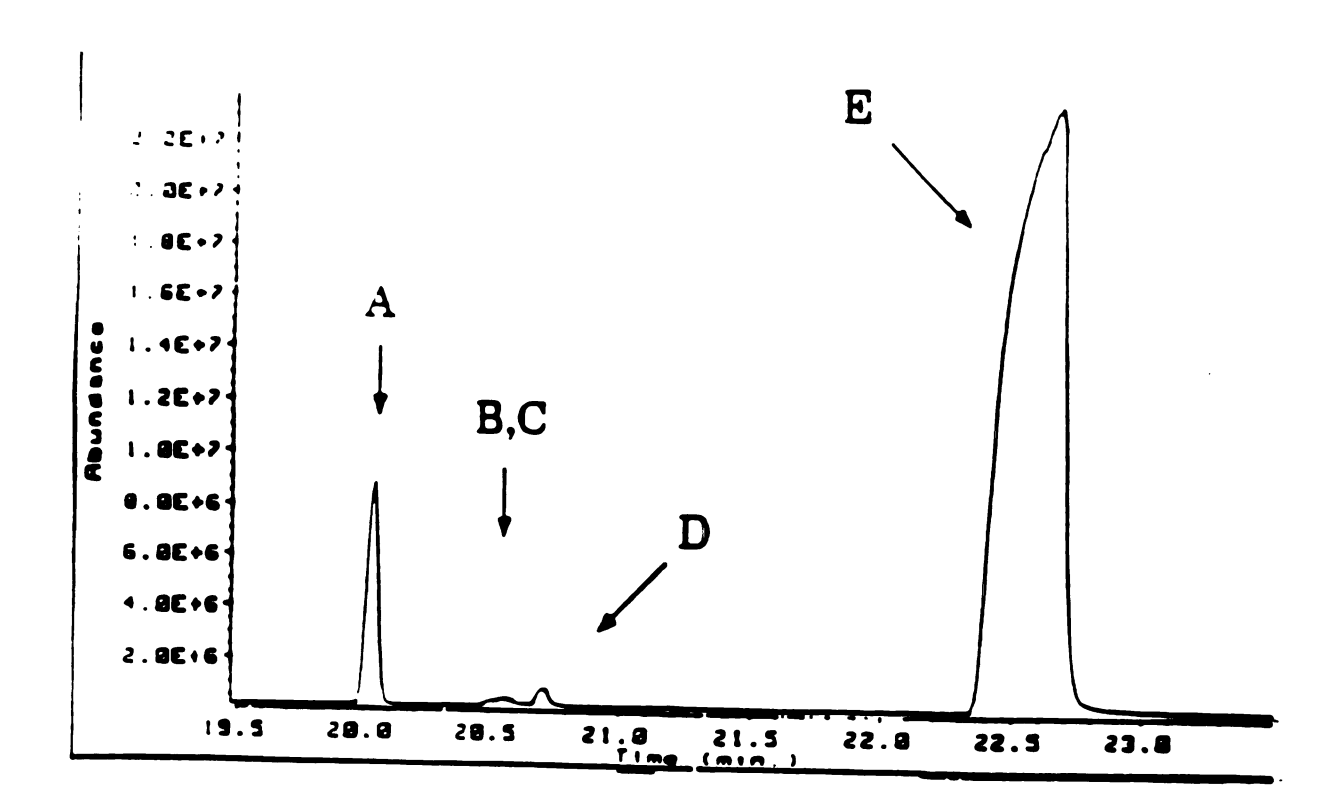


Figure 5-10. RTIC of the 2-D GC/MS analysis of region 2. The five peaks indicate the presence of five compounds, labeled A-E, in this region.

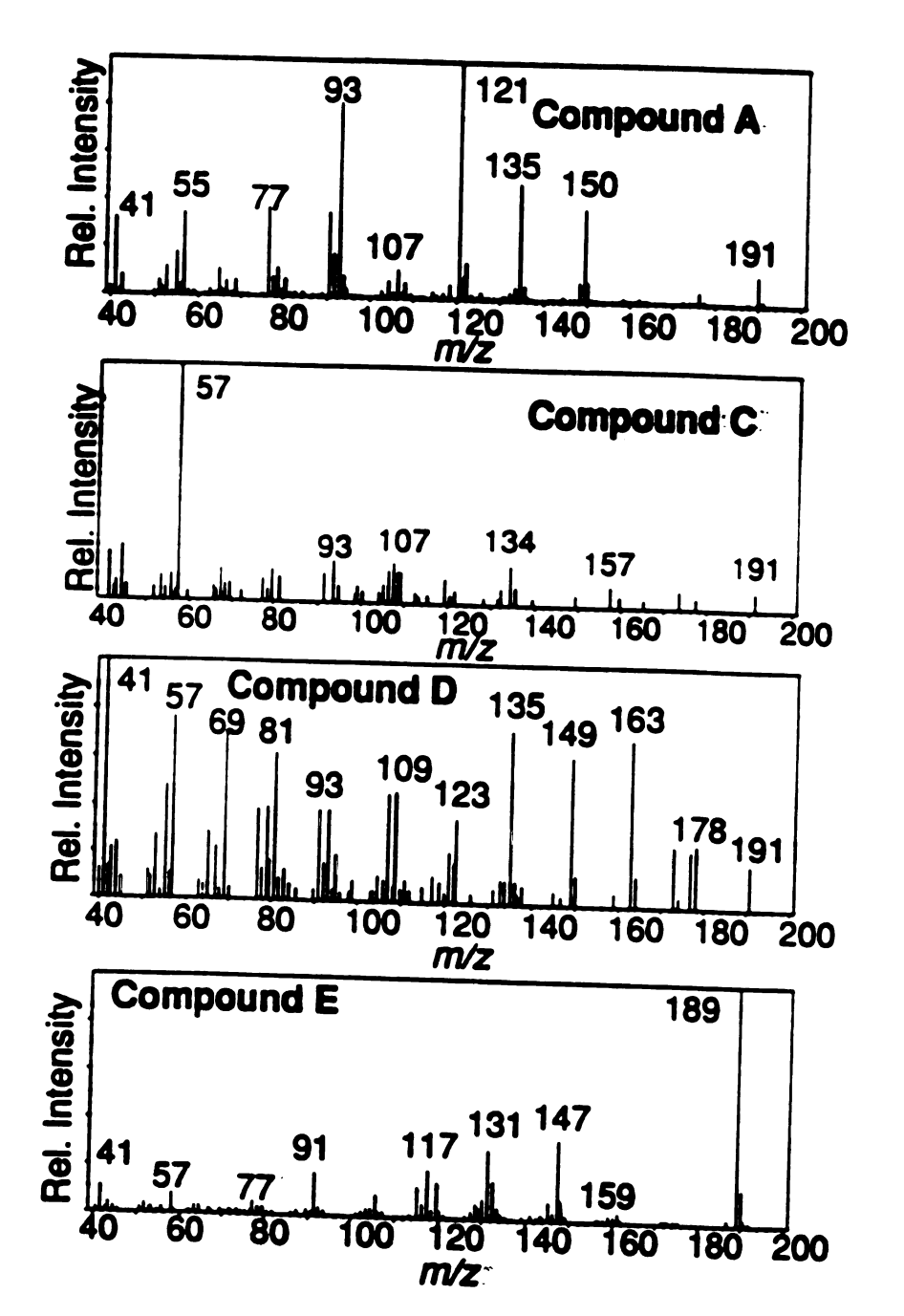


Figure 5-11. Mass spectratof four of the five compounds located by 2-D. GGMes: (Figure 5-10). The intensity of compound B. was so low that no representatives mass spectrum could be obtained. Because these compounds were proprietary; they were not identified via library-searcheer:

only two pairs of spectra that agree in composition and intensity. The spectra of compounds 2 and 3 from the deconvolution data match those of compounds E and A from the 2-D GC/MS data, respectively. The inversion in the retention order is a result of the selectivity of the second column in the 2-D GC/MS analysis. The intensities of compounds C and D comprise less than 1% of the total mass contained in region 2 and were probably present at levels near the detection limits of the TOFMS/TAD system. Unfortunately, simply increasing the on-column sample concentration would not permit detection of compounds C and D by the deconvolution approach. The peak-finding algorithm requires that the intensities of all m/z values lie within the dynamic range of the mass spectrometer. The detector was saturated in region 2 for some m/z values when the sample concentration was increased to a suitable amount. The inability of 2-D GC/MS analysis to find the first compound located by the deconvolution intrinsic weakness. approach reveals its Compounds must be chromatographically resolved from any compound in the region, especially those with similar mass spectra. The most likely elution time for this compound was nearly the same as that of compound E. Coelution of these two isomers explains the asymmetrical shape of the elution profile for peak E, but the large degree of similarity between the mass spectra of the two compounds disguises the presence of a second compound.

Combining the results of the two approaches, a total of six compounds were located in this region. Only two of these six compounds were identified by both approaches. The dynamic range of the TOFMS/TAD system restricted the

deconvolution approach to locating and identifying the three compounds with the largest intensities. Five of the six compounds were located by 2-D GC/MS including the three compounds with the lowest intensities. Spectra for all of these compounds could be obtained with little difficulty. However, 2-D GC/MS failed to locate the compound with second largest intensity of those in region 2. Although this compound was partially resolved from its isomer by the first GC column, the selectivity of the second column caused the retention times of the two isomers to converge.

5.4 Conclusions

Each of the two techniques increases the amount of information available from chromatographically coeluting regions of complex mixtures over the traditional GC/MS approach. When these two techniques were applied to the two regions of interest, the results were sometimes complementary, revealing the strengths and weaknesses of each approach.

A great advantage of GC/high-speed MS with data deconvolution is the reduced analysis time. The deconvolution approach operates on data acquired in a single chromatographic run, no matter how many regions are selected for detailed analysis. For 2-D GC/MS, separate runs are required for each region suspected of needing further resolution. The MCPPP lines provide information about the degree of structural similarity and the retention time of coeluting compounds. The use of high-speed MS detection also provides more information

about the shape of the elution profiles for all masses, allowing the location of compounds not visible by traditional GC/MS. Since our present deconvolution approach is based on the presence of a unique m/z value for each coeluting compound, chromatographically unseparated compounds with very similar mass spectra will not be located or identified. A compound will also not be located if the detector is saturated for any significant m/z value because the MCPPP locates the point of maximum intensity for each mass in a chromatographic peak. Thus, the dynamic range of this approach is limited by the need to maintain the integrity of the chromatographic profile for all mass chromatograms.

The major strength of 2-D GC/MS is its capability to physically separate compounds with similar mass spectra that coelute in the primary GC analysis. The dynamic range of this approach is larger because intense responses by compounds present at high concentrations can saturate the detector without affecting regions of the chromatogram containing smaller responses. The presence of trace compounds can be determined by overloading the first chromatographic column to pass a detectable amount of material into the second chromatographic dimension. Chromatographic resolution of these trace compounds reduces the background and permits their detection at very small concentrations. The intrinsic limitation of 2-D GC/MS is the need to chromatographically resolve all of the components placed onto the second column by the differing selectivity of the chromatographic columns. Sometimes, as occurred in region 2, this approach backfires and the retention times of compounds become more similar. When this occurs, scrutiny of the shape of the

elution profile may reveal the presence of multiple components. These compounds are not otherwise detectable.

These two approaches, designed for the same purpose, may reveal complementary information about the same coelution. Use of both techniques is desirable for this reason. The deconvolution approach can provide a large fraction of the information about the regions containing coeluting compounds in a relatively small amount of time. Deconvolution data, through MCPPP and elution profile information, and sniff-port results can be used to locate those regions requiring more chromatographic resolution or dynamic range. The structural information available from the data used to generate the MCPPP can also be used as a tool in selecting the conditions for 2-D GC/MS analysis. Increased information about coeluting species and the need to analyze fewer regions via 2-D GC/MS can significantly reduce the time required to characterize a complex mixture of unknown composition.

5.5 Summary

Compounds that coelute when analyzed by GC/MS may be analyzed using 2-D GC with mass spectrometric detection or by deconvoluting GC/MS data acquired using the MTOF/ ITR system. While 2-D GC/MS instrumentation is commercially available, this approach is time-consuming due to the need to physically isolate coeluting compounds onto the analytical column. The deconvolution approach has the potential to reduce the time without sacrificing

any information. The perfume sample of unknown composition used for this study revealed strengths and weaknesses in each technique. Combining these two techniques could reduce the time required to analyze complex mixtures and use the strengths of each technique.

Analysis of complex natural mixtures is difficult because of the presence of many isomeric species that possess similar retention and spectral characteristics. This problem is exacerbated when a sample of unknown composition contains hundreds of components. Chromatographic resolution of all of these compounds often cannot be achieved in the limited separation space available with even capillary column GC. Compounds with very similar mass spectra are difficult to locate when they coelute from a chromatographic column.

References

- 1. Guiochon, G.; Gonnard, M. F.; Zakaria, M.; Beaver, L. A.; Siouffi, A. M., Chromatographia 1983, 17, 121.
- 2. Davis, J. M.; Giddings, J. C., *Anal. Chem.* **1983**, *55*, 418.
- Tecklenburg, R. E., Jr.; McLane, R. D.; Grix, R.; Sweeley, C. C.; Allison, J.; Watson, J. T.; Holland, J. F.; Enke, C. G.; Gruner, U.; Gotz, H.; Wollnik, H., Proceedings of the 38th ASMS Conference on Mass Spectrometry and Allied Topics, Tucson, AZ, June 3-8, 1990.

- 4. Rodriguez, P. A.; Eddy, C. L.; Marcott, C.; Fey, M. L.; Anast, J. *J. Microcol. Sep.* **1991**, *3*, 289-301.
- 5. Holland, J. F.; Newcome, B.; Tecklenburg, R. E., Jr.; Davenport, M.; Watson, J. T.; Enke, C. G. Rev. Sci. Instrum. 1991, 62, 69.

Chapter 6

Photodissociation in Tandem Mass Spectrometry

6.1 Introduction

The same problems that have limited GC/MS analysis are present in tandem mass spectrometry (MS/MS). Several factors unique to tandem mass spectrometry increase the time required to acquire complete product spectra of all precursors. These factors primarily result from the processes necessary to isolate the precursor ion of interest, fragment the selected precursor and acquire the product ion spectrum. The same trade-off between scan speed and intensity present in sector and quadrupole instruments plays a role in the time needed for precursor ion selection and product ion analysis. Acquisition of a single product ion spectrum requires setting the conditions for the mass analyzer used for precursor ion selection and scanning the mass analyzer used for product ion analysis. Commercial MS/MS instruments often require several minutes to acquire complete MS/MS data sets (all products of all precursors).

6.2 Qualities Required For MS/MS Using TOF Instruments

The keys to MS/MS analysis in a TOF instrument are high resolution for selection of the precursor m/z value, effective fragmentation of the selected

precursor, transmission of a large fraction of the product ions formed to the detector and at least unit resolution of product ions. Since resolution in a TOF instrument is related to the flight time of an ion, both precursor and product ion resolution increase with the length of the flight path. Ion packets have their narrowest spatial distribution at the space-focus plane(s) of a TOF instrument. Thus, precursor ion selection is best achieved at a space-focus plane a significant distance from the ion source.

Effective fragmentation and high transmission of the precursor ion are dependent on the dissociation technique. A dissociation technique must introduce energy into the precursor ions under conditions that cause a significant fraction of them to fragment and reach the detector. These requirements have led to the use of SID and PID as the two major dissociation techniques for TOF instruments. When PID is used, the laser power must be sufficient to insure that a significant fraction of the selected ions in the packet absorb a photon and fragment. The laser pulse rate should be the same as the extraction rate of the ion source to provide maximum sensitivity for the production of product ions.

After fragmentation has occurred, the newly-formed product ions travel at the same velocity as their precursor. These product ions have a fraction of the kinetic energy distribution of their precursor as well as the energy acquired in the photodissociation process. Acceleration to a higher energy just after fragmentation occurs imparts mass-dependent velocities to the product ions. Mass separation now occurs in a manner similar to the first TOF mass analyzer

except that the product ions are not monoenergetic. Ions have the energy received in the acceleration region plus the fraction of precursor ion energy retained after fragmentation. For an ion mirror to achieve perfect energy focusing, all of the ions should have the same approximate energy. Since the second mirror is optimized for the energy of the precursor ions, the product ions will not be perfectly focused. The best product ion resolution can be achieved as the energies of the precursor and fragment ions become more similar. Thus, as the acceleration voltage at the interaction region is increased and as the initial energy of the precursor ion is decreased, a wider range of product ion masses will be focused. Unit mass resolution should be achieved for all product ions of precursors compatible with GC analysis.

6.3 Photodissociation in Mass Spectrometry

Photodissociation (PID) as a means of inducing the fragmentation of ions has been used with several different types of mass spectrometers and light sources (see Table 6-1). Photodissociation efficiency plays a major role in the selection of the choice of mass spectrometer and light source to be used in an analysis. If the photon and ion densities are uniform and overlap completely when laser excitation occurs, photodissociation efficiency can be described by the relation

Efficiency =
$$\frac{N_c}{N_l}$$
 = $\phi \sigma$

where N_c is the number of fragmentation-inducing collisions occurring between photons and ions in one laser pulse, N_l is the number of ions in the irradiated area, ϕ is the photon density of the laser pulse in the region populated by ions, and σ is the photon interaction cross-section for the selected ion at a given wavelength. Thus photodissociation efficiency can be improved by increasing the number of photons given the opportunity to interact with an ion, increasing the number of ions present in the laser beam and choosing the radiation wavelength judiciously. These factors all play roles in the approaches used to perform photodissociation in mass spectrometers.

The orientation of the laser to the ion beam is dependent on a variety of factors including ion densities and type of mass spectrometer used. Many researchers have sought to maximize the ion exposure time to the laser beam by irradiating the sample for up to 3 s in an ion cyclotron resonance mass spectrometer (ICR) or by making the laser beam coaxial to the ion beam in sector or quadrupole instruments. Ion sources in sector and quadrupole mass spectrometers usually form and analyze ions continuously. The ion densities in these instrument are relatively small. McGilvery and Morrison [1], and Krailler and Russell [2,3] have directed the laser perpendicularly to the low-density ion beam in quadrupole and sector mass spectrometers, respectively. The sensitivity problems that they experienced forced them to adopt a coaxial geometry that increased the number of ions intercepted by the laser light path. Trapped ions in ICRs can be exposed to the laser for relatively long periods of time (up to 3 s) allowing single and multiphoton PID processes to occur. But

Table 6-1. Historical Background of Photoionization/Photodissociation in MS.

Investigator:	Morrison ¹	Eyler ^{4,5}	Russell ^{2,6}	McIver ⁷	Dunbar ⁸	Hunt ⁹	Freiser & Russell ¹⁰ ICR
Instrument:	TQMS (axial)	ICR	Sector (axial)	ICR	ICR	FTMS	
Light Source:	Dye Laser	CO, Laser	Ar Ion Laser	Excimer	Ar Ion Laser	Excimer (ArF)	3.5 kW Xe Arc Lamp
Wavelength:	606 nm (vis)	10.61 μ <i>m</i> (IR)	514-458 nm (vis)	193 nm (VUV)	515 nm (vis)	193 nm (VUV)	(300-400 nm)
Energy/ Photon:	2.0 eV	0.8 eV	2.4-2.6 eV	6.4 eV	2.4 eV	6.4 eV	3.1-4.1 eV
Pulse Width:	1 μs	CW/1 μs- 500 ms	•	5 ns	100 ms	•	2-3 s
Power Density:	30 mW/cm ²	5-10 W/cm ²	-	2.2 MW/cm ²	400 mW/cm ²	-	•
Photons Required:	1	-	1	1	2	1	-
% Fragment.:	<cid(1%)< td=""><td>-</td><td>-</td><td>10-20%</td><td>30%</td><td>-</td><td>50-80%</td></cid(1%)<>	-	-	10-20%	30%	-	50-80%
Photon Density:	9x10 ¹⁰ / cm ²	2.3x10 ²¹ / cm ²	-	1.1x10 ¹⁶ / cm ²	1x10 ¹⁷ / cm ²	-	-

photon-induced neutral ionization and fragmentation is hard to distinguish from PID because ions in an ICR are not separated energetically from the neutrals.

Choice of laser frequency is important in PID experiments, and more than one approach has been successfully adopted. Dunbar [11] has shown that the photofragmentation of larger molecules is less dependent on their overall structure than on the presence of specific chromophores. This chromophoric functionality is the primary determinant of the photon interaction cross-section for a class of ions and typically ranges from 10-17-10-19 cm² [12]. Since trapped ions can be irradiated for longer periods of time than in beam instruments, infrared [13,14], visible [15] and ultraviolet [16] radiation have been used to induce fragmentation in them. Multiple photons from infrared light sources are needed to cause photofragmentation because only a small amount of energy is deposited into an ion by a single photon. Multiphoton PID can either occur when the ion is excited to a virtual or a real state by absorption of the first photon. In the former case, The second absorbed photon must arrive in the same laser pulse. Thus, multiphoton PID through a virtual state is a highly unfavored process and rarely observed. When multiphoton photodissociation is induced via a real state, the successive photon(s) can be absorbed from the same or subsequent laser pulses. Since multiphoton PID is often used to analyze ions with a large number of electronic states, photodissociation via a real state is performed in mass spectrometers capable of trapping the ions so that they may be exposed to many laser pulses. Visible and ultraviolet wavelengths are often employed to cause photofragmentation in beam mass spectrometers because of the larger amounts of energy deposited into an ion by a single photon. Nearly all examples of photodissociation in beam mass spectrometers have been single photon processes. In all cases, the laser may be tuned to be selective or non-selective for analyte(s) through the choice of laser wavelength and power.

Photodissociation has been performed on organic and inorganic ions of a wide variety of sizes. These range from peptides [17] and oligopeptides [6] to metal clusters [18] and relatively small molecules such as benzene [19,20], methyl iodide [21], ethyl acetate and 1,4-dioxane [22]. Molecules as large as 12,000 *u* have been successfully photofragmented [23]. In direct contrast to CID, PID is not mass limited. The amount of energy deposited into an ion is only dependent on the amount of energy possessed by a photon and the number of photons interacting with that specific ion. Hill, Annan and Biemann [24], and Tecklenburg and Russell [25] have successfully photodissociated fairly large biomolecules in sector mass spectrometers. Biemann found that the product ions of two model proteins, angiotensin III and melittin, provided useful sequencing information.

The key to photodissociation for any size of ion is wavelength selection. Tecklenburg, Miller and Russell [26] have shown that derivatization of peptides by adding a chromophore to them produced mass spectra dominated by ions resulting from loss of the chromophore. Thus, the target chromophore should be an intrinsic part of the ion of interest. For instance, a light source set at about 193 *nm* has proven useful in the analysis of peptides. Photons of this energy are absorbed by the amide linkage of the peptide and fragmentation is dominated by B and Y type fragments resulting from cleavage of the amide bond.

Although photodissociation may be targeted for classes of compounds, it can also be used as a very selective technique. Photodissociation crosssections of ions are different for ions of different structures at different wavelengths. In 1981, Wagner-Redeker and Levsen [27] measured the relative intensities of five [C₅H₈]+ ions. These ions were generated from 1,2-pentadiene, 1,3-pentadiene, 2-pentyne, 3-octyne and cyclopentene. The [C₅H₈]+ produced by these structures possess different chromophores due to numbers and locations of conjugated double bonds, triple bonds. The photodissociation crosssections of these compounds were measured at multiple wavelengths including 351 and 515 nm. Krailler and Russell [2] were able to discriminate between cis and trans isomers of 1,3-pentadiene and the cis, trans and trans, trans isomers of 2,4-hexadiene based on their wavelength-dependent branching ratios. Another way of differentiating ions with similar structures is to measure their translational energy release upon PID. Beynon and coworkers [28] studied the three xylene isomers and found that the three isomers could be discriminated by examining their energy release at different wavelengths.

Although Table 2-1 does not contain examples of PID in time-of-flight mass spectrometers, photodissociation has been studied in conjunction with multiphoton ionization (MPI) and, more recently, by itself. Boesl *et al.* [29] and Bernstein [19], among others, noted the dependence of the degree of fragmentation achieved in MPI on laser intensity. Segar and Johnston [30] have used controlled MPI and subsequent PID of the ion to study benzyloxycarborbonyl derivatized dipeptide methyl esters of nonaromatic amino acids by TOFMS. In their studies, they noted that MPI required two 266 *nm*

photons and that photodissociation occurred upon absorption of a third 266 *nm* photon.

6.4 Time-of-Flight Instruments in MS/MS Analysis

The speed and simplicity of time-of-flight mass spectrometers make them attractive candidates for MS/MS systems. TOFMS has previously been combined with other mass dispersive devices such as magnetic (B) and electric (E) sectors and quadrupoles to form MS/MS instruments. Glish et al. [31] have combined TOF with a quadrupole mass filter for trace analysis. This instrument achieved direct product spectra via TOF, but suffered from poor product ion resolution and low sample efficiency. In 1977, Gandy and coworkers [32] reported the development of a magnetic sector/time-of-flight instrument which was used to study CID. The combination of TOF with a magnetic sector produced a technique called time-resolved ion momentum mass spectrometry (TRIMS) [33]. This work led to the ability to acquire a complete MS/MS spectrum in about 10 s. Although this is exceedingly fast for MS/MS analysis, it is barely adequate for low-resolution (packed column) GC. This approach is also limited by the inherently low scan rates of magnetic sectors since acquisition of any MS/MS spectrum requires scanning of the magnet. In 1990, Russell and coworkers [34,35] constructed an EB/TOF instrument. lons, generated using a pulsed Cs+ ion gun operated at 30 keV, are separated in the sector portion of this instrument. The use of an EB instrument provides high resolution of precursor ions. The selected precursor ions are decelerated from 8 kV to 1 kV and fragmented using CID or photodissociation. The unfragmented precursor ions and products are reaccelerated to 8 kV, reflected by a mirror and detected. A detector placed behind the mirror in the TOF portion of this instrument to detects neutral species resulting from PID. Since acquisition of a product spectrum requires adjustment of the electric and magnetic sectors, the time required to acquire a complete MS/MS map is not reduced by this instrument.

A number of instruments have been developed that use TOF for both precursor ion selection and product ion analysis. Initial MS/MS analysis developed from the observation of metastable decay in sector instruments. Both Standing *et al.* [36] and Della-Negra and LeBeyec [37] have detected fragment ions produced by metastable decomposition using a single stage time-of-flight instrument. Their instruments use pulsed ionization, an electrostatic ion mirror, a detector to measure the reflected ion spectrum (precursors and products) and a neutral detector, placed behind the mirror to identify the precursor ion that has fragmented. This approach is limited to metastable ions and is only effective when a few ions are in the flight path at one time. Thus, it is not suitable for use as a chromatographic detector.

In 1987 Schey et al. [38] developed a TOF/TOF instrument based on SID fragmentation. Precursor ion selection is performed via a set of deflection plates placed 40 cm into the ion path. The SID surface deflects the ion beam so that it is accelerated into and travels through a second mass analyzer placed at a 90° angle to the first mass analyzer. Although this approach was successful in the generation of product ions, the instrument was limited by poor resolution in precursor selection by beam deflection and poor product ion resolution.

Photodissociation has been performed at several locations in TOF instruments. Colby et. al. [39] performed MS/MS analysis on benzene and aniline with limited success by relying on their ability to selectively photofragment a chosen ion based on its behavior in the ion source of a TOFMS instrument. The precursor ion resolution of this approach was about 20; inadequate for any further consideration. Duncan and coworkers [40] performed PID at the turn-around point in the mirror of a time-of-flight mass spectrometer. Laser timing in this approach is simplified because ions spend a significant amount of time at their turn around point in the mirror. Unit mass resolution is achieved to m/z 200 for both precursor and product ions. This instrument has been used to analyze metal clusters and other compounds that do not require the resolution needed by a chromatographic detector. Weinkauf et al. [41] developed a TOF instrument that combines laser PID at the space-focus plane of the ion source and acceleration of the resulting product ions through a flight path containing a reflectron to the detector. This scheme is very similar in concept to our instrument with one very notable exception. The space-focus plane on this instrument is only 12 cm from the ion source. Precursor ion selection by the gate and laser are limited by this short distance especially for higher masses where the isomass ion packets are close together spatially. The duration and focusing of the laser pulse are not so precise that only one mass can be irradiated by a single laser pulse for high mass ions. These ions are resolved temporally but the isomass packets of adjacent masses are very close together. Thus, they proposed constructing an instrument identical to ours. Photodissociation will be performed at the space-focus plane of the first mirror to provide high resolution for selected precursor ions. Nearly all known TOF

instruments that use PID and SID are characterized by poor precursor and/or product ion resolution [42-44].

The lone exception to those instruments with poor product and/or precursor ion resolution was proposed by Cornish, Lys and Cotter [45]. Following laser desorption ionization, ions are accelerated and separate as they travel down the flight path through mirror 1 and back to the interaction region. A gate will be used to select the precursor m/z value. The precursor ion will be fragmented by either PID or SID. The resulting product ions and unfragmented precursor ions will be accelerated, travel down the flight path and be reflected by mirror 2 onto the detector. Presently this instrument only operates as a high resolution MS instrument. Resolution of 4000 has been achieved for desorbed samples when TOFMS is performed using the entire flight path.

6.5 The Tandem Time-of-Flight Mass Spectrometer

A tandem time-of-flight mass spectrometer (TOF/TOF), consisting of two consecutive MTOF instruments, was developed to use the speed and sensitivity advantages of the MTOF instrument for MS/MS analysis. A conceptual diagram of the TOF/TOF instrument is shown in Figure 6-1. Continuously-formed, stored ions are extracted from the ion source every few milliseconds. Temporal separation occurs as these ions travel through the flight tube and are deflected and focused by the first mirror. Precursor ion selection is accomplished by the gate or the gate/laser pulse combination for surface-induced dissociation or photodissociation respectively. The resulting product ions and unfragmented

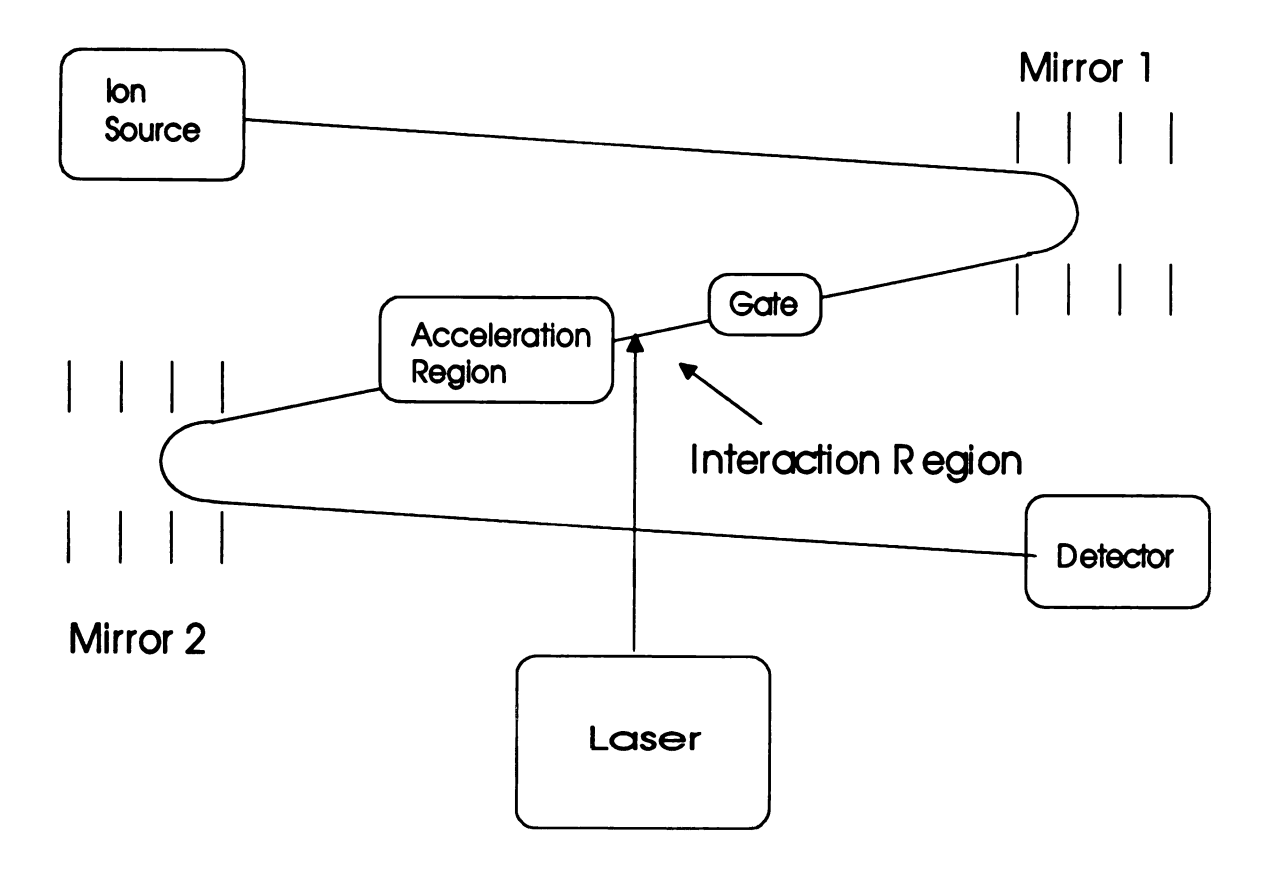


Figure 6-1. Conceptual diagram of the TOF/TOF instrument.

precursor ions are accelerated to impart mass dependent velocities. Temporal separation occurs as these ions travel to the detector via the second mirror.

This instrument can produce up to 500 product spectra per second. The mass spectrum generation rate is limited by the maximum repetition frequency of the excimer laser. Each ion source extraction pulse produces a transient waveform at the detector containing the product spectrum of the selected precursor ion. When coupled with TAD, the increased sample utilization of the TOF/TOF instrument should increase MS/MS sensitivity by a factor of 1000 over commercially available instruments. With these qualities, the addition of an ITR for time-array detection should produce an instrument capable of acquiring ten or more product spectra as a compound elutes from a capillary GC column.

6.6 Theoretical Considerations

The previously described MTOF instrument serves as the basis for the TOF/TOF instrument. The combination of a storage ion source and non-linear mirror in the MTOF instrument results in a large number of ions in a narrow packet at the detector (positioned at the space-focus plane of the first mirror). Thus, unit resolution or better is achieved for all precursor masses up to about 1200 in the TOF/TOF instrument.

The interaction region of the TOF/TOF instrument occupies the same position as the detector in the MTOF. All of the isomass ion packets are temporally and spatially focused at the interaction region. This focusing occurs

in the same place but at different times for ions of different mass-to-charge ratios. Precursor ion selection is initially accomplished by a gate placed before the interaction region. The requirements placed on the gate are dependent on the selected dissociation technique. When photodissociation is used, the gate deflects all ions with m/z values less than the selected precursor so that they do not reach the detector. (These ions can interfere with product ion analysis.) Final precursor ion selection is achieved by timing an excimer laser pulse so that its occurrence at the interaction region coincides with that of the desired precursor m/z value. The length of the laser pulse is approximately the same as the 20 ns temporal width of an isomass ion packet at the interaction region. Since only those ions in the interaction region at the time when the laser fires can photodissociate and the laser may not irradiate all ions in the isomass packet passed by the gate, the laser serves as the ultimate selector of the precursor ions. A second concern is that the laser must be made to irradiate only the selected precursor ion isomass packet. The Z-shaped flight path of the TOF/TOF instrument is tilted to guarantee that the laser beam only has the opportunity to interact with those ions in the interaction region. The physical space between ion packets of adjacent masses decreases as the m/z value increases. The dimensions of the isomass ion packets are determined by the physical dimensions of the ion source. The spatial width remains constant for ions of all m/z values. The time an ion spends in the interaction region is velocity- and thus mass-dependent. As the velocity of an ion packet decreases the arrival times become closer together and the focusing of the laser becomes more crucial.

The gate must pass only the precursor ion isomass packet if other dissociation techniques are employed. Unlike the laser pulse, the dissociation medium is present in the ion path for a substantial amount of time. Lighter ions will still interfere in product ion analysis, but so can ions with m/z values greater than that of the chosen precursor. When these heavy ions fragment, their products may have small enough m/z values to intrude into the product spectrum of the selected precursor. Thus, operating the gate in the mode required for these techniques means that its opening and closing must be precisely controlled. Fortunately, Karataev et al. [46] found the arrival time difference between m/z 866 and 867 was 105 ns for a one-meter instrument with an ion mirror. Since these dimensions are similar to the TOF/TOF instrument, a similar amount of time is present between adjacent masses.

Photodissociation of relatively small ions typically occurs within a few hundred femtoseconds of photon absorption by the ion [47]. The excited ion will travel less than a millimeter in this short time span. Thus, PID should only occur in the interaction region of the TOF/TOF instrument.

Separation of product and unfragmented precursor ions is achieved by accelerating them to a higher energy. They assume mass-dependent velocities which are dependent on the mass of the precursor ion as well as the mass of the generated product ion. If the product ions are not accelerated after formation, all of the product ions and the unfragmented precursor ions will travel at the same velocity to the second mirror. The field in this mirror will mass separate the ions. Unfortunately, using an ion mirror as a mass analyzer eliminates its ability to

energy-focus. Acceleration of the product ions after the interaction region will give them mass-dependent velocities. They now separate prior to arriving at the second mirror. Ions arriving at the second mirror are no longer monoenergetic as they were when entering the first mirror. For the second mirror to achieve perfect energy focusing, all of the ions should have approximately the same kinetic energy. When the difference in kinetic energy is minimized for all precursor and product ions, a wider range of product ion masses will be focused by the second mirror. Increasing the acceleration voltage after the interaction region to a larger value and reducing the initial energy of the precursor ion will minimize the energy differences between precursor and product ions. The maximum acceleration given to product ions is limited by instrumental considerations.

6.7 Design and Construction of the TOF/TOF Instrument

The responsibilities for design and construction of the TOF/TOF instrument have been divided into three areas: (a) source and flight path design and construction, (b) gate design and construction and (c) system control, sample introduction and implementation of the laser. My responsibilities are for system control. They include selection and purchasing of hardware capable of delivering the required critical timing and developing the software to control data acquisition. These items include the laser and necessary optics, transient recorder, delay generator and computer. Sample inlets were assembled to interface a gas chromatograph and a direct leak inlet to the ion source of the mass spectrometer. Work in these areas will be the focus of Chapter 6 of this thesis. A brief synopsis of the other areas of the instrument, principally

developed by Mary Puzycki/Seeterlin and Paul Vlasak, is presented in the following sections.

6.8 Overview of Other Areas

6.8.1 Ion Generation and Storage

The electron-impact ion source used in the TOF/TOF instrument is based on the Wollnik design shown in Figure 2-5. A diagram of the TOF/TOF source is shown in Figure 6-2. The most obvious difference between the two designs is the use of two opposing linear filaments in the TOF/TOF instrument rather than the cylindrical filament present in the Wollnik design. Electrons generated by the opposing filaments are accumulated in the ionization region between G2 and G3. The potential well is created by a combination of the electron space charge and the potentials on the source electrodes, G2 and G3. Storage times on the *ms* time scale have been achieved when the pressure of the ion source is ~10-7 *torr.* This should provide for efficient use of the ionized sample and a density of ions in each precursor isomass packet even though introduction of the helium carrier gas from the gas chromatograph will reduce this storage time. A 200 *V* pulse is applied to the rear electrode, G3, accelerating the ions out of the source. A second acceleration field, established between G2 and G1, raises the potential applied to the ions to 500 *V*.

Source

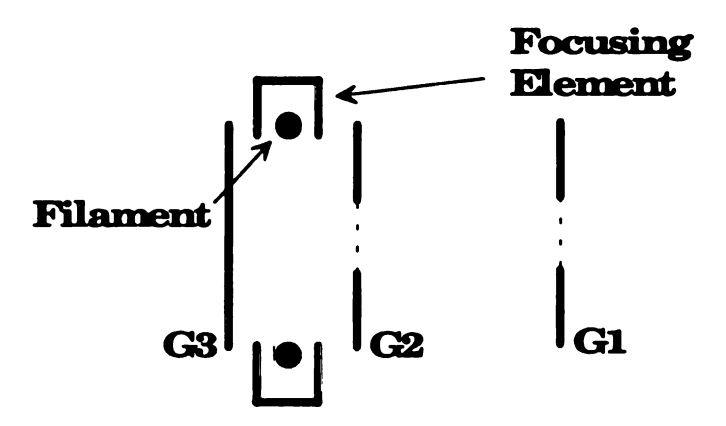


Figure 6-2. Ion source for the TOF/TOF instrument. This source is similar to the Wollnik source with the exception of the use of two opposing filaments.

6.8.2 Time-of-Flight Separation of Precursor lons

At the space focus plane, the precursor packet has a temporal distribution on the order of 20-40 *ns*. The ions in this packet also have a significant kinetic energy distribution introduced from their spatial distribution in the source. An Einzel lens and two pairs of steering plates are located just outside of the source. The former, in conjunction with the lensing effect of the mirror focuses the ions radially. The steering plates allow the ion beam to be directed onto the surface of the detector.

The ions travel down the flight path to a ten element grid-free mirror. This non-linear mirror reflects the ions to the space-focus plane of the first mirror. The flight path to the interaction region is 2.4 *m* and the resolution of separated ions is 1200 or more (FWHM definition).

6.8.3 Gating of the Precursor lons

The ion gate is placed on an optical rail in the flight path between the first mirror and the interaction region. The gate is of the variety described by Weinkauf et al. [41]. Two interleaved combs of fine wire are placed across the flight path of the ions. A voltage is applied to each of the sets of wires. A zero difference in the voltage applied between the two sets of wires passes ions through to the detector. When a potential difference is applied between the two wire sets, the beam is deflected away from the beam path.

The ability of the gate to keep ions of m/z values other than that of the desired precursor from reaching the interaction region is shown in Figure 6-3. These data were collected by placing the gate 6" in front of the interaction region. A 0.5" orifice was located 1.5" in front of the ion gate to prevent the gate from deflecting ions that would not normally strike the detector from being deflected onto it. The 1" detector face was allowed to limit the area at the interaction region. The fraction of ions reaching a detector placed in the interaction region was monitored as a function of the difference in the voltage applied between the two sets of wires in the gate. Ion transmission through the gate is high when the two combs are operated within 20 V of each other. As expected, the transmission efficiency drops as the voltage difference increases. Based on the experimental results and calculations, the voltage difference between the two sets of wires should be about 260 V for rejection when ions were accelerated to 500 V in the first mass analyzer. This potential difference will need to be exceeded because ion packets with m/z values similar to that of the selected precursor will experience only a fraction of the deflection field due to their spatial and temporal proximity to the precursor.

The gate conditions described above satisfy the requirements of precursor ion selection those for CID or SID in a multichannel plate. When these techniques are used for fragmentation, only the precursor ion packet must be allowed to enter this region. Photodissociation puts less stringent requirements on the gate. Ions of all m/z values may travel through the interaction region. The goal of the gate is simply to impart a trajectory on all ions with masses less than the selected precursor which will keep them from striking the detector surface.

Gate Deflecting Power

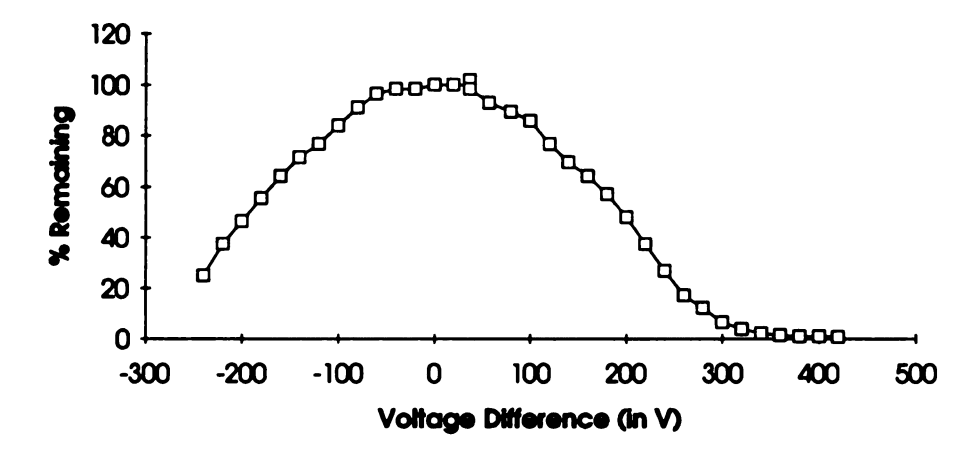


Figure 6-3. Graph showing the percent of ions transmitted from the gate to the interaction region as a function of the voltage difference between the two elements in the gate assembly.

Since the flight path from the gate to the detector is several meters, the voltages applied to the gate may be correspondingly smaller.

6.8.4 Time-of-Flight Analysis of Product Ions

Acceleration of the ions just following the interaction region, gives the product ions mass-dependent velocities and reduces the relative product ion kinetic energies. The product ions will be permitted to fragment prior to this acceleration. The acceleration grid is placed on an optical rail between the interaction region and the second mirror to allow the time between excitation and acceleration of the ions to be fragmented. Since the time between excitation and fragmentation is may depend on many factors, adjustment of the acceleration region position will facilitate its optimization.

Acceleration of ions after the interaction region allows temporal separation of the product ions. With a precursor ion energy of 500 V and a secondary acceleration of 1000 V, the range of energies for a selected precursor and its products will be 1000 to 1500 V. The focusing power of the second mirror is increased as the relative differences in kinetic energy between precursor and product ions is reduced. Simulation using a simple linear mirror indicates that resolving power of the second mass analyzer should yield unit mass resolution for all products of precursors with m/z as high as 1000. The use of a non-linear mirror should improve this value somewhat.

6.9 Summary and Conclusions

This chapter describes the MS/MS instruments based on time-of-flight analysis and the role of photodissociation in mass spectrometry. Although this description does not include all investigators in these fields, all significant advances have been described for both topics.

Some time-of-flight MS/MS instruments are hybrids consisting of a time-of-flight instrument coupled with another type of mass spectrometer. These instruments may have good resolution of precursor and product ions, but achieve it at the cost of slower mass spectral acquisition. Other instruments use TOF analysis for both precursor ion selection and product ion analysis. All tandem time-of-flight mass spectrometers which do not have a mirror in each section that is devoted to energy focusing have suffered from poor resolution of precursor and/or product ions.

Photodissociation has great potential as a fragmentation technique and seems ideally suited for TOF instruments where collisions with a surface or gas can adversely affect resolution. A photon introduces a discrete amount of energy into an ion without altering its velocity and dissociation occurs within a few hundred femtoseconds of photon absorption for small ions. Photodissociation efficiency for an ion depends on the structure of the ion, photon flux of the laser and laser wavelength.

The MTOF/ITR system also serves as the foundation for the development of the TOF/TOF instrument. The ion source/mirror combination that provides the resolving power and sensitivity of the MTOF can be extended to tandem mass spectrometry. The TOF/TOF instrument has been designed and constructed to realize the possibility of MS/MS on the capillary chromatographic time scale. The second portion of this thesis will describe the hardware and software that have been developed and integrated to provide the critical timing required for the TOF/TOF instrument.

References

- McGilvery, D. C.; Morrison, J. D. Int. J. Mass Spectrom. Ion. Physics 1978, 28, 81.
- 2. Krailler, R. E.; Russell, D. H. Anal. Chem. 1985, 57, 1211.
- 3. Krailler, R. E.; Russell, D. H. Int. J. Mass Spectrom. Ion Processes 1985, 66, 339.
- 4. Watson, C.H.; Baykut, G.; Eyler, J. R., ACS Symp. Ser., 1987, 359 (FTMS), 140.
- Baykut, G.; Watson, C. H.; Weller, R. R.; Eyler, J. R. J. Am. Chem. Soc.
 1985, 107, 8036.
- 6. Krailler, R. E.; Russell, D. H. *Int. J. Mass Spectrom. Ion Phys.* **1985**, *66*, 339.

- Bowers, W. D.; Delbert, S. S.; McIver, R. L. J. Am. Chem. Soc. 1984, 106,
 7288.
- 8. Honovich, J. P.; Dunbar, R. C. J. Am. Chem. Soc. 1982, 106, 7288.
- 9. Hunt, D. F.; Shabanowitz, J.; Yates, J. R., III, *J. Chem. Soc., Chem. Commun.* 1987, 548.
- Cassaday, C. J.; Fresier, B. S.; Russell, D. H. *Org. Mass Spectrom.* 1983,
 18, 3789.
- 11. Honovich, J. P.; Dunbar, R. C. J. Am. Chem. Soc. 1982, 104, 6220.
- 12. Dunbar, R. C. in *Gas Phase Ion Chemistry, Vol.* 2, M. T. Bowers, Ed., Academic: New York, 1979, 187.
- Watson, C. H.; Baykut, G.; Battiste, M. A.; Eyler, J. R. Anal. Chim. Acta
 1985, 178, 125.
- 14. Dunbar, R. C. in *Gas Phase Ion Chemistry, Vol. 3*, M. T. Bowers, Ed., Academic: New York, 1984, 129.
- 15. Dunbar, R. C. Anal. Instrum. 1988, 17, 113.
- 16. Dunbar, R. C. J. Chem. Phys. 1989, 91, 6080.
- 17. Sheil, M. M.; Derrick, P. J. Org. Mass Spectrom. 1988, 23, 429.
- Vaida, V.; Welch, J. A. in *Advances in Laser Spectroscopy, Vol. 3*, B. A.
 Garetz and J. R. Lombardi, Eds., John Wiley and Sons: New York, 1986, 159.

- 19. Zandee, L. Bernstein, R. B. J. Chem. Phys. 1979, 70, 2574.
- 20. Boesl, U.; Weinkauf, R.; Walter, K.; Weickhardt, C; Schlag, E. W. *J. Phys. Chem.* **1990**, *94*, 8567.
- Chupka, W. A.; Colson, S. D.; Seaver, M. S.; Woodward, A. M. Chem.
 Phys. Lett. 1983, 95, 171.
- 22. Baykut, G.; Watson, C. H.; Weller, Eyler, J. R. *J. Am. Chem. Soc.* 1985, 107, 8036.
- 23. Hunt, D. F.; Shabonowitz, J.; Yates, R. J. *J. Chem. Soc., Chem. Commun.* **1987**, 548.
- 24. Hill, J. A.; Annan, R. S.; Biemann, K., Presented at the 38th ASMS Conference on Mass Spectrometry and Allied Topics, Tucson, AZ, June 3-8, 1990.
- 25. Tecklenburg, R. E., Jr., Russell, D. H. Mass Spectrom. Reviews 1990, 9, 405.
- Tecklenburg, R. E., Jr.; Miller, M. N.; Russell, D. H. J. Am. Chem. Soc.
 1989, 111, 1161.
- 27. Wagner-Redeker, W.; Levsen, K. Org. Mass Spectrom. 1981, 16, 538.
- 28. Mukhtar, E. S.; Griffiths, I. W.; Harris, F. M.; Beynon, J. H. *Org. Mass Spectrom.* **1981**, *16*, 51.
- 29. Boesl, U.; Neusser, H. J.; Schlag, E. W. *J. Chem. Phys.* **1980**, *72*, 4327.

- 30. Segar, K. R.; Johnston, M. V. Org. Mass Spectrom. 1989, 24, 176.
- 31. Glish, G. L.; McLuckey, S. A.; McKown, H. S. Anal. Instr. 1987, 16, 191.
- 32. Gandy, R. M.; Ampulski, R.; Prusaczyk, Johnston, R.H. Int. J. Mass Spectrom. Ion Physics 1977, 24, 363.
- 33. Stults, J. T.; Enke, C. G.; Holland, J. F. *Anal. Chem.* **1983**, *55*, 1323.
- 34. Russell, D. H.; Strobel, F.; White, M. A., Presented at the 38th ASMS Conference on Mass Spectrometry and Allied Topics, Tucson, AZ, June 3-8, 1990.
- 35. Strobel, F. H.; White, M. A.; Preston,. L.; Russell, D. H., Presented at the 39th ASMS Conference on Mass Spectrometry and Allied Topics, Nashville, TN, May 19-24, 1991.
- 36. Standing, K. G; Beavis, R.; Bolbach, G.; Ens, W.; Lafortune, M.; Main, D.; Schueler, Tang, X.; Westmore, J. *Anal. Instr.* **1987**, *16*, 173.
- 37. Della-Negra, S.; LeBeyec, Y. L. Anal. Chem. 1985, 57, 173.
- 38. Schey, K.; Cooks, R. G.; Grix, R.; Wollnik, H. Int. J. Mass Spectrom. Ion Processes 1987, 77, 49.
- 39. Colby, S. M.; Yang, M.; Reilly, J. P., Presented at the Pittsburgh Conference, Atlanta, GA, March 7, 1989.
- 40. LaiHing, K.; Cheng, P. Y.; Taylor, T. G.; Willey, K. F.; Peschke, M.; Duncan, M. A. *Anal. Chem.* 1989, *61*, 1458.

- 41. Weinkauf, R.; Walter, K.; Weickhardt, C.; Boels, U.; Schlag, E. W. Z. Naturforsch. 1989, 44a, 1219.
- 42. Geusic, M. E.; Jarrold, M. F.; McIlrath, T. J.; Freeman, R. R.; Brown, W. L. *J. Chem. Phys.* 1987, *86*, 3862.
- 43. Liu, Y; Zhang, Q.-L.; Tittle, F. K.; Curl, R. F.; Smalley, R. E. *J. Chem. Phys.* **1986**, *85*, 7434.
- 44. Brucat, P. J.; Zheng, L.-S.; Pettiete, C. L.; Yang, S.; Smalley, R. E. J. Chem. Phys. 1986, 84, 3078.
- Cornish, T.; Lys, I.; Cotter, R. J., Presented at the 39th ASMS Conference on Mass Spectrometry and Allied Topics, Nashville, TN, May 19-24, 1991.
- 46. Karataev, V. I.; Mamyrin, B. A.; Shmikk, D. V. Sov. Phys. Tech. Phys. 1972, 37, 45.
- 47. Rosker, M. J.; Dantos, M.; Zewail, A. H. Science 1988, 241, 1200.

Chapter 7

System Control of the TOF/TOF Instrument

7.1 Introduction

The focal point of the tandem time-of-flight MS/MS instrument is the interaction region. Here precursor ions are selected and fragmented, and the resulting product ions are accelerated to mass-dependent velocities. When photodissociation is used as the fragmentation technique, the overlap between the arrival of the ion packet and light from the laser emission also serves as the final selector of the precursor m/z value. The ion source extraction pulse, gate trigger and laser emission all play a role in precursor selection and must be adjusted to an optimal value to maximize photodissociation efficiency. The TOF/TOF instrument can generate thousands of transients per second. The instrument components, which provide trigger signals, produce the photon beam and acquire transients, must all function at these high repetition rates with high precision. Since precursor ions of different masses arrive at the interaction region at different times, the timing must be adjustable as well as precise. Thus, the selection of the laser, timing elements and transient recorder are crucial to the development of this instrument. A control system is required to fully use the capabilities of each component and integrate all of them into a photodissociation system.

7.2 Spatial-Temporal Considerations for the Interaction Region

The amount of time that an ion spends in the region irradiated by the laser beam is mass-dependent. Assuming that the laser beam is focused to a width of 0.1 mm, an isomass ion packet with a m/z value of 100 will travel through the area irradiated by the laser in about 20 ns while an ion packet with m/z 1000 will remain in the interaction region for 60 ns. Despite the large variation in the amount of time that ions of different m/z values spend in the irradiated region of the interaction region, all isomass ion packets have the same spatial dimensions. Final selection of precursor ions is determined by the duration and size of the laser beam. This overlap will also determine the initial spatial and temporal distribution of product ions. Thus, all of the critical timing for precursor ion selection and product ion formation must be performed with variations less than about 5 ns to provide a large and reproducible amount of parent ion/laser pulse overlap.

7.3 Laser Considerations

Acquiring MS/MS data sets on the chromatographic time scale places stringent requirements on the photodissociation laser. The laser must be capable of operating at high repetition rates to provide the largest possible number of transients containing MS/MS information per second. Photodissociation in this instrument is intended to produce a great deal of fragmentation. The laser must have high power to produce photon densities

,

large enough to fragment a significant fraction of the selected precursor ions. In our case the number of photons involved in the dissociation process is unimportant. The large difference between one and two-photon photodissociation cross-sections reveals that most of the PID products will result from single-photon interactions. The laser should be able to operate in the UV region to allow significant amounts of energy to deposited into a precursor by a single photon. The duration of the laser pulse should be the same amount of time as an isomass ion packet spends in the interaction region. Finally, the time at which laser emission occurs should have no more than a few nanoseconds of pulse-to-pulse variation. Laser emission should also be reproducible over several hours differing by only a few nanoseconds. The laser power should be very reproducible pulse-to-pulse and for operation over several hours.

Few lasers can operate at repetition rates compatible with the TOF/TOF instrument and still have high power. Two types of lasers that have the qualities necessary to fulfill the requirements of the TOF/TOF instrument are excimers and Neodymium:YAG (Nd:YAG) lasers. Although most excimer and Nd:YAG lasers are designed to run at much slower repetition rates, a few are able to provide high power at high repetition rates. Features of two of these—the Questek 2580vB excimer and Quantel International Vertex 1000 Nd:YAG laser are shown in Table 7-1. Although neither of these lasers operates at the desired level of 1 kHz or more, these two approach the desired goal of high repetition rates and high power. One major advantage of the excimer is its power at UV frequencies. The excimer can operate at any one of six fundamental frequencies

Table 7-1. Comparison of Excimer and Nd:YAG Lasers

	Excimer (QUESTEK 2580vB)	Nd:YAG Laser (QUANTEL VERTEX 1000)
Maximum Repetition Rate (Hz)	500	840
Pulse Duration (ns)	9-31	7-12
Available Wavelengths (nm)	157, 193, 222, 248, 308, 351	1064, 532, 355, 266
Pulse Energy (mJ)	500 at 248 nm	3 at 266 nm
Jitter (ns)	±2	2.5
Energy Stability (%)	± 3-8	3.5-10

and produce high energy pulses (300 *mJ* or more). Although the Vertex 1000 has an energy of 85 *mJ* at its fundamental frequency, quadrupling the frequency to 266 *nm* reduces the pulse energy to a mere 3 *mJ*. This is 100 times less energy than is available from the excimer. Both types of laser are capable of producing pulses with durations in the irradiated portion of the interaction region similar to that of an ion packet in the GC/MS mass range. Thus, the laser pulse durations range from 7-12 *ns* and 9-31 *ns* for the Nd:YAG laser and excimer respectively; these compare favorably with mass peaks that remain in the interaction region for about 20 *ns*. The jitter between pulses and pulse-to-pulse energy variations are both in an acceptable range for use with the TOF/TOF instrument.

A Questek 2580vB excimer was selected as the photodissociation laser for the tandem time-of-flight instrument based on its ability to provide high power at high repetition rates. A dye laser, pumped by the excimer, was also purchased to increase the number of wavelengths available for photodissociation studies and for use in fundamental studies of photodissociation in mass spectrometers.

Only those ions irradiated by the laser pulse are potential precursors. The initial dimensions of the laser beam are about 10 mm tall by 20 mm wide. Since final precursor selection is performed by the laser, focusing of the laser beam will improve precursor ion resolution. Assuming that the accelerating voltage applied to ions leaving the ion source is 700 V and that the length of the effective flight path to the interaction region is 2.4 m, ions of m/z 1000 will reach

the interaction region 140 ns before ions with m/z 1001. After traveling from the ion source to the interaction region, ions from these two adjacent masses are separated by about 1.2 mm. Under these same conditions, ions with m/z 600 will reach the interaction region 188 ns before those of m/z 601. The isomass ions from these packets will be separated by a distance of about 2 mm in the first mass analyzer. Simulations and initial ion source studies indicated that the ion beam would be circular with a diameter of about 1 cm. Accordingly, the laser beam was focused to 10 mm tall \times 1 mm wide. These dimensions are adequate for all m/z values in the GC/MS mass range in the TOF/TOF instrument.

7.4 System Control

The key to MS/MS in a tandem time-of-flight mass spectrometer is to produce the largest possible overlap between the arrival of the precursor ion packet and laser beam in the interaction region. The system that controls the elements needing critical timing—the ion source, gate, laser and transient recorder—must be accurate to provide the proper timing and flexible to allow different types of experiments to be performed.

The control system for the TOF/TOF instrument is shown in Figure 7-1. Critical timing for the photodissociation system is provided by a delay generator which is controlled by a Zenith 486 computer with 33 *MHz* clock. All components involved in the critical timing were equipped with a general purpose information bus (GPIB) to allow communication with the computer. Elements of the critical

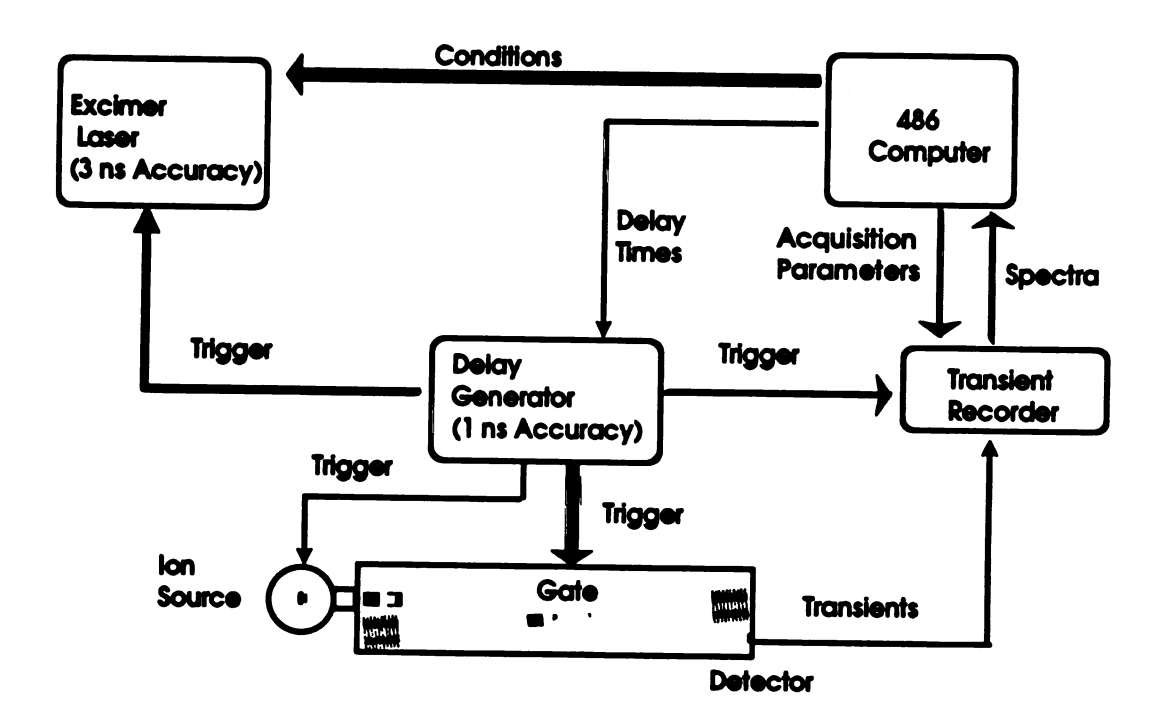


Figure 7-1. System control for the tandem time-of-flight mass spectrometer.

r

Sh

[86 [3]

370

, e. s.

3€ 30 90 timing system include the delay generator, transient recorder, and laser. The requirements and capabilities for each of these components are described in the following sections. Although the ion source and gate require a precise trigger, they will not be included in this discussion since they respond to the trigger signal.

7.4.1 Delay Generator

The most critical element involved in controlling the timing for photodissociation for the TOF/TOF instrument is the delay generator. The delay pulses that trigger the laser, ion source, gate and transient recorder must be controlled precisely. Thus, a minimum of three independent output channels are needed to trigger the ion source, gate and laser. (The transient recorder can be triggered at the same time as any of these components.) The delay generator for this system would ideally trigger each component with picosecond precision to produce only small variations in the overlap of the selected precursor ion packet and laser emission. The output pulse of the delay generator should have a fast rise-time to increase the precision in triggering the ion source, laser and gate. The values in the delay generator must be changed to allow acquisition of the product ions for different precursors. Resetting the delay values for each channel of the delay generator must be performed in a small amount of time to avoid wasting laser pulses and achieve our goal of 10 product spectra per second.

è

A LeCroy Model 4222 delay generator was chosen to supply all of the necessary delays for the TOF/TOF instrument. This CAMAC module supplies 170 *ns*- 16.7 *ms* delays over four channels triggered with a common input. Although the 1 *ns* resolution for each channel is larger than the desired picosecond range, this variation is still small enough to allow irradiation of a portion of the precursor ion packet since the ion packet is typically wider than the duration of the laser pulse. The LeCroy delay generator can be retriggered 100 *ns* after the last delay without any external input. The output from the delay generator is a 5 *V* pulse with a 1 *ns* rise-time.

7.4.2 Transient Recorder

The most important feature required for a transient recorder used with a time-of-flight mass spectrometer is the ability to sum the transient signals from the mass spectrometer as rapidly as possible. While an integrating transient recorder can perform this function for ion source extraction rates of 5 kHz [1], no commercially available instruments had this capability. Most commercial digital oscilloscopes acquire summed data using a weighted approach. This is not useful for a mass spectrometer which requires true summing capabilities. These instruments also have a trade-off between the number of data points acquired by the scope and summing rate. The highest summing rates are attained when only a few data points are summed. Unfortunately, acquisition of only a few points requires sacrificing resolution or mass range from a mass spectrum. Another desired feature for the transient recorder is a wide dynamic range to allow

acquisition of signals of very different intensities. Finally, the transient recorder should be interfaced to the computer to load acquisition parameters and to provide computer processing of the data acquired by the transient recorder.

The LeCroy 9450 digital oscilloscope provides true summed averages, 450 megasamples per second, 10 bit analog-to-digital conversion, storage for acquisition parameters and acquired data, and a Motorola 68020 microprocessor that controls operation of the oscilloscope and performs data processing storage. This transient recorder can be controlled remotely by the 486 computer via the GPIB network to load acquisition conditions or download data to the computer. The LeCroy 9450 digital oscilloscope can store seven complete sets of acquisition conditions internally. Since the GPIB network is relatively slow when compared to the internal microprocessor of the transient recorder, conditions are most easily changed by loading the stored front-panel setups. The transient recorder can then operate independently from the computer and acquire data for the selected conditions.

Like most of the available transient recorders, the LeCroy 9450 digital oscilloscope possessed the trade-off between the number of points acquired and the summing rate. This model acquires summed averages rather than just sums. A study was conducted to determine the amount of time required to acquire summed averages of 300 transients while acquiring different numbers of points across each waveform. A TTL signal from a function generator was operated over a range of frequencies compatible with the TOF/TOF instrument. The

number of summed averages performed per second for different numbers of data points at a variety of triggering rates is shown in Table 7-2. According to its manufacturer, this digital oscilloscope can acquire about 30 sums each second. This is confirmed by the data in Table 7-2. This rate is only achieved if the number of points acquired is 2000 or less. The information contained in a complete mass spectrum is not adequately sampled when only 2000 points are acquired unless the points are acquired over a narrow time window. When the range is extended to include 50,000 points per sum, the summing rate remains at about 5 Hz for all triggering frequencies between 20 and 500 Hz. Another concern is the ability of the transient recorder to use the information in as many transients as possible. Efficiency of the summed average procedure for a 5000 point window is shown in Figure 7-2. As expected, the transient recorder has its highest efficiency when it is triggered between 20 and 40 times per second. However, the fastest summing rates are available when the transient recorder is triggered more 200 times per second. Operation of the laser and transient recorder at high repetition rates will decrease the time required for acquisition of a product ion spectrum while using only a small fraction of the transients.

The above data show that the transient recorder will be the component that limits the data acquisition time. Under ideal circumstances, only about 30 transients can be summed per second regardless of the repetition rate of the mass spectrometer or laser. This translates to acquiring a product ion spectrum every 1.67 s if 50 transients are summed to make a mass spectrum. When the laser is operated at 500 Hz, summing the same number of transients would

Table 7-2. Summing Times (Summed Averages per Second) for Different Numbers of Points at Different Frequencies

Number of Points	50	100	200	500	1000	2000	5000	10,000	50,000
Frequency									
20 Hz	6.71	6.69	6.61	6.68	6.61	6.66	6.56	6.34	5.06
27 Hz	6.85	6.87	6.84	6.88	6.86	6.85	6.72	6.72	5.30
36 Hz	12.17	11.09	11.01	11.09	11.34	11.24	10.65	10.56	5.39
50 Hz	12.52	12.33	12.38	12.41	12.33	12.05	12.33	11.26	5.33
60 Hz	11.15	11.17	11.14	11.43	11.19	11.34	10.75	10.40	5.37
100 Hz	18.76	19.46	19.08	19.57	19.65	18.90	18.73	18.38	6.13
133 Hz	19.76	19.49	19.88	19.80	19.88	19.69	19.12	18.21	6.66
200 Hz	27.62	27.62	27.55	26.95	26.60	27.32	26.74	19.16	6.72
250 Hz	27.10	27.25	26.95	26.60	26.95	26.95	25.91	19.16	6.72
294 Hz	28.17	28.33	27.62	27.55	27.86	27.10	27.40	19.19	6.71
357 Hz	28.09	27.93	27.86	28.01	27.86	27.93	27.10	19.34	6.71
500 Hz	29.24	29.24	29.15	29.41	29.24	29.07	23.26	17.64	5.30

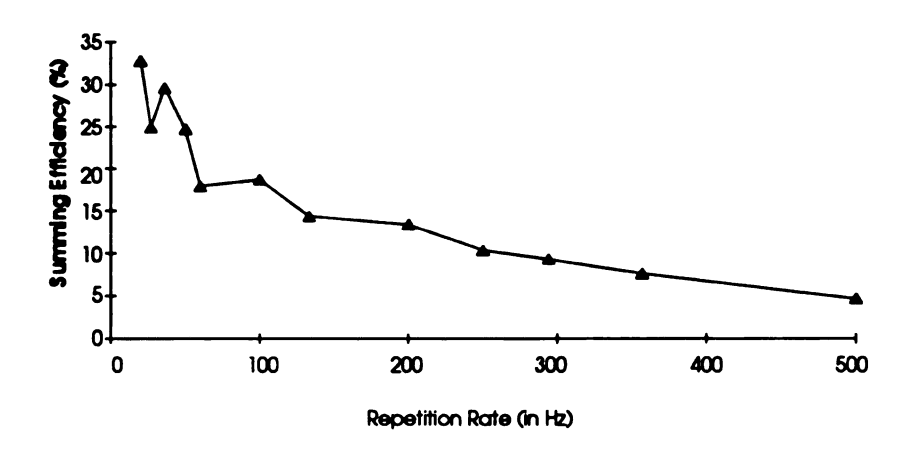


Figure 7-2. Percent of transients used by the LeCroy 9450 for a 5000 point acquisition window at triggering rates between 20 and 500 Hz.

result in acquisition of a product ion spectrum every 0.1 s. Obviously, true GC/MS/MS analysis requires the more efficient use of ions provided by an integrating transient recorder.

7.4.3 Laser

The Questek 2580vB laser can be triggered in several modes. The mode that provides the best accuracy and precision in the time at which light is emitted happens when the laser is triggered by an external source with the command charge feature turned off. When command charge is off, the high voltage power supply is charged continuously. The other option for the command charge feature is to charge the high-voltage supply only after receiving the trigger signal. The laser jitter with the command charge off is 2 ns or less according to the manufacturer. The manufacturer also reports that the excimer trigger signal should be about 7 V in intensity and several microseconds in duration for reproducible operation. We were able to externally trigger the excimer using a variety of signals including a TTL signal from a function generator, a square wave generated by a National Instruments AT-MIO-16F-5 board, and the signal from the delay generator. The most interesting result of these experiments was that the laser was consistently triggered by signals that were only 3 V in intensity. The delay generator signal was more intense but had a width of 150 ns. Thus, controlled triggering of the laser can be performed from several components in the system.

A second concern with laser operation was the need to know the time delay between triggering and light emission and any litter or long-term drift associated with this process. The delay between triggering the excimer and thyratron discharge is fairly constant for a given repetition rate once the instrument has reached a stable operating temperature (about 15 minutes). Consultation with Questek revealed two possible pathways that can be used to estimate when light is emitted by the laser: monitor the time at which the thyratron discharges and use a fast photodiode to determine when light is emitted. The first of these approaches is the simplest and also the least accurate. The thyratron discharge occurs within only a few nanoseconds of light emission, giving this approach accuracy to about 10 ns. This procedure can be performed using an oscilloscope. The laser trigger is also given to the oscilloscope. An oscilloscope lead is placed on top of the covered laser. When the thyratron switches and releases the 26-32 kV charge stored in the capacitors of the excimer, this signal can monitored on the oscilloscope. An example of the signal produced is shown in Figure 7-3. The thyratron discharge occurs at the time of the first fluctuations in the oscilloscope signal. The second approach has accuracy to about one nanosecond and measures light emission itself. A beam splitter is inserted into the path of the laser beam and a portion of the beam is directed onto a piece of white cardboard such as a business card. When the laser beam strikes the card, it fluoresces. The signal from the fast photodiode which detects the fluorescence is measured to determine the delay between triggering the laser and light emission.

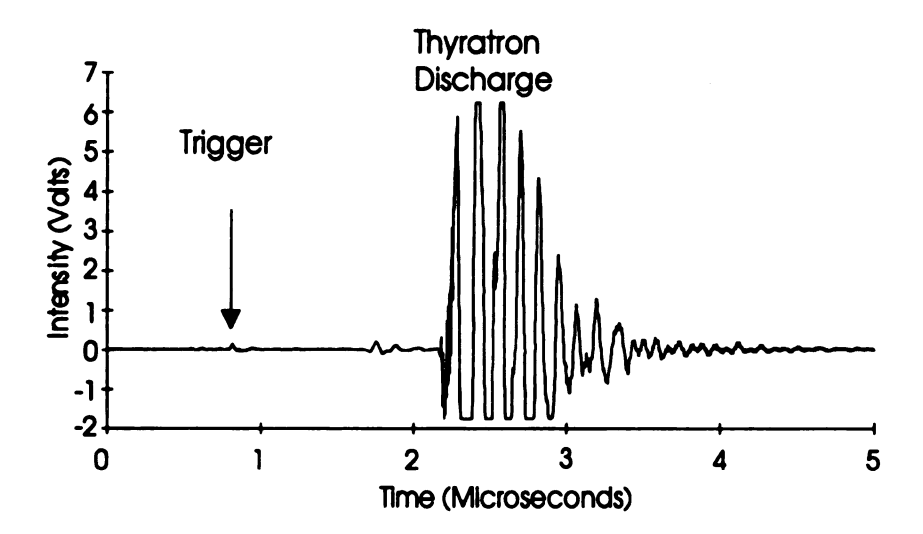


Figure 7-3. The signal produced by the thyratron discharge. The delay time is the time between triggering the excimer and the first response in the thyratron discharge signal.

The delay between triggering of the excimer and thyratron discharge was found to change by 50 *ns* as the repetition rate of the laser was increased from 20 to 325 Hz. Changes in repetition rate produced different, but precise trigger/discharge delay times. This delay time was monitored at several different frequencies over the course of several hours. Once the laser had warmed to operating temperature and been stabilized by fifteen minutes of operation at the desired repetition rate, these times were monitored. Delay times remained within a few nanoseconds for each of these repetition rates, but were of different durations for different laser repetition rates. Thus, the laser can be fired reproducibly and the time of light emission can be determined. Actual optimization of the delay times to produce the best overlap between the laser pulse and ion packet is an empirical process that is greatly simplified by characterization of the laser delays.

7.5 Command Flow for Data Acquisition

Acquisition of product ion data sets from an unknown compound involves several different steps. The first of these is to acquire a normal mass spectrum. The *m/z* values and arrival times at the interaction region can be determined for all precursor ions from this mass spectrum. A product spectrum is then collected using the arrival times of the precursor ions at the interaction region determined from the normal mass spectrum. The components of the TOF/TOF must function differently for the acquisition of normal mass spectra and product spectra. The steps required for the collection of both types of spectra are described below.

Normal mass spectra are acquired by allowing ions of all *m/z* values to be detected. The gate must be left open and the laser off to make sure that all potential precursor ions are detected. Conditions for the transient recorder and delay times for the ion source extraction pulse are loaded, and the transient recorder performs a summed average on a selected number of transients. The mass spectrum is transferred to the computer where further data processing is performed.

Acquisition of product spectra involves a different sequence of events. The normal mass spectrum is inspected to determine precursor ion m/z values and the arrival time of these m/z values in the irradiated portion of the interaction region. Delay times for the ion source extraction pulse, gate pulse and transient recorder are selected for each precursor. Conditions are then loaded into the transient recorder. The previously determined source and gate delay times are loaded into the delay generator and a mass spectrum is acquired. The acquired mass spectrum is transferred from the transient recorder to the computer to complete the acquisition of a single product spectrum. The laser is operated at a constant repetition rate during this process to provide it with the best operating environment. Subsequent product spectra are acquired by changing the delay times for the gate and ion source, capturing the data on the transient recorder and transferring them to the computer. The transient recorder conditions should not require alteration to acquire different product spectra under most circumstances. Since the transient recorder requires the greatest amount of time for configuration, leaving its conditions unchanged while acquiring several

product spectra reduces the time required to collect a complete product ion data set.

The data flow through the system is the same for both normal and product spectra. Transients are detected and summed averaging is performed by the transient recorder. The captured spectra are transferred to the computer where the spectral information is converted to mass intensity pairs for both types of spectra. Because the flight time of a product ion is dependent on the m/z value of its precursor as well as the mass of the product ion, calibration is more complex and a separate calibration is required for each product spectrum. This problem is more fully discussed in Chapter 8 of this thesis.

7.6 System Control Software

The software for the TOF/TOF instrument must combine the capabilities of each of the system elements involved in critical timing, and manipulate the data generated by the mass spectrometer. The laser, transient recorder and delay generator are all microprocessor controlled. These components function most efficiently when allowed to perform their functions independently. For instance, once conditions are loaded into the delay generator, the delay values are used every time the delay generator is triggered until a new set of conditions are loaded. The role of the computer in the operation of the microprocessor-controlled components is to provide the information necessary for the instrument

to begin its functioning. Once data have been acquired by the transient recorder, it must be transferred to the computer for display and other types of processing.

The instrument control programs for the TOF/TOF instrument were written using LabWindows version 2.0, a software package available from National Instruments. LabWindows provides an integrated programming environment for data acquisition using a personal computer (PC). Instruments can be constructed using instrument drivers and libraries that comprise the software. This flexibility of LabWindows allows rapid creation of simple data acquisition routines using either Basic or C languages. More complex, permanent programs can also be constructed using the same building blocks.

7.6.1 Overview of the TOF/TOF Instrument System Control Programs

Data acquisition and processing are accomplished using a series of three programs. The first of these allows the user to select a set of data acquisition conditions including the file name, trigger rate, delay generator and transient recorder settings. (Drivers supplied as a part of the LabWindows software provide communication with the delay generator and transient recorder via the GPIB network.) This program acquires data, transfers it to the host Zenith 486 computer and displays it. The second program provides the capability for a user to review the acquisition conditions which are stored within a LeCroy binary format. The final program converts data from the LeCroy binary format into a tab delimited ASCII file. This ASCII file may be imported into other programs for

further processing. These programs, associated function panels, and instrument drivers that I created are included in the Appendix.

7.6.2 Instrumental Characteristics Requiring Special Attention

Some features of the system components and their drivers have required special attention in the TOF/TOF instrument control program and in achieving MS/MS on the chromatographic time scale. These qualities and special concerns are described in this section.

The GPIB network can transfer 1 *Mb* of information per second for read and write operations [2]. Although a significant amount of data can be handled per second, a typical compressed binary file acquired by the LeCroy 9450 digital oscilloscope occupies about 10 *Kb*. Transferring a single data file of this size requires 0.01 *s*. Acquisition of ten product ion spectra per second requires 0.1 *s* to simply transfer the acquired spectra from the transient recorder to the computer. This does not include the time needed to configure the instrumental components for each spectral acquisition or the time required by each component to implement these conditions. Communication via a GPIB network is not viable for acquisition of complete product ion data sets for GC/MS/MS analyses unless the network is confined to carrying small amounts of information.

Drivers for the LeCroy instruments restrict the amount of data that can be stored in a single file and the number of files that can be acquired in a single run. Data from an array collected by the transient recorder are written to a data file. Although the LeCroy 9450 digital oscilloscope is capable of acquiring data sets containing 50,000 points, this array (called "spec" in the TOF/TOF instrument control program) is defined as an integer which can only contain 8192 elements. Portions of the acquired data set can be stored to different arrays which can be transformed into data files. Unfortunately, the value of the first point in the array also has an upper limit of 8192. Thus, even when 50,000 of data points are acquired by the transient recorder, only the first 16,384 can be captured by the computer. Accurate display of mass spectral information requires multiple data points over a peak. Since adequate sampling of a wide mass range requires the acquisition of a large number of data points, the mass range must sometimes be reduced to provide a suitable number of samples across a mass peak. Multiple runs may be needed to adequately characterize a wide range of m/z values.

The driver for the transient recorder did not contain several options including the summed average feature that we use predominantly. Transferring all of the acquisition conditions across the GPIB network is slower than allowing the transient recorder to load a set of conditions that are stored internally. I chose to limit the time required for loading the appropriate acquisition parameters by recalling the conditions from one of the six sets of front panels stored by the oscilloscope. This has the added benefit of fully using the

capabilities of the 80286 microprocessor in the transient recorder and freeing the computer to communicate with other components of the TOF/TOF instrument.

The lack of any options in the driver for the LeCroy 9450 digital oscilloscope also means that the computer is unable to determine when summing is complete for a series of transients. Without any modifications in the TOF/TOF instrument control program, the computer captures a single transient rather than the summed average of many transients. The Finished_Summing routine was included in the instrument control program to insure that the computer acquires the desired summed average. This routine monitors the status of a specific bit to determine when data acquisition is complete. This bit can give false positive responses when gueried by the computer depending on the instrumental channels involved in the summing process. A data acquisition pathway must be determined by the user prior to acquisition of the summed average. If the pathway for the summed average includes either of the two function channels (E or F), but not both, the user selects one Finished Summing routine. If the pathway includes both functions E and F, a second routine is selected. The false positive response can occur when the first route is designated by the user when both of the function channels are involved in the data collection. During acquisition of the summed average, the bit will show a value that is identical to that required to end the Finished_Summing routine. The computer then captures a summed average signal that does not contain the selected number of sums.

7.7 Summary and Future Work

One of the major challenges in the construction of the TOF/TOF instrument was to cause a 20 ns laser pulse to arrive in a 1 mm section of the interaction region at the same time as an ion packet of selected mass. This ion packet may be present in this region for 50 ns or less. In addition to stringent timing requirements, the laser must have high power while operating at high repetition rates. Components to trigger the ion source, gate and laser, and detect the transients were selected and integrated via software. Additional software was written for processing of the mass spectral data.

Although the transient recorder is presently the slowest element in the TOF/TOF instrument. construction of an integrating transient recorder will eliminate this problem. This leaves the laser as the factor that limits the maximum possible acquisition rate for the system. The 500 Hz repetition rate maximum for the excimer is only half of the rate at which the mass spectrometer is easily capable of attaining. Decreasing the time required to acquire a normal mass spectrum may be achieved by extracting the contents of the ion source twice for every laser pulse. A normal mass spectrum can be obtained from one of these pulses while photodissociation is performed on the other. Simultaneous acquisition of a normal mass spectrum will allow the laser to be used more efficiently without any loss in information.

Addition of the ITR can also reduce the role of the relatively slow GPIB network to controlling the delay generator. This is a significant time savings especially when files must be transferred to the computer. A typical mass spectrum acquired by the transient recorder fills 10 *Kb* of space. Our present system requires 0.01 s to transfer this data to the computer. When the laser is operated at its maximum repetition rate, this means that the product ions from a minimum of five laser pulses are not detected. Assuming that summing 50 transients produces usable product ion spectra, this inefficiency will cause at least one product spectrum to be lost across a chromatographic peak. The ITR can easily generate ten spectra per second [3] and use the product ion information in every PID transient.

The software in its present state is adequate for instrumental construction and feasibility testing, but will require modifications to operate on the chromatographic time scale. Delay time computations for the ion source and gate will need to be performed as a chromatographic peak elutes. The software will need to choose the precursor m/z values and appropriate delay times, and load them into the delay generator.

References

- 1. Holland, J. F.; Newcombe, B.; Tecklenburg, R. E., Jr.; Davenport, M.; Allison, J.; Watson, J. T.; Enke, C. G. Rev. Sci. Instrum. 1991, 62, 69.
- 2. Application Note 030, National Instruments, Austin, TX 78730-5039, 1991.
- 3. Holland, J. F.; Newcombe, B.; Tecklecburg, R. E., Jr.; Davenport, M.; Allison, J.; Watson, J. T.; Enke, C. G. Rev. Sci. Instrum. 1991, 62, 69.

Chapter 8

Characteristics of the Ion Fragmentation Process in the TOF/TOF Instrument

8.1 Introduction

The critical timing system was combined with the mass spectrometer to form the TOF/TOF instrument. Our initial version of the instrument was operated without the gate while this portion of the instrument was being developed. Upon its completion, the gate will provide initial selection of precursor ions and eliminate any species that could interfere with detection of product ions. The remainder of the instrument was in place and operational for the characterization studies described in this chapter.

Optimal product ion formation for the TOF/TOF instrument depends on the precursor ion resolution and photodissociation efficiency. Since the laser should serve as the ultimate selector of those precursor ions to be fragmented, spatial and temporal features of the laser beam and precursor ion packets allow their overlap to be increased. Precursor ion resolution is heavily dependent on the dimensions of the laser beam at the interaction region. As the beam becomes more focused, precursor resolving power increases. Photodissociation

		:

Bromobenzene and toluene were selected for initial photodissociation studies because they have been previously characterized using ICR mass spectrometers [1-5]. These compounds are volatile enough for steady-state introduction into the mass spectrometer via a direct leak inlet throughout long periods of time. The photodissociation zero-Kelvin threshold of bromobenzene is $2.81 \pm 0.07 \ eV$ at $440 \pm 10 \ nm$, as determined by Dunbar and Honovich [6] using an ICR mass spectrometer. These and related compounds are also known to undergo PID at 193 nm [1,2]. The 6.4 eV photons present at this wavelength have been used to achieve efficiencies of 15% for conversion of precursor ions to product ions in ICR instruments [1].

8.2 Characteristics of the Isomass Ion Packets

Precursor ion resolution and the number of ions permitted to photodissociate depend on the spatial and temporal characteristics of the selected isomass ion packet. The ideal target for laser photodissociation has the same approximate dimensions as the laser pulse spatially and temporally. Under optimal conditions, the 20 ns laser pulse will irradiate ions of only one m/z value and all of the ions in the selected isomass packet would be irradiated for the entire duration of that pulse.

A detector was placed at the interaction region of the mass spectrometer to permit characterization of the target isomass ion packets. A steady-state concentration of bromobenzene was introduced into the ion source. Mass spectra were acquired using the LeCroy 9450 digital oscilloscope by

accumulating a summed average of fifty transients. A region from the mass spectrum of bromobenzene acquired under these conditions is shown in Figure 8-1. The isomass packets for these m/z 156 and 158 ions have temporal widths (FWHM) of 34 and 30 ns, respectively, where PID is initiated. Assuming an accelerating voltage of 700 V, these temporal widths translate to spatial widths of about 0.7 mm thick for ion packets of all masses. Ions with m/z 156 and 158 will travel about 1 mm during a 20 ns period when accelerated to 700 V. Arrival times at the interaction region for these isomass ion packets differ by about 550 ns. Ions with m/z 157 reach the interaction region approximately 260 ns after those with m/z 156. When mass 156 is the selected precursor ion, the m/z 157 ion packet is about 13 mm away from the interaction region when the laser pulse interacts with the precursor ion.

The diameter and uniformity of the ion beam were initially examined by placing a multichannel plate detector (MCP) that contained a phosphor in the path of the ion beam outside of the ion source and at the interaction region. The ion source extraction voltage was adjusted to provide a constant ion beam from the residual gases in the mass spectrometer, and the surface of the phosphor was observed to determine the size of the ion beam. The ion beam was consistently larger than the 1" detector surface even when the MCP was located just outside of the ion source. As the potentials applied to the plates of the MCP were reduced, the image revealed a portion of the beam about 0.25" in diameter that showed a slightly greater ion abundance than the edges of the beam.

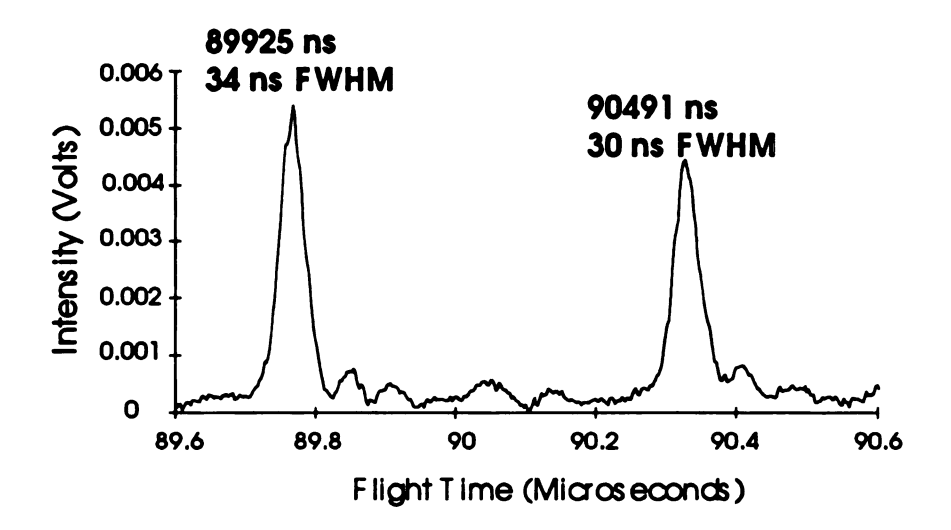


Figure 8-1. Portion of a bromobenzene mass spectrum acquired with detector placed at the interaction region

The uniformity and divergence of the ion beam were then studied by placing an adjustable aperture was placed 8" in front of a detector located at the interaction region. After the aperture was calibrated, the intensity of m/z 18 (H_2O) was monitored as the aperture was closed with the shield voltage of the first TOF analyzer set to its normal value of 500 V. Since ion beam divergence is time-dependent, decreasing the flight-time of ions to a detector will reveal its effects on the ion signal. The experiment was repeated with the shield voltage of the first mass analyzer set to 1000 V. Examination of ion beam uniformity was performed by attenuating its intensity via reduction of the filament bias current. Data from these three studies are plotted in Figure 8-2 as a function of the area of the aperture opening.

When the aperture opening is large, the relative intensity of the m/z 18 signal decreases more rapidly under normal operating conditions than when the shield voltage is raised or the ion beam is attenuated. As the area of the aperture approaches 2 cm^2 , the loss in relative intensity is very similar for all three sets of conditions. Since attenuation of the ion beam will reveal the uniformity of the ion density across the beam, a slow initial loss in the attenuated signal supports the possibility of a non-uniform ion beam. This is further substantiated by the similar loss rates observed as the aperture is closed further. The diameter of the more intense portion of the ion beam can also be estimated from these data. Since the relative intensity curves are very similar when the aperture opening is 2 cm^2 or smaller, the intense portion of the ion beam probably has diameter of about 15 mm.

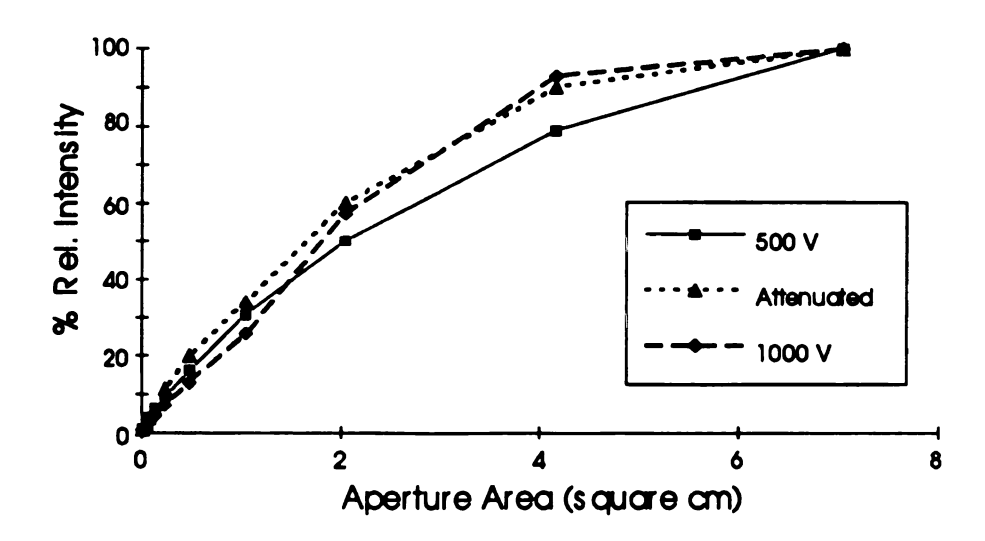


Figure 8-2. Plot of the relative intensity of m/z 18 as an aperture was closed under normal operating conditions, to study the uniformity of the ion beam and to examine divergence of the ion beam.

Not all of the ions reaching the interaction region will strike a detector placed at the end of the flight path (about 2.2 m away). Since beam divergence is related to the flight-time of an ion, the relative intensity of the ion should be larger as long as ions accelerated to a greater velocity strike the detector more frequently than accelerated to 500 V. The relative intensity of the ion beam decreases less rapidly than under normal conditions when the shield voltage of the first TOF analyzer is increased to 1000 V until the area reaches about 2 cm². The relative intensities become similar as the aperture is closed further. From these data, the more intense central portion of the ion beam is also less divergent than the more diffuse surrounding part of the beam. This portion should define the area to be irradiated by the laser pulse.

8.3 Laser Timing and Focusing

Integration of the laser into the TOF/TOF instrument required several steps. The two major challenges, proper alignment of the laser and coordination of the timing for the laser firing, were both evolutionary processes. The steps involved in development of the present instrument also give insight into processes that affect instrumental operation. Although portions of these two processes were performed simultaneously, they are more easily understood when discussed separately.

8.3.1 Laser Beam Characteristics

The excimer beam is 24 mm wide by 13 mm tall when it exits the laser. If the beam is not focused, these dimensions remain constant for the entire light path (about 1 m). A two-inch cylindrical lens with a 300 mm focal length is placed just before the mass spectrometer. The lens is adjusted to produce the smallest image where the ion and laser beams intersect. The laser beam is about 2.5 mm wide and 13 mm tall at this point. Although this image is larger than desired, the uniform beam image exiting the laser now has a more intense region at its center. This region is about 0.3-0.5 mm in width. The laser beam diverges and exits the mass spectrometer with slightly smaller dimensions than when it entered the TOF/TOF instrument.

8.3.2 Laser Alignment

Proper laser alignment is absolutely critical to the functioning of the TOF/TOF instrument. The laser beam must be allowed to interact with the photons without allowing any other interactions. If the laser beam is permitted to strike a metal surface, the detected ion signal is attenuated. In an early experiment, the laser beam was directed through the mass spectrometer in a path that traveled through a total of four grids. Not only was the laser intensity reduced before it reached the interaction region, the 500 mJ laser pulse ablated the metal surface forming ions and neutrals that reduced the ion signal by 75%. A light isolation tube was designed and constructed by Mary Seeterlin to eliminate the fringing-field problems that affected the ion signal. This one inch

square tube provides a clear path for the laser pulse to follow through the mass spectrometer. The isolation tube also prevents the field leakage that results from removal of the grids from affecting the flight path or transmission of ions. The ions travel through this tube only in the interaction region. Removal of the grids allowed the ion beam to remain at a constant intensity even when the laser was operating. This is especially significant when one considers the need for the laser beam to enter an ICR analyzer cell through a metal mesh when PID is performed in an ICR mass spectrometer [1].

Even when the laser beam is properly aligned and does not strike any metal surfaces inside the mass spectrometer, it still passes through windows on each side of the instrument. In another experiment, the laser was allowed to run with the light isolation tube in place. The intensity of the ion beam and pressure inside the mass spectrometer were monitored. In a period of about thirty seconds, the pressure rose from 3×10^{-6} torr to 1×10^{-5} torr. This phenomenon was reproducible and, unlike earlier experiences, did not attenuate the ion beam. Water and other species coating the surface of the windows were removed by the laser beam. This problem has been minimized by heating the flanges to which the windows are attached. Pressure rises now average about 2×10^{-6} torr during several hours of operation.

8.3.3 Laser Timing

One of the major challenges in the TOF/TOF instrument is to synchronize the laser pulse so that it arrives at the interaction region at the same time as the

isomass ion packet of interest. The best way to determine the arrival time of the precursor ion and to locate the space-focus plane of the first mirror at the interaction region is to insert a detector in the ion path just prior to the interaction region. Inserting a MCP detector in this position allows ion source and mirror settings to be adjusted to insure that the space-focus plane of the first mirror is located at the irradiated portion of the interaction region and provides the flight-time of ions with specific m/z values to be determined.

8.4 Photodissociation in the TOF/TOF Instrument

Since the flight time, temporal width of the isomass ion packet and delay between laser triggering and emission are all known, the delay times between the ion source extraction pulse and laser triggers can be calculated. The flight time of an ion from the source to the interaction region can be expressed as:

$$t_f = t_{t,x} + lv - t_{t,d} \tag{1}$$

where t_f is the delay time between triggering the ion source and triggering the laser pulse, $t_{t,x}$ is the delay between triggering the ion source extraction pulse and pulsing, I is the effective length of the flight-path, v is the ion's velocity and $t_{t,d}$ is the delay time between laser triggering and thyratron discharge. The delay in the ion source extraction pulse is constant and can be measured. The laser delay is constant for a given repetition rate although it may vary slightly day-to-day. The length of the effective flight path can be calculated from the arrival time of ions of a known m/z value. The velocity of an ion is dependent on its mass, charge and the accelerating voltage. The charge on an ion can be assumed to be one for most compounds analyzed in the TOF/TOF instrument. The length of

			!
			•
			3
			:

the effective flight-path may be determined using ions with known m/z values using this equation. Once the value of l is known, delay times can be calculated for ions of any m/z value.

Although calculations provide a starting point, initial location of the precursor ion packet still must actually be performed experimentally. The laser delay time is varied about the expected arrival time for an ion at the interaction region while monitoring the intensity of the precursor ion signal. This signal depletes only when the laser pulse strikes the isomass ion packet. When the delay time differs from the arrival time by even a few nanoseconds, no parent ion depletion is observed. The selectivity of this procedure is illustrated in Figures 8-3 to 8-6. Bromobenzene was introduced into the ion source at about 1×10-6 torr. The excimer was operated at a 30 Hz repetition rate with an average energy of 145 mJ per pulse. With the laser beam focused to 3 mm wide \times 13 mm tall at the interaction region, the summed average of 200 transients was accumulated to produce a mass spectra. The laser pulse passes through the interaction region prior to the arrival of m/z 156 for the data shown in Figure 8-4. This spectrum is identical to one in which no light was permitted into the mass spectrometer. Selective depletion of m/z 156, 157 and 158 is shown in Figures 8-4 through 8-6, respectively. The intensity of the selected precursor ion is reduced to less than 50% of its original value without affecting the intensity of the other two potential precursor ions for each of the three m/z values studied.

Although selective depletion of the precursor ion indicates that photodissociation has probably occurred, the best proof is the appearance of

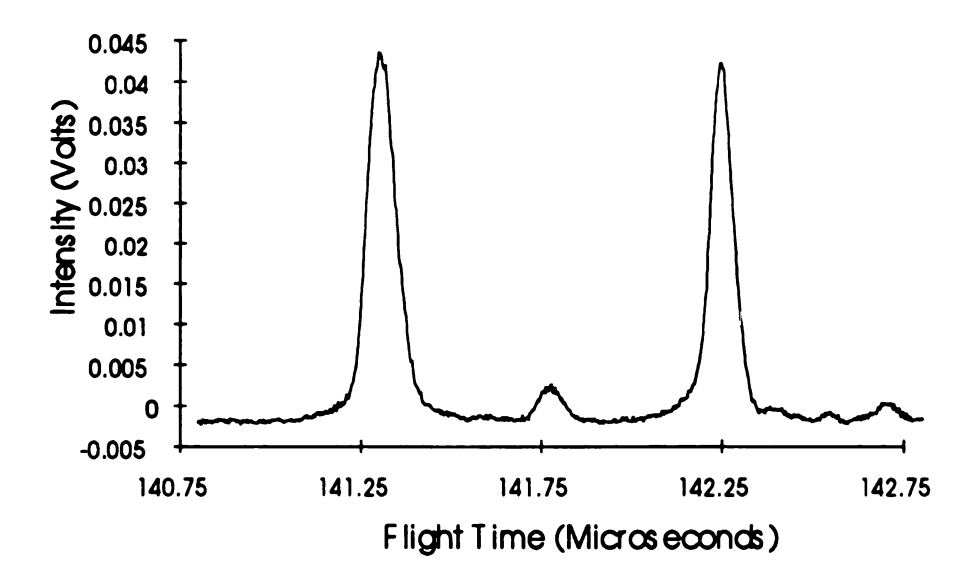


Figure 8-3. Region of bromobenzene mass spectrum showing no depletion of m/z 156, 157, or 158. Laser emission occurred 50 ns before the arrival time of m/z 156.

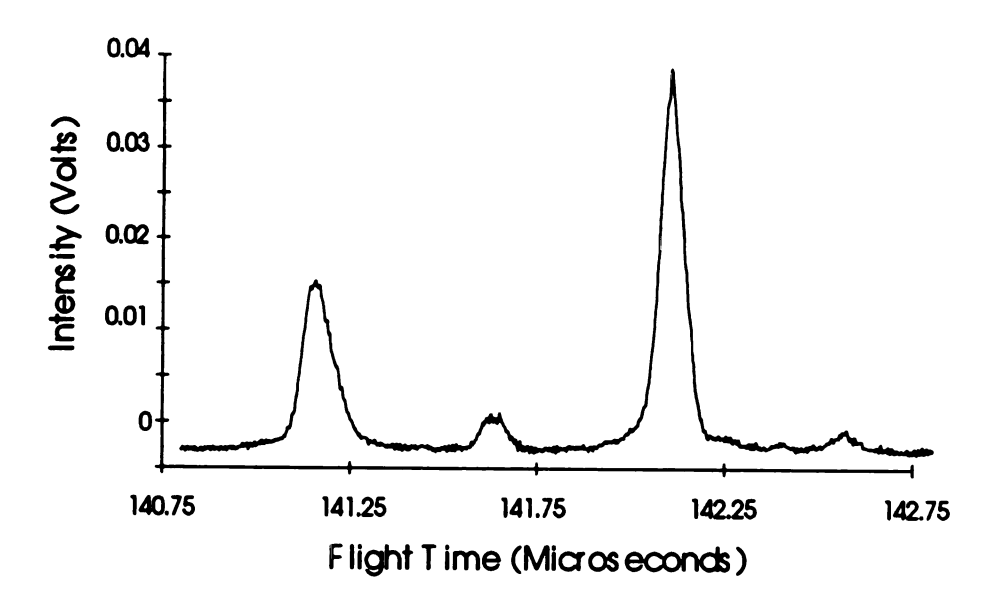


Figure 8-4. Laser triggered to deplete m/z 156.

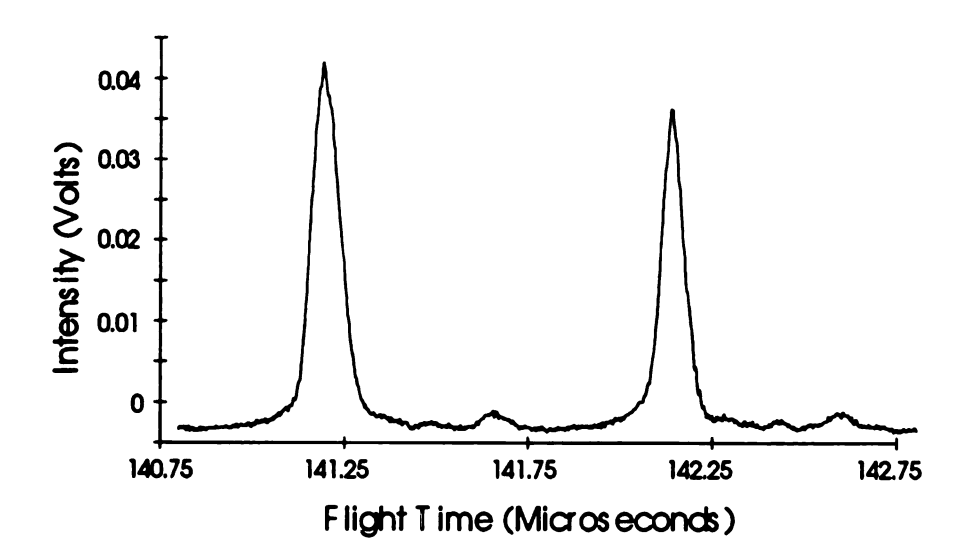


Figure 8-5. Laser triggered to deplete m/z 157.

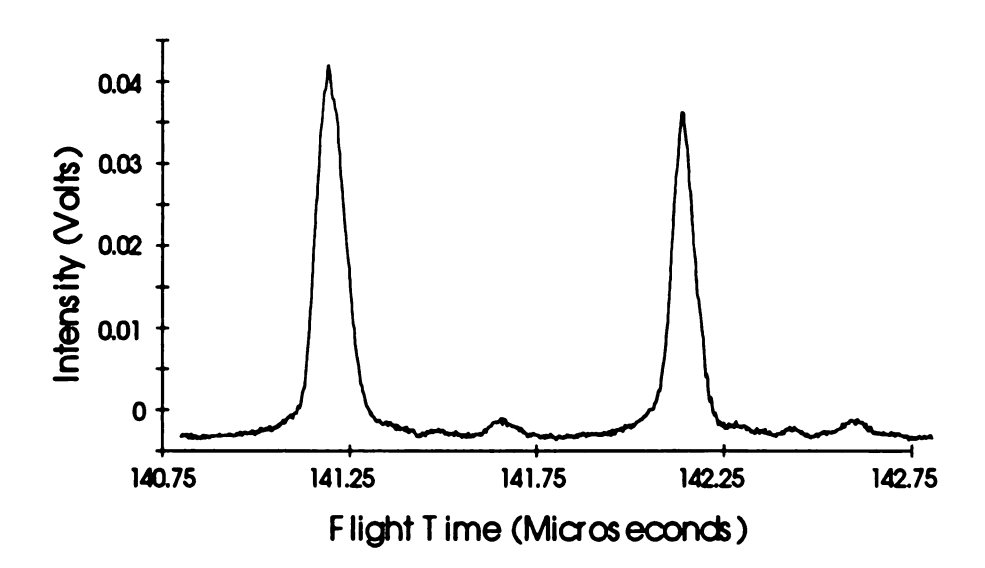


Figure 8-6. Laser triggered to deplete m/z 158.

product ions. The region containing the predicted arrival time of m/z 77 is shown in Figure 8-7. This is the predominant PID product ion from m/z 156 of bromobenzene. Mass spectra were acquired using summed average of 200 transients and the focused 3 mm x 13 mm excimer beam. The laser pulse was timed to pass through the interaction region before the arrival time of m/z 156 for Figure 8-7A. The spectrum shown in 8-7B was acquired when the laser pulse coincided with the arrival of m/z 156 in the interaction region. The appearance of a response at the expected arrival time of m/z 77 shows that photodissociation has occurred. The molecular ion from toluene (m/z 92) was analyzed under the same conditions as were used for the m/z 156 product ions from the bromobenzene. A portion of the photodissociation spectrum from this analysis is shown in Figure 8-8. This spectrum was obtained by subtracting a spectrum with the laser pulse not overlapping the ion packet in the interaction region from the spectrum when the excimer pulse overlaps with the precursor ion packet. Depletion of the precursor ion and appearance of the product ion with m/z 91 are visible in this spectrum. Assuming that all of the precursor ions photofragment to form ions with m/z 91 and that all product ions are detected by the mass spectrometer, about 22% of the m/z 92 precursor ion was converted to the m/z 91 product ion and detected. This value is the lowest possible photodissociation efficiency for toluene in our system since m/z 92 may photofragment to form ions other than m/z 91. Thus, very efficient photodissociation is occurring in the TOF/TOF mass spectrometer.

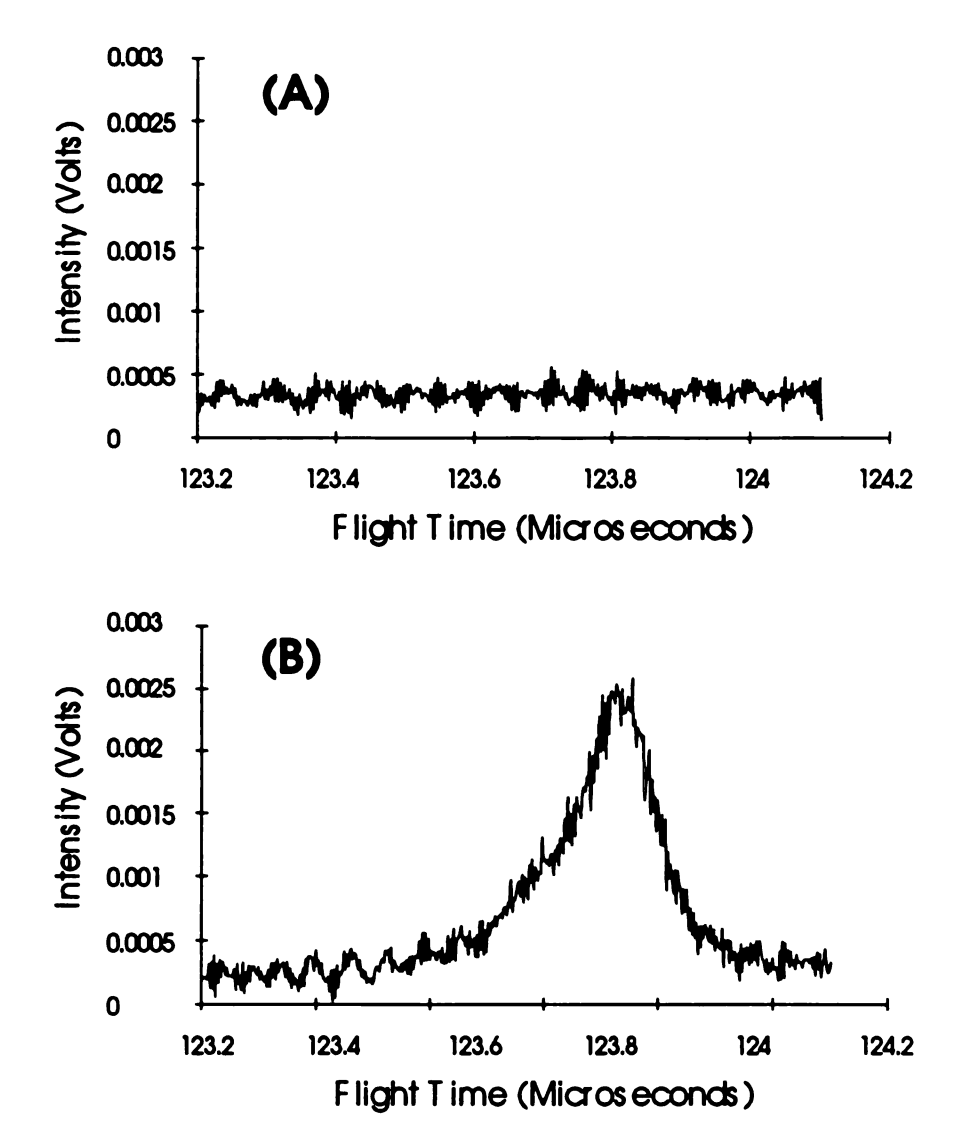


Figure 8-7. Region containing the predicted arrival time of the m/z 77 product ion (from m/z 156) at the detector (A) without laser pulse ion packet overlap and (B) with overlap of the laser pulse and selected ion packet.

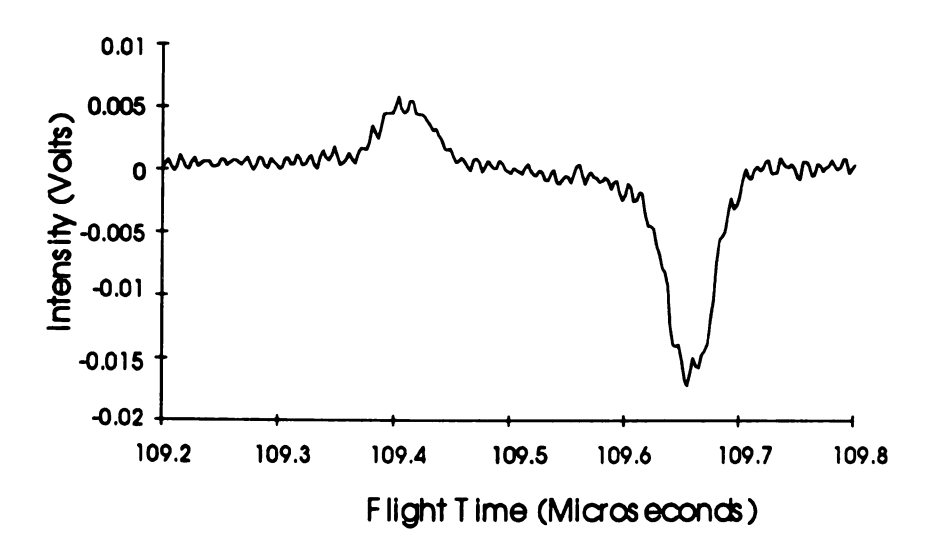


Figure 8-8. Photodissociation spectrum showing the appearance of the m/z 91 product ion and depletion of the m/z 92 parent ion.

8.4.1 Precursor Ion Resolution

Since final precursor selection is performed by the laser, the resolving power of the laser was examined using the 3 $mm \times 13$ mm dimensions. The average laser power for this experiment was 5.75 W at 193 nm when the laser was operated at 30 Hz. A one microsecond time window that included the response from m/z 156 and 158 was examined in 10 ns increments. Each mass spectrum acquired by the LeCroy 9450 digital oscilloscope was the summed average of 200 transients. The percent of the m/z 156 and m/z 158 precursor ion remaining as a function of the laser trigger delay time is shown in Figure 8-9. The average precursor ion resolution provided by the laser for these two masses was about 200 using the FWHM definition.

8.4.2 Photodissociation Characteristics

One advantage of performing PID in the TOF/TOF instrument is our ability to obtain a true background signal by causing the laser pulse to travel through the interaction region only a few nanoseconds prior to the arrival of the precursor ion packet. When the laser beam is directed into the mass spectrometer, it may cause reactions other than PID to occur. The laser pulse may cause neutrals and/or ions to be present in the interaction region. These species will remain in the interaction region for a significant amount of time (at least microseconds). Neither precursor ion intensity depletion nor product ion appearance have been observed when this experiment is performed. Although all of these competing processes can occur, photodissociation is the most likely

cause for diminution of the precursor ion intensity as well as formation of product ions. Mass spectra obtained in this manner make ideal blanks for photodissociation studies.

The precursor ion intensity was reduced to 7.8% of its original value for both m/z 156 and m/z 158 for the data shown in Figure 8-9. assuming this depletion is due to no other process, more than 90% of the ions in the isomass packet of the precursor ion were photodissociated by the laser pulse. This efficiency agrees with our predictions and is larger than any of those listed in Table 6-1. The TOF/TOF instrument is capable of such high efficiencies because the large ion density of the focused precursor packet is highly overlapped with an intense laser pulse. No other type of mass spectrometer provides this high ion density as a target for the photodissociation laser.

The photodissociation cross-section can be determined from the results in Figure 8-9. The photodissociation cross-section for an ion at a selected wavelength can be expresses as:

$$\sigma = e / \phi \tag{2}$$

where σ is the PID cross-section, ϕ is the photon flux and e is the photodissociation efficiency. The average laser pulse contained 192 mJ of energy for this study. This translates to a photon flux of 4.8×10^{17} cm^{-2} for this experiment. Based on this photon flux and 92.2% efficiency, the photodissociation cross-section for bromobenzene was found to be about 1.9×10^{-18} cm^{-2} at 193 nm in our system. Variations in the overlap between the laser pulse and precursor ion packet affect photodissociation cross-sections

determined from the TOF/TOF instrument. The position of the precursor ion packet is not stationary for the duration of the laser pulse. The amount of time that an ion spends in the interaction region depends on its velocity. While heavier precursor ions have slower velocities and may remain in the interaction region for the laser pulse duration, faster, smaller ions will remain in the interaction region for only a small fraction of the laser pulse. These factors reduce the validity of the 100% overlap assumption in the calculation. In addition, the relationship between fraction dissociated and cross-section will not be linear for large degrees of depletion. If such a large fraction of the ions are being excited, there is a substantial possibility for multiphoton processes. These factors would result in a low estimate of the PID cross-section. Another limitation of using a TOF/TOF instrument for determination of PID cross-sections is the need to transmit all of the product ions to the detector. While transmission for TOFMS instruments is normally high, a portion of the product ions will not reach the detector.

When the cross-section for bromobenzene was calculated using the data of Bowers *et al* [2], a value of 1.8×10⁻¹⁷ cm² at 193 *nm* was obtained. The laser pulse can cause reactions other than just photodissociation to occur during the ten or more milliseconds between photoexcitation and product ion analysis. The light opening to the ICR analyzer cell used in this experiment was covered with an electroformed copper mesh. The laser can ablate neutrals and ions from any metal surface that it strikes. The instantaneous concentration of these species in the cell can cause CID or other reactions to occur in addition to PID. All reaction products are assumed to result from photodissociation since the ICR cannot

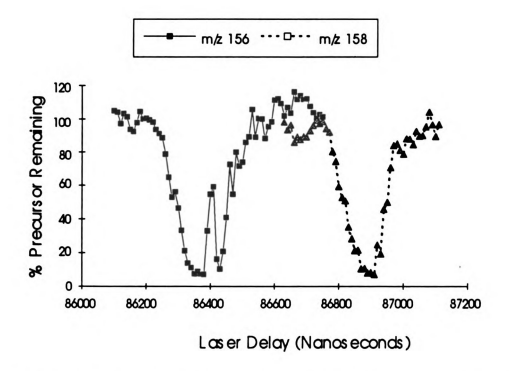


Figure 8-9. Percent of the precursor ion remaining from the photodissociation of bromobenzene as a function of the laser trigger delay time.

distinguish between PID products and products occurring via other mechanisms. These factors would result in a high estimate of the PID cross-section. Almost all product ions formed in the ICR are detected, making this instrument the traditional choice for studying photodissociation cross-sections.

The TOF/TOF instrument has the potential to become an excellent platform for studying photodissociation on the microsecond time scale. The ability of this instrument to isolate PID from many other competing processes is a major advantage over the ICR mass spectrometer. Product ions of ion/neutral reactions have different arrival times at the detector than those resulting from PID. Timing the laser to fire only a few nanoseconds before the arrival of the precursor ion at the interaction region gives the best blank for photodissociation since all processes associated with introduction of the laser light to the mass spectrometer can occur.

8.4.3 Critical Timing Precision

A major concern in performing photodissociation in the TOF/TOF instrument is the need to consistently strike the selected precursor ion packet with the laser pulse. The jitter and drift associated with the triggering of the excimer have been described in Chapter 7 of this thesis. Both of these variable fluctuate by only a few nanoseconds even when the laser is operated for several hours. The other major contributor controlling the overlap of the ion packet and the laser pulse is the mass spectrometer. Since all other voltages in the instrument are static, the ion source extraction pulse is the largest contributor to

jitter in the arrival times of isomass ion packets at the interaction region and also the detector.

A series of ten single-shot mass spectra were acquired of the *m/z* 156 to 158 region from bromobenzene on the LeCroy 9450 digital oscilloscope. One of these spectra is shown in Figure 8-10. The arrival times for m/z 156 and 158, their mean value and standard deviation are shown in Table 8-1. The average standard deviation in the arrival times was about 25 *ns*. This value is greater than the duration of the laser pulse and limits both timing and photodissociation efficiency. As the number of summed averaged transients per mass spectrum is increased from one to two hundred, the base width of the arrival time signal increases from 30 *ns* to about 65 *ns*.

Drift in the laser discharge delay time or the arrival time of the precursor ion packet at the interaction region will also affect photodissociation efficiency. The static voltages in the mass spectrometer drift slightly and require readjustment every few hours. The greatest effect arises from changing the mirror voltages which can alter the length of the flight path. Since the flight time of an ion is dependent on the length of the flight path, this drift will reduce the overlap with the laser pulse. Operation of the excimer at high repetition rates (more than 300 Hz) will cause the it to gradually warm over a few hours. The discharge delay time between triggering the laser and thryratron discharge is temperature dependent. At this time, the delay between triggering and thyratron discharge has varied only a few nanoseconds over a few hour period. Thus, drift will require optimization of the TOF/TOF instrument every few hours to keep a

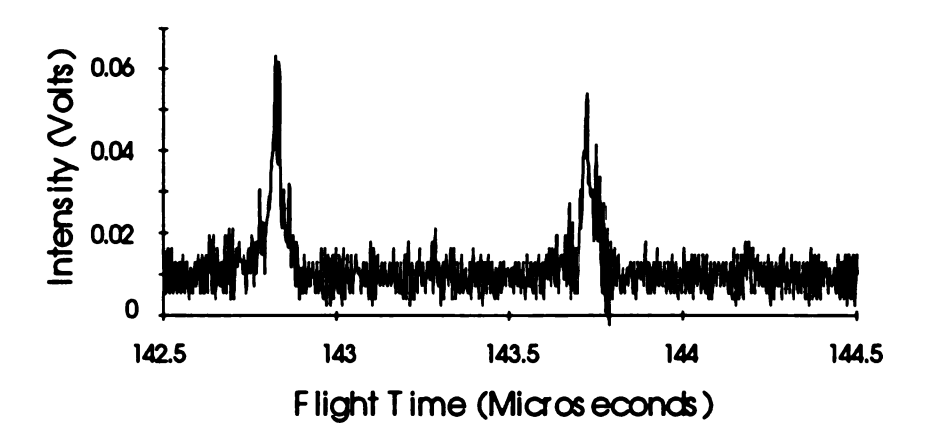


Figure 8-10. Single-shot mass spectrum of bromobenzene showing the arrival times of m/z 156 and m/z 158. These spectra were acquired with the detector at the end of the ion flight-path.

Table 8-1. Arrival times for m/z 156 and m/z 158 from acquisitions of one transient per mass spectrum using bromobenzene.

Trial	<i>m/z</i> 156	<i>m</i> ∕z 158
	(±3 <i>ns</i>)	(±3 <i>ns</i>)
1	142, 897 <i>ns</i>	143,936 <i>ns</i>
2	142,914 <i>ns</i>	143,987 <i>ns</i>
3	142,939 <i>ns</i>	144,004 <i>ns</i>
4	142,939 <i>ns</i>	144,004 <i>ns</i>
5	142,872 <i>ns</i>	143,937 <i>ns</i>
6	142,906 <i>ns</i>	143,996 <i>ns</i>
7	142,923 <i>ns</i>	144,004 <i>ns</i>
8	142,906 <i>ns</i>	143,979 <i>ns</i>
9	142,872 <i>ns</i>	143,970 <i>ns</i>
10	142,887 <i>ns</i>	143,937 <i>ns</i>
Mean	142,906 <i>ns</i>	143,977 <i>ns</i>
Standard Deviation	24 ns	27 ns

large amount of temporal overlap between the precursor ion packets and the laser pulse.

8.5 Summary and Conclusions

Photodissociation has been performed at the focal plane of the first ion mirror in a tandem time-of-flight mass spectrometer. The unique ability of TOF/TOF instruments to provide high ion densities at the interaction region allows a large overlap with photons from an intense laser pulse. Precursor depletion efficiencies of more than 90% have been achieved for bromobenzene and toluene. The keys to effective photodissociation in this instrument include obtaining optimal excimer pulse/ion packet overlap in the interaction region and providing a clear light path through the mass spectrometer for the laser pulse. Precursor ion resolution is controlled by the focus of the laser beam. The variation in ion packet arrival times poses the greatest difficulty in achieving complete overlap with the laser pulse.

The tandem time-of-flight mass spectrometer has many advantages for studying photodissociation on the microsecond time scale. These include its high efficiency, ability to discriminate between product ions resulting from different fragmentation processes and highly defined excitation region. The high photodissociation efficiencies of the TOF/TOF instrument result from the large temporal and spatial overlap of ions at the interaction region. Both the laser pulse and ion packet have high densities at the interaction region. They also have similar durations. No other type of mass spectrometer has this capability.

Many processes can occur when laser emission enters a mass spectrometer. When the excimer pulse reaches the interaction region only a few nanoseconds before the precursor ion packet in the TOF/TOF instrument, all processes associated with the laser emission except photodissociation occur. This true background signal permits photodissociation product ions to be isolated from products of other processes. Photoexcitation gives each ion a mass-independent discrete amount of energy. Unlike other types of mass spectrometers, the high ion density and known ion path allow photodissociation to be performed in a small region that is well defined. The wide laser beam used in ICR experiments and the longer coaxial interaction region used in sector mass spectrometer do not define the time or location of the photoexcitation or dissociation processes.

8.6 Future Work

Photodissociation after a mirror in tandem time-of-flight mass spectrometers is still in its infancy. Although high photodissociation efficiencies have been achieved for a few selected compounds, our goal of GC/MS/MS requires the ability to successfully photodissociate all ions. Since the structures of these ions may vary greatly, several classes of compound must be examined to determine the generality of photodissociation at 193 *nm*.

Another major area of emphasis is the need to improve the resolving power for precursor ion selection. Precursor selection is determined by the gate and dimensions of the laser pulse. When the gate is completed and its resolving power known, the laser beam dimensions required for the optimal combination of

photodissociation efficiency and precursor selection can be determined. One way of reducing the dimensions of the laser pulse is to add an adjustable slit to the light path. If the slit width can be increased or decreased precisely without changing the position of its center, calibration of the arrival times of masses at the interaction region can be simplified. An added benefit of this approach is that the precursor resolving power can be adjusted to provide unit mass resolution for all m/z values in the sample. As the slit is closed and the width of the laser beam reduced, the number of photons reaching the interaction region is also reduced.

The addition of the dye laser to the photodissociation system will permit fundamental photodissocation studies for processes that occur on the microsecond time scale. The ability to produce a true blank signal allows ion photodissociation products to be isolated from all other events caused by the laser pulse. The range of wavelengths provided by the dye laser can be used to acquire photodissocation spectra for ions produced by electron ionization.

References

- 1. Williams, E. R.; McLafferty, F. W. *J. Am. Soc. Mass Spectrom.* 1990, 1, 361.
- Bowers, W. D.; Delbert, S. S.; McIver, R. T., Jr. Anal. Chem. 1986, 58, 969.
- 3. van Velzen, P. N. T.; van der Hart, W. J. Chem. Phys. 1981, 61, 325.

- 4. Rosenstock, H. M.; Stockbauer, R. L.; Parr, A. C. *J. Chem. Phys.* **1980**, *73*, 773.
- 5. Dunbar, R. C.; Fu, E. W. J. Phys. Chem. 1977, 81, 1531.
- 6. Dunbar, R. C.; Honovich, J. P. Int. J. Mass Spectrom. Ion Processes 1984, 58, 25.



System Control Programs for the Tandem Timeof-Flight Mass Spectrometer

This appendix contains LabWindows C code and panels for the three major control programs for the TOF/TOF instrument. Programs for instrument control, header viewing and file conversion to an ASCII format are contained in this appendix. These programs, differing from one another in many respects including design and functionality, are described below.

The instrument control program integrates the functions of the laser, transient recorder, delay generator and mass spectrometer by precisely controlling the timing of several events (via the LeCroy 4222 delay generator). This program requests user input and loads information into the system components through a series of pop-up panels. Data are acquired, down-loaded to the computer as a LeCroy binary file and displayed by this program.

The header program allows examination of data files acquired using the TOF/TOF instrument. This program extracts information including acquisition date, time, sampling rate, and first acquired data point from the stored binary file.

The third of these programs converts the stored binary file into an ASCII format. A new instrument driver was created for this program to make the actual operating program very simple. A LabWindows instrument may be either real or virtual. Creation of an instrument reduces the possibility of user errors causing program failure. Instrument drivers are not accessible to the casual user but may be easily amended by a system programmer. ASCII files generated by this program are tab delimited to simplify loading into Microsoft Excel 4.0.

A.1 TOF/TOF Instrument Control Program

This program allows the user to input the file name, trigger rate, and conditions for the LeCroy 4222 delay generator and LeCroy 9450 transient recorder. These conditionas are loaded into the appropriate instruments and data are collected. The acquired data are transferred to the host computer and displayed #include "C:\lw\programs\toftof\tofdev.h" #define FALSE 0 #define TRUE 1 Global Variables static char file name[128]; static double spec[8192]; static int error: static int delay handle; static int file handle: static int graph handle; static int trans handle; static int tof handle; static int pulse_handle; static int sig source: static int instrum prog; static int pts_to_array; static int pts_to_graph; static int first_pt; static double frequency; static double duty_fraction; static long delay1;

```
static long delay2;
static long delay3;
static long delay4;
static long number_pts;
static long start pt;
Formal function declarations
void Change File Name (void):
void Get Delay Info (void):
void generate tone (double freg. double duration):
void Get_Trans_Info (void);
void Get Graph Info(void):
int Acquire_Data(void);
void Show Var Values(void):
void Setup_Run(void);
int finished summing(void):
void Pulse Rate(void);
main ()
Load the five panels for the TOFTOF instrument control.
*/
int panel, ctrl, power_switch;
int handle:
error = 0:
delay_handle = LoadPanel ("C:\\lw\\programs\\toftof\\tofdev.uir", 2);
if (delay_handle < 0) {
  FmtOut ("Unable to load the Delay panel from the resource file.\n");
  return;
  }
```

```
pulse handle = LoadPanel ("C:\\lw\\programs\\toftof\\tofdev.uir", 5);
if (pulse handle < 0) {
  FmtOut ("Unable to load the Pulse Rate Instrument Control panel from the
resource file.\n"):
  return:
graph handle = LoadPanel ("C:\\lw\\programs\\toftof\\tofdev.uir", 4);
if (graph handle < 0) {
  FmtOut ("Unable to load the Graph panel from the resource file.\n");
  return:
trans_handle = LoadPanel ("C:\\lw\\programs\\toftof\\tofdev.uir", 1);
if (trans handle < 0) {
  FmtOut ("Unable to load the Transient Recorder panel from the resource
file.\n");
  return:
file handle = LoadPanel ("C:\\lw\\programs\\toftof\\tofdev.uir", 3);
if (file handle < 0) {
  FmtOut ("Unable to load the File Name panel from the resource file.\n");
  return:
tof_handle = LoadPanel ("C:\\lw\\programs\\toftof\\tofdev.uir", 0);
if (tof_handle < 0) {
  FmtOut ("Unable to load the TOFTOF Instrument Control panel from the
resource file.\n");
  return;
HidePanel (delay_handle);
HidePanel (pulse_handle);
HidePanel (trans_handle);
HidePanel (file_handle);
HidePanel (graph handle):
DisplayPanel (tof_handle);
Turn on the power switch to activate the pulse button on the screen
*/
```

```
while (TRUE) {
  GetUserEvent (1, &panel, &ctrl);
  switch (ctrl) {
     case tofpan power:
       GetCtrlVal (tof handle, tofpan power, &power switch);
       SetCtrlVal (tof handle, tofpan led, power switch);
       SetInputMode (tof_handle, tofpan_power, power_switch);
       SetInputMode (tof_handle, tofpan_hes, power_switch);
       SetInputMode (tof_handle, tofpan_trans, power_switch);
       SetInputMode (tof_handle, tofpan_graph, power_switch);
       SetInputMode (tof_handle, tofpan_start, power_switch);
       SetInputMode (tof handle, tofpan name, power switch);
       SetInputMode (tof handle, tofpan rate, power switch);
       if (power switch == 0){
         /* Stop Delay Generator*/
         lecCAMAC init (5):
         lec4222_set_module_location (5, 1);
         lec4222_disable_trigger ();
         lecCAMAC_close ();
         /* Reset counter 1 */
         CTR_Stop (3, 1);
         CTR Reset (3, 1, 1);
          DefaultPanel (file_handle);
         DefaultPanel (trans_handle);
         DefaultPanel (delay handle);
         DefaultPanel (pulse_handle);
         DefaultPanel (tof handle):
          UnloadPanel (file handle):
         UnloadPanel (trans handle):
          UnloadPanel (delay_handle);
          UnloadPanel (pulse handle);
         UnloadPanel (tof handle);
         return;
       break;
```

```
Data Acquisition
    case tofpan hes:
       InstallPopup (delay_handle);
       Get Delay Info (); /* actions on delay panel */
       break:
    case tofpan trans:
       InstallPopup (trans handle);
       Get_Trans_Info (); /* actions on transient recorder panel*/
       break:
     case tofpan_graph:
       InstallPopup (graph handle);
       Get_Graph_Info(); /* actions on graph panel */
       break:
    case tofpan_start:
       Acquire_Data(); /* data acquisition occurs here. */
       WaveformGraphPopup (spec, pts_to_graph, 4, 1.0, 0.0, first_pt, 1.0);
       break:
    case tofpan_name:
       InstallPopup (file handle):
       Change_File_Name (); /* change file name */
       break:
    case tofpan_rate:
       InstallPopup (pulse_handle);
       Pulse Rate (); /* set pulse rate and start Trigger */
       break:
  }
Functions called by the various panels to process changes in their contents
*/
```

This function sets the trigger frequency and the duty cycle

```
for the National AT-MIO-16F-5 board.
void Pulse Rate()
  int rate event:
  int board, HI_period, LO_period;
  int timebase:
  GetPopupEvent (1, &rate_event);
  switch (rate_event) {
     case rate_frequency:
       break;
     case rate_duty_fraction:
       break:
     case rate_return:
       GetCtrlVal (pulse handle, rate frequency, &frequency);
       GetCtrlVal (pulse handle, rate duty fraction, &duty fraction);
       if( frequency == 0.0 )
          frequency = 10.0:
       if( frequency >= 5001.0 )
          frequency = 10.0;
       if( duty_fraction == 0.0 )
          duty fraction = 0.1;
       if( duty_fraction >= 1.0 )
          duty_fraction = 0.9;
       /* Initialize timer and start pulsing */
       Init_DA_Brds (3, &board);
       CTR Rate (frequency, duty_fraction, &timebase, &HI_period,
&LO period):
       CTR_Square (3, 1, timebase, HI_period, LO_period);
       delay(0.1);
       RemovePopup (0);
       break:
    }
  }
```

```
This function sets the number of points to be
displayed in the popup graph.
*/
void Get_Graph_Info()
  int graph event;
  GetPopupEvent (1, &graph_event);
  switch (graph event) {
     case graph_pts_to_graph:
       break;
     case graph_return:
       GetCtrlVal (graph_handle, graph_pts_to_graph, &pts_to_graph);
       GetCtrlVal (graph_handle, graph_first_pt, &first_pt);
       if (first_pt < 0)
          first pt = 0;
       if (pts_to_graph > 8192)
          pts to graph = 8192;
       RemovePopup (0);
       break;
     case graph_first_pt:
       break:
     case graph regraph:
       RemovePopup (0):
       GetCtrlVal (file_handle, name_file, file_name);
       GetCtrlVal (trans_handle, trans_start_point, &start_pt);
       GetCtrlVal (trans handle, trans number_pts, &number_pts);
       GetCtrlVal (trans handle, trans pts to array, &pts_to_array);
       GetCtrlVal (graph_handle, graph_pts_to_graph, &pts_to_graph);
       GetCtrlVal (graph_handle, graph_first_pt, &first_pt);
       if (first pt < 0)
          first pt = 0;
       if (pts to graph > 8192)
          pts to graph = 8192;
       WaveformGraphPopup (spec, pts_to_graph, 4, 1.0, 0.0, first_pt, 1.0);
       return;
       break:
```

```
}
}
This functions sets the delay values to be used by
the LeCroy 4222 delay generator.
*/
void Get_Delay_Info(void)
  int delay event;
  int temp:
  GetPopupEvent (1, &delay_event);
  if (delay_event== hes_return) {
     GetCtrlVal (delay_handle, hes_hes1, &delay1);
     GetCtrlVal (delay handle, hes hes2, &delay2);
     GetCtrlVal (delay_handle, hes_hes3, &delay3);
     GetCtrlVal (delay_handle, hes_hes4, &delay4);
     if (delay1 < 170) {
       delay1 = 170;
       MessagePopup ("Delay1 set to smallest legal value.");
     if (delay2 < 170) {
       delay2 = 170;
       MessagePopup ("Delay2 set to smallest legal value.");
     if (delay3 < 170) {
       delay3 = 170;
       MessagePopup ("Delay3 set to smallest legal value.");
     if (delay4 < 170) {
       delay4 = 170;
       MessagePopup ("Delay4 set to smallest legal value.");
     if (delay1 > 16777385){
       delay1 = 16777385;
       MessagePopup ("Delay1 set to largest legal value.");
```

```
if (delay2 > 16777385){
       delay2 = 16777385;
       MessagePopup ("Delay2 set to largest legal value.");
     if (delay3 > 16777385){
       delay3 = 16777385;
       MessagePopup ("Delay3 set to largest legal value.");
     if (delay4 > 16777385){
       delay4 = 16777385;
       MessagePopup ("Delay4 set to largest legal value.");
     RemovePopup (0);
     return;
}
This function sets the values for components of the
transient recorder.
*/
void Get_Trans_Info ()
  int trans_event;
  GetPopupEvent (1, &trans_event);
  if (trans_event == trans_return){
     GetCtrlVal (trans_handle, trans_instrum_prog, &instrum_prog);
     GetCtrlVal (trans_handle, trans_source, &sig_source);
     GetCtrlVal (trans handle, trans start point, &start pt);
     GetCtrlVal (trans handle, trans number pts, &number pts);
     GetCtrlVal (trans_handle, trans_pts_to_array, &pts_to_array);
     if (instrum prog < 0)
       MessagePopup ("Error in Instrument Program Selections");
     if (sig source < 0)
       MessagePopup ("Error in Signal Source Selections");
     if (start pt < 0)
       start pt = 0:
```

```
if (start pt > 50000) {
       start_pt = 50000;
        MessagePopup ("The starting point has been set to 50000.");
     if (number pts <= 0)
       number_pts = 5000;
     if (number_pts > 50000) {
       number pts = 50000;
        MessagePopup ("The number of points to be acquired has been set to
       the legal limit.");
     if (pts_to_array <= 0)
       pts_to_array = 5000;
     if (pts_to_array > 8192)
       pts_to_array = 8192;
     RemovePopup (0);
     return;
}
This function changes the name of the file to be acquired.
*/
void Change_File_Name ()
{
  int num;
  int temp;
  GetPopupEvent (1, &num);
  if (num == name_return) {
     GetCtrlVal (file_handle, name_file, file_name);
     RemovePopup (0);
     return;
  }
}
```

```
This function acquires and graphs the data using
the entries into all of the user interface panels.
*/
int Acquire Data()
  int delay_status;
  int num_pts;
  double interval;
  cls();
  Setup_Run();
/* The LeCroy 8901 CAMAC controller is initialized at GPIB
address 5. The LeCroy 4222 delay generator is initialized and the
delay times are set to appropriate values. The delay generator
is then triggered and the CAMAC controller closed.*/
/*
  lecCAMAC_init (5);
  lec4222_set_module_location (5, 1);
  lec4222_disable_trigger();
  lec4222_set_delay_times (delay1, delay2, delay3, delay4);
  lec4222 enable trigger ();
  delay_status = lec4222_get_status ();
  lecCAMAC_close ();
/* Data are acquired on the LeCroy 9450 digital oscilloscope.
The instrument is initialized at GPIB address 4. The default analysis
conditions are loaded by recalling the contents of Setup Panel 4
and the data are acquired. The acquired data are written to a
file. The contents of the file are then writtento an array called
"spec". (Both the file and the array contain 5000 elements.)*/
  error = lec94xx init (4, 0);
     if (error != 0){
```

```
MessagePopup ("Transient Recorder Initialization Error");
       FmtOut("Transient Recorder Initialization Error:\t%d\n", error);
       return (-1);
  error = lec94xx save load setup inst (1, instrum prog);
    if (error != 0){
       MessagePopup ("Error Loading Instrument Program");
       FmtOut("Instrument Program Loading Error:\t%d\n", error);
       return (-1);
  finished_summing ();
 error = lec94xx_read_wvfm_to_file (sig_source, file_name, 1, start_pt,
number_pts);
    if (error != 0){
       MessagePopup ("Error Writing Waveform to File");
       FmtOut("Could not write waveform to file. Error:\t%d\n", error);
       return (-1);
       }
  error = lec94xx_read_wvfm_file_arr (file_name, pts_to_array, spec, &interval,
&num pts);
    if (error != 0){
       MessagePopup ("Error Writing File to Array");
       FmtOut("Could not waveform to array. Error:\t%d\n", error);
       return (-1);
       }
  error = lec94xx_close ();
    if (error != 0){
       MessagePopup ("Error Closing Transient Recorder");
       FmtOut("Error closing Transient Recorder:\t%d\n", error);
       return (-1);
       }
 }
```

```
This function gets the values for all variables used
by the Acquire Data function. The number of points
contained in the file, graph and array are compared
to produce the most appropriate values for display.
*/
void Setup Run ()
{
  GetCtrlVal (file_handle, name_file, file_name);
  GetCtrlVal (delay_handle, hes_hes1, &delay1);
  GetCtrlVal (delay handle, hes hes2, &delay2);
  GetCtrlVal (delay_handle, hes_hes3, &delay3);
  GetCtrlVal (delay handle, hes hes4, &delay4);
  GetCtrlVal (trans_handle, trans_instrum_prog, &instrum_prog);
  GetCtrlVal (trans_handle, trans_source, &sig_source);
  GetCtrlVal (trans_handle, trans_start_point, &start_pt);
  GetCtrlVal (trans_handle, trans_number_pts, &number_pts);
  GetCtrlVal (trans_handle, trans_pts_to_array, &pts_to_array);
  GetCtrlVal (graph_handle, graph_pts_to_graph, &pts_to_graph);
  GetCtrlVal (graph_handle, graph_first_pt, &first_pt);
  GetCtrlVal (pulse_handle, rate_frequency, &frequency);
  GetCtrlVal (pulse_handle, rate_duty_fraction, &duty_fraction);
  if (pts_to_graph > pts_to_array)
     pts to graph = pts to array;
}
This function gueries the LeCroy 9450 to determine
whether or not the procedures performed by functions
E and F (particularly averaging) are complete. When
this procedure fails, a negative number is returned.
Success is indicated by a return value of 0.
*/
int finished summing ()
```

```
int user_req;
  int error:
  int comm_err;
  int exec_err;
  int dev_spec;
  int inr val:
  int event status;
  int status byte;
  inr_val = 0;
  GetCtrlVal (trans_handle, trans_source, &sig_source);
If using Fcn E or Fcn F, but not both functions simultaneously,
the following section of code should be used. The program will
not work properly if both functions are used together.
*/
  if (sig_source == 10){
     while (inr val != 2049){
       error = lec94xx_read_stat (&status_byte, &event_status, &inr_val,
&dev _spec, &exec_err, &comm_err, &user_req);
  if (sig_source == 9){
     while (inr val != 1025){
       error = lec94xx_read_stat (&status_byte, &event_status, &inr_val,
&dev spec, &exec err, &comm err, &user req);
*/
If using Function F of the LeCroy 9450 via a signal processed by
Function E, use the following special routine. This routine should
not be commented and the preceding section MUST be commented for
the program to run properly.
*/
    if (sig source == 10){
     while (inr_val != 3073){
       error = lec94xx_read_stat (&status_byte, &event_status, &inr_val,
&dev spec, &exec err, &comm err, &user reg);
     }
}
```

A.1.1 Include File Called by the TOF/TOF Instrument Control Program

```
This program defines the response to buttons
used by the TOF/TOF instument control program.
/* LabWindows User Interface Resource (UIR) Include File
                                                             */
/* Copyright (c) National Instruments 1991. All Rights Reserved.
                                                             */
/* WARNING: Do not add to, delete from, or otherwise modify the contents */
      of this include file.
                                             */
#define tofpan 0
#define tofpan power 0
#define tofpan hes 1
#define tofpan trans 2
#define tofpan graph 3
#define tofpan start 4
#define tofpan_name 5
#define tofpan led 6
#define tofpan rate 7
#define trans 1
#define trans instrum prog 0
#define trans source 1
#define trans_start_point 2
#define trans_number_pts 3
#define trans pts to array 4
#define trans_return 5
#define trans message1 6
#define trans message2 7
#define trans message3 8
#define hes 2
#define hes hes1 0
#define hes hes2 1
#define hes hes3 2
#define hes hes4 3
```

```
#define hes_return 4
#define hes_times 5

#define name 3
#define name_file 0
#define name_return 1
#define graph 4
#define graph_pts_to_graph 0
#define graph_return 1
#define graph_first_pt 2
#define graph_regraph 3

#define rate 5
#define rate_frequency 0
#define rate_duty_fraction 1
#define rate_return 2
```

A.1.2 Function Panels Called by the TOF/TOF Instrument Control Panel

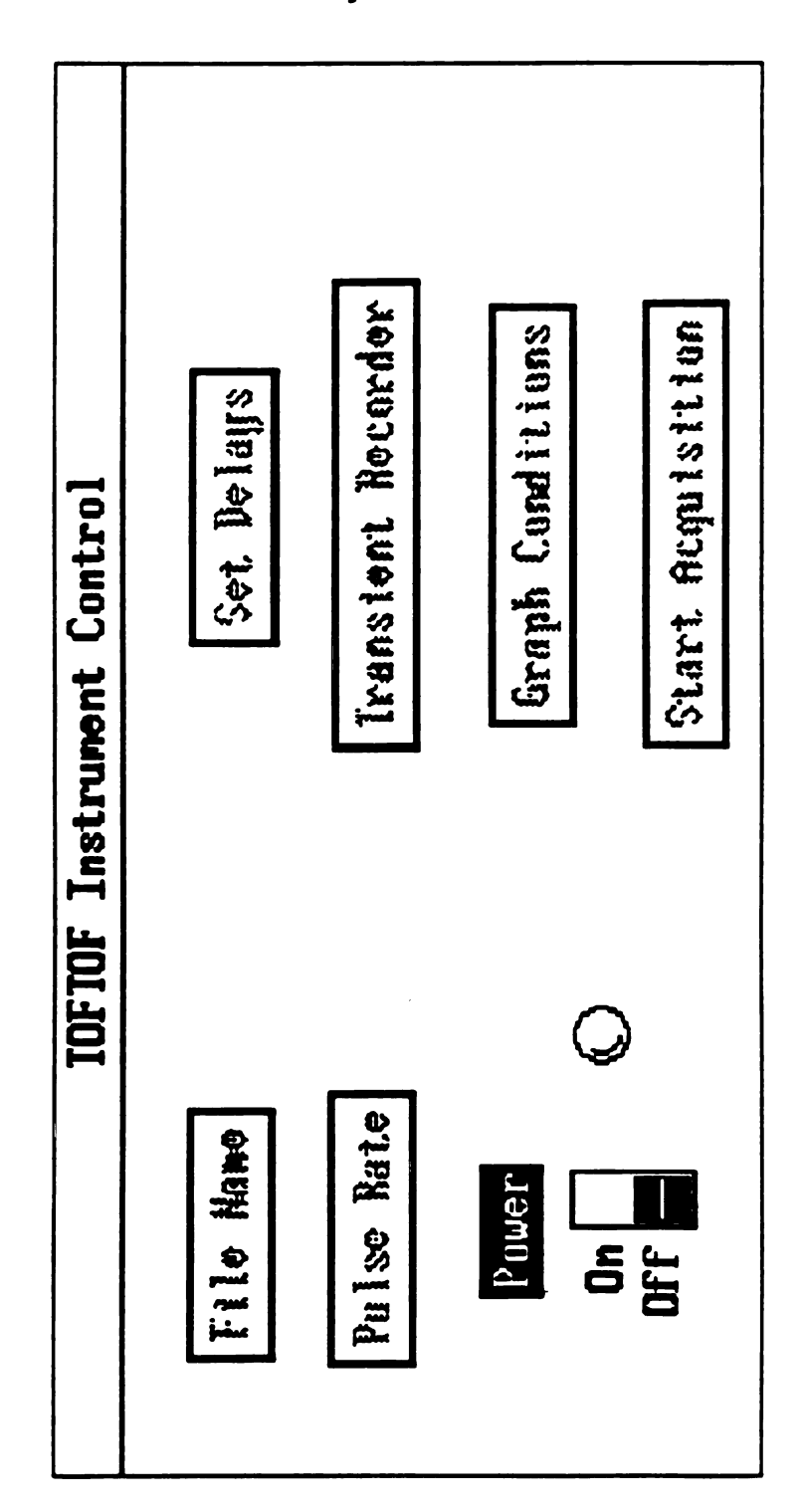


Figure A-1. The system control function panel for the TOF/TOF instrument

File Name	File to Be Acquired	ii:\lw\data\spec.dat	Directories must be separated by \ for this panel.	Return
			Direc	

Figure A-2. Function panel for the name of the file to be acquired

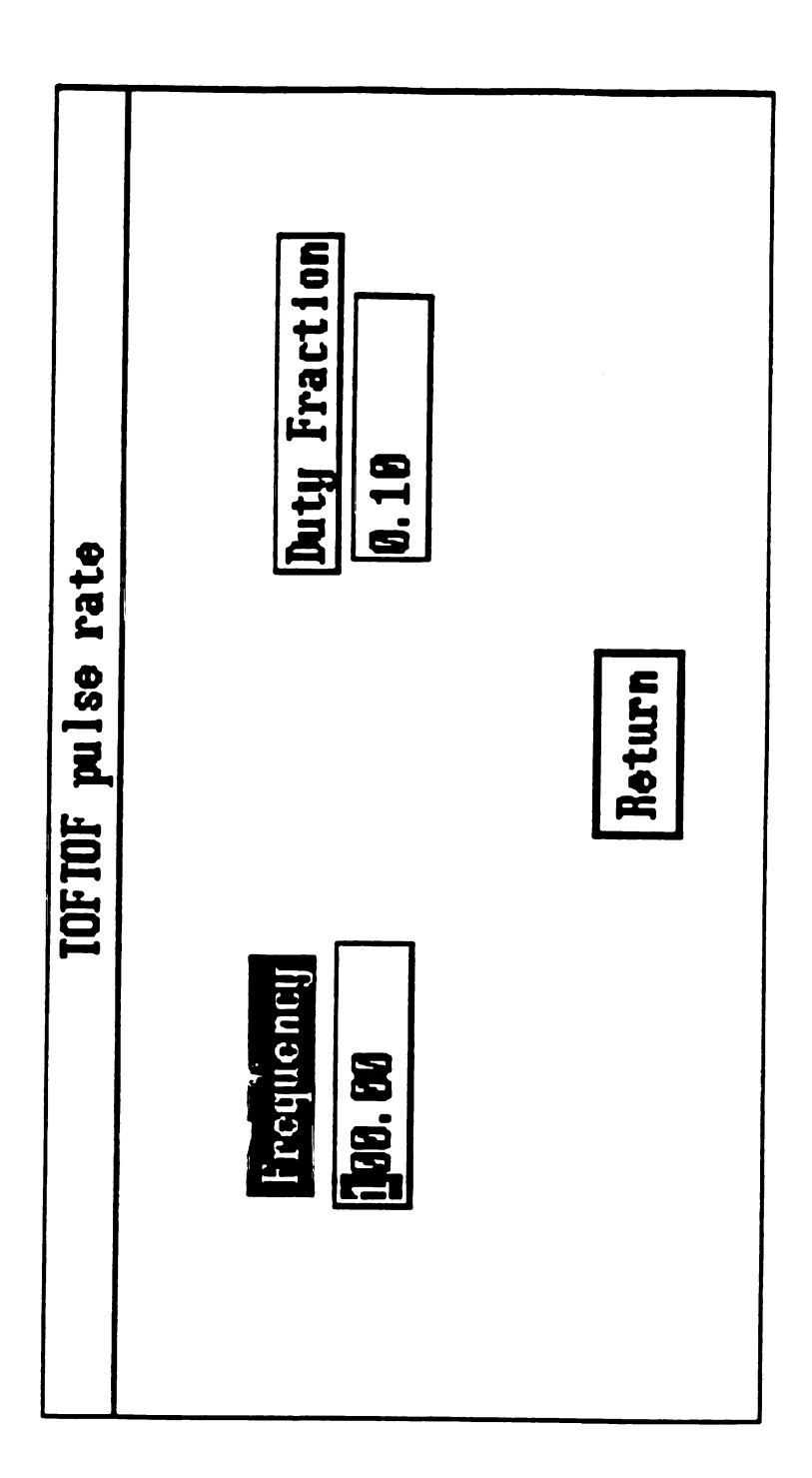


Figure A-3. The repetition rate of the square wave trigger signal is entered into this function panel.

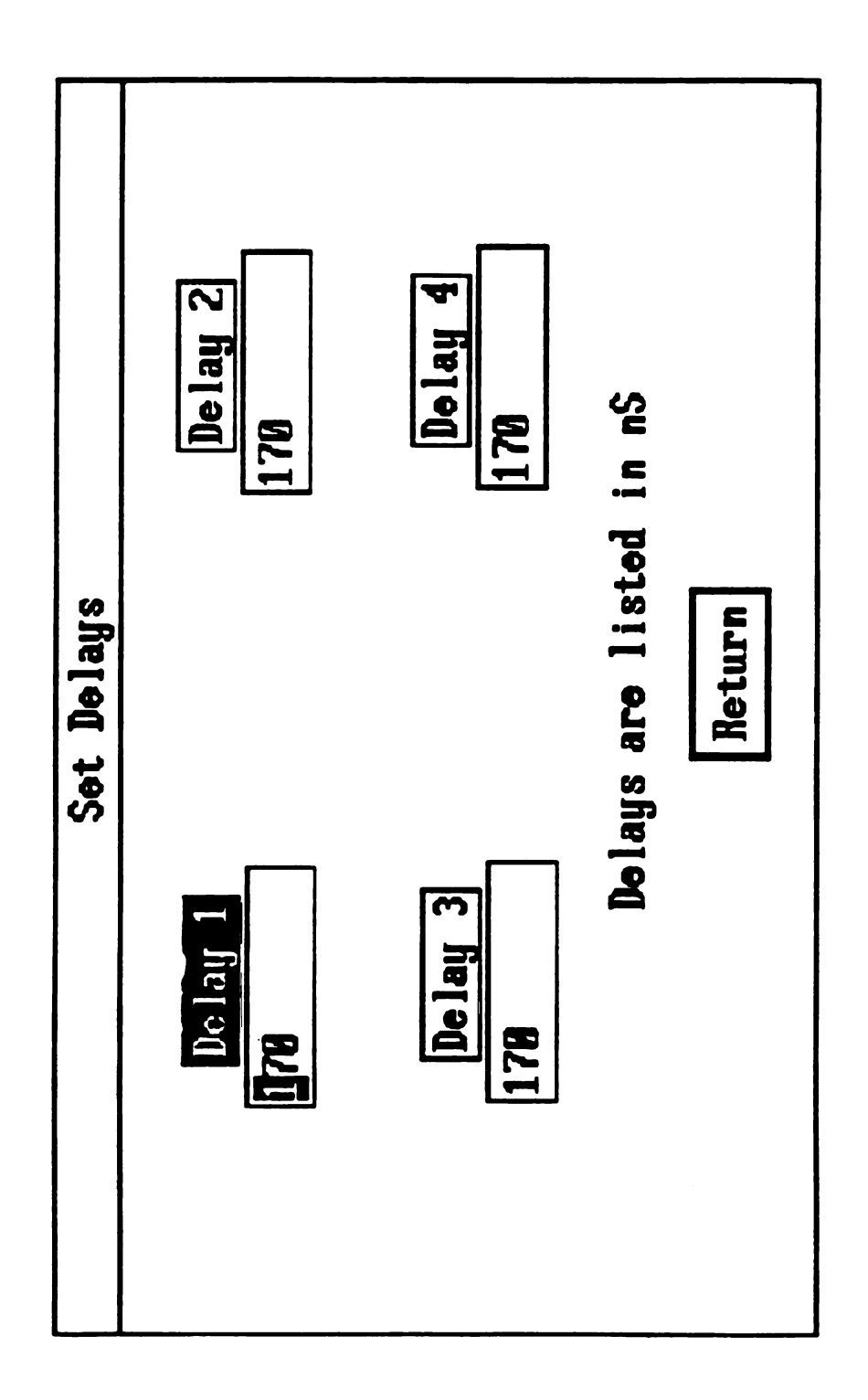


Figure A-4. Function panel to enter delay times for the LeCroy 4222 delay generator

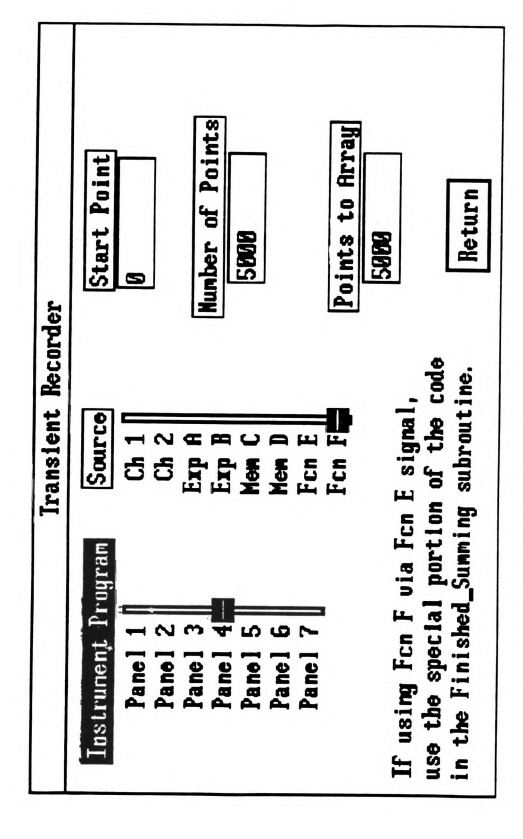


Figure A-5. Function panel for entry of conditions for the LeCroy 9450 transient recorder

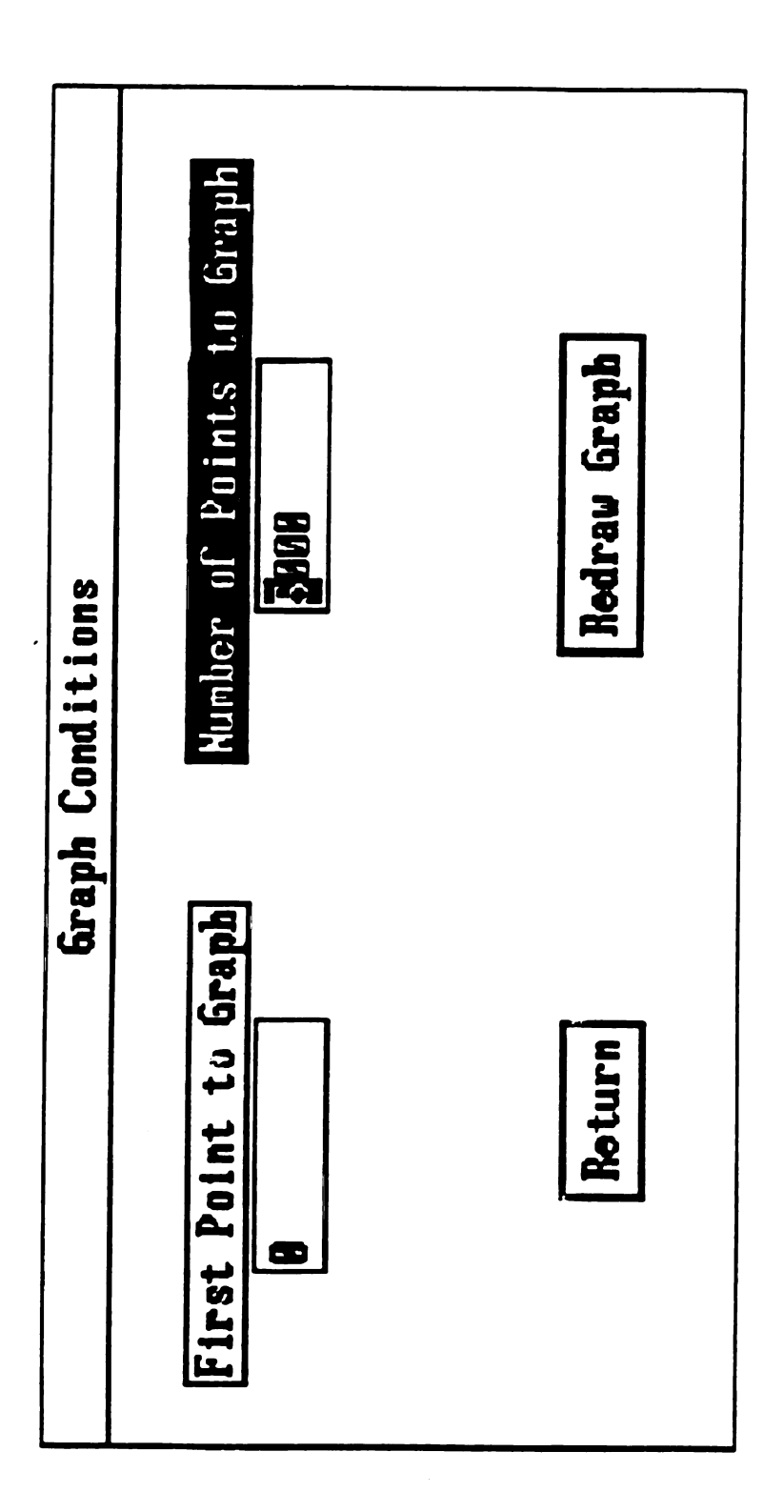


Figure A-6. Function panel for screen displayed graph conditions

A.2 Program to Parse Data File Header for Acquisition Information

/* This file parses the header of a binary file acquired by the LeCroy 9450 to determine pertinent information for further data processing. The only line in this program that should be edited by a user is the constant "FILE NAME". This value should be changed to an appropriate name prior to running the program. */ #define FILE NAME "F:\\lw\\data\\brb6.dat" char out0[15]; char out1[15]; char out2[15]; char out3[15]; char out4[15]; char out5[15]; char out6[15]; char out7[15]; main () ASCII header (FILE NAME, 0, out0); ASCII header (FILE_NAME, 1, out1); ASCII header (FILE NAME, 2, out2); ASCII_header (FILE_NAME, 3, out3); ASCII_header (FILE_NAME, 4, out4); ASCII header (FILE NAME, 5, out5); ASCII header (FILE NAME, 6, out6); /* ASCII_header (FILE_NAME, 7, out7); */ cls(); FmtOut ("The name of the file is: \t%s\n", FILE NAME); FmtOut("The acquisition time was:\t%s\n", out0): FmtOut("The acquisition date was:\t%s\n", out1); FmtOut("The number of points was:\t%s\n", out2): FmtOut("The sampling interval was:\t%s\n", out3); FmtOut("The number of points per screen was:\t%s\n",out4); FmtOut("The first point was:\t%s\n", out5);

FmtOut("The probe attenuation was:\t%s\n", out6);

```
/* FmtOut("The channel coupling was:\t%s\n", out7); */
}
```

A.3 Program to Convert LeCroy Format Binary Data to ASCII Format

This program converts a binary data stored in the format used by the LeCroy 9450 transient recorder to a tab delimited ASCII file.

static int error; static int num_of_pts; static double sample_int; static double spec[8192];

main () {

ASCII_gen ("F:\\lw\\\data\\brb5.dat", 5000, spec, &sample_int, &num_of_pts, error, "F:\\lw\\xldata\\brb5.dat");

A.3.1 ASCII gen Instrument Used by the Format Conversion Program

```
This program is a modification of a format conversion program
used by the LeCroy 9450. The major feature change is that this
program does not require the 9450 to be turned on or initialized
before the file format is transformed.
static char buffer [17000];
static int lec9450_invalid_integer_range (int, int, int, int);
static int lec9450_file_exists (char *);
static int lec9450_err;
static char *channel_cp[5];
         /* This function reads the information from a waveform header file.
int ASCII_header (file_name, info_type, out_str)
char *file name:
int info_type;
char *out_str;
  int handle;
  int pad;
  int temp time[2];
  int year;
  int coup;
  int sp:
  int temp int;
  double temp_doub;
  double sec:
  long temp_long;
 /* if (lec9450 device closed () != 0)
    return lec9450 err; */
  if (!file_name[0]) {
    lec9450_err = -2;
```

```
return lec9450 err;
  if (!lec9450_file_exists (file_name)) {
     lec9450 err = 310:
     return lec9450_err;
  handle = OpenFile (file name, 1, 0, 1);
  if (ReadFile (handle, buffer, 500) < 0) {
     CloseFile (handle);
     lec9450 err = 315;
     return lec9450 err:
  if (CloseFile (handle) < 0) {
     lec9450_err = 316;
     return lec9450 err:
  pad = FindPattern (buffer, 0, -1, "WAVEDESC", 0, 0);
  switch (info_type) {
  case 0:
     pad += 296:
     if (Scan (buffer, "%1f[i*z]>%f", pad, &sec) != 1) {
       lec9450_err = 236;
       return lec9450 err;
    }
     pad += 8;
     if (Scan (buffer, "%2d[b1zi*]>%2d", pad, temp_time) != 1) {
       lec9450 err = 236:
       return lec9450 err:
     Fmt (out_str, "%s<%d[p0w2]:%d[p0w2]:%f[p2]", temp_time[1], temp_time[0],
sec);
     break:
  case 1:
     pad += 306;
    if (Scan (buffer, "%2d[b1zi*]>%2d", pad, temp_time) != 1) {
       lec9450_err = 236;
       return lec9450 err;
    }
    pad += 2:
    if (Scan (buffer, "%1d[zi*]>%d", pad, &year) != 1) {
       lec9450 err = 236;
       return lec9450 err;
    }
```

```
Fmt (out str. "%s<%d[p0w2]/%d[p0w2]/%d", temp_time[1], temp_time[0],
year);
     break:
  case 2:
     pad += 116;
     if (Scan (buffer, "%1d[i*b4z]>%d[b4]", pad, &temp_long) != 1) {
       lec9450 err = 236:
       return lec9450_err;
     Fmt (out_str, "%s<%d[b4]", temp_long);
     break;
  case 3:
     pad += 136:
     if (Scan (buffer, "%1d[i*b4z]>%d", pad, &sp) != 1) {
       lec9450 err = 236;
       return lec9450_err;
     pad += 40;
     if (Scan (buffer, "%1f[i*b4z]>%f", pad, &temp_doub) != 1) {
       lec9450_err = 236;
       return lec9450 err:
     temp doub *= (double)sp;
     Fmt (out_str, "%s<%f", temp_doub);
     break:
  case 4:
     pad += 120;
     if (Scan (buffer, "%1d[i*b4z]>%d[b4]", pad, &temp_long) != 1) {
       lec9450 err = 236;
       return lec9450 err;
     Fmt (out_str, "%s<%d[b4]", temp_long);
     break:
  case 5:
     pad += 132:
     if (Scan (buffer, "%1d[i*b4z]>%d[b4]", pad, &temp_long) != 1) {
       lec9450 err = 236;
       return lec9450_err;
     Fmt (out_str, "%s<%d[b4]", temp_long);
     break:
  case 6:
     pad += 328;
     if (Scan (buffer, "%1f[b4zi*]>%d", pad, &temp_int) != 1) {
```

```
lec9450 err = 236:
       return lec9450 err;
     Fmt (out str. "%s<%d", temp int);
     break:
 /* case 7:
     pad += 326:
     if (Scan (buffer, "%1d[zi*]>%d", pad, &coup) != 1) {
       lec9450 err = 236;
       return lec9450_err;
     Fmt (out_str, "%s<%s", channel_cp[coup]);
     break;
 /* return lec9450_err; */
   This function reads a waveform file into an array.(from the LeCroy 9450 file)
int ASCII_gen (file_name, num_of_pts, wvfm, x_incr, acq_pts, lec9450_err,
output file)
char *file_name;
char output_file[35];
int num of pts;
double wvfm[8192];
double *x_incr;
int *acq pts:
{
  int pad;
  int handle;
  int i:
  int output;
  int count;
  int num_of_bytes;
  int num_read;
  long wav arr cnt;
  long sp;
  long new_sp;
  long wv_desc_len;
```

```
long usr_txt_len;
double vert_gain;
double vert_offset;
double val;
/* if (lec9450_device_closed () != 0)
   return lec9450_err; */
if (!file_name[0]) {
   lec9450_err = -2;
   return lec9450_err;
if (lec9450 invalid_integer_range (num_of_pts, 0, 8192, -2) != 0)
  return lec9450_err;
if (!lec9450_file_exists (file_name)) {
   lec9450_err = 310;
   return lec9450_err;
handle = OpenFile (file_name, 1, 0, 1);
if (ReadFile (handle, buffer, 500) < 0) {
   CloseFile (handle);
   lec9450_err = 315;
   return lec9450_err;
if (CloseFile (handle) < 0) {
   lec9450 err = 316;
   return lec9450 err;
pad = FindPattern (buffer, 0, -1, "WAVEDESC", 0, 0);
pad += 36:
if (Scan (buffer, "%1d[i*b4z]>%d[b4]", pad, &wv_desc_len) != 1) {
   lec9450_err = 236;
   return lec9450_err;
}
pad += 4;
if (Scan (buffer, "%1d[i*b4z]>%d[b4]", pad, &usr_txt_len) != 1) {
   lec9450_err = 236;
   return lec9450 err;
}
pad += 76;
if (Scan (buffer, "%1d[i*b4z]>%d[b4]", pad, &wav_arr_cnt) != 1) {
   lec9450_err = 236;
   return lec9450_err;
pad += 20;
```

```
if (Scan (buffer, "%1d[i*b4z]>%d[b4]", pad, &sp) != 1) {
  lec9450_err = 236;
  return lec9450 err;
pad += 20:
if (Scan (buffer, "%1f[i*b4z]>%f", pad, &vert_gain) != 1) {
  lec9450 err = 236;
  return lec9450_err;
pad += 4;
if (Scan (buffer, "%1f[i*b4z]>%f", pad, &vert_offset) != 1) {
  lec9450 err = 236:
  return lec9450_err;
pad += 16:
if (Scan (buffer, "%1f[i*b4z]>%f", pad, x_incr) != 1) {
  lec9450_err = 236;
  return lec9450_err;
new_sp = wav_arr_cnt / (long)num_of_pts;
if (new_sp == 0L) {
  *acq_pts = (int)wav_arr_cnt;
  *x_incr *= (double)sp;
  num_of_bytes = 2;
else {
  *acq pts = num_of_pts;
  *x incr = *x incr * (double)sp * (double)new sp;
  num_of_bytes = (int)(2L * new_sp);
handle = OpenFile (file_name, 1, 0, 0);
SetFilePtr (handle, wv_desc_len + usr_txt_len + (long)pad - 176L, 0);
for (count = 0; count < *acq_pts; count++) {
  num_read = ReadFile (handle, buffer, num_of_bytes);
  if (num_read <= 0) {
     CloseFile (handle);
    lec9450 err = 315;
    return lec9450 err;
  if (Scan (buffer, "%1d[z]>%f", &val) != 1) {
     CloseFile (handle);
    lec9450_err = 236;
    return lec9450 err:
  }
```

```
wvfm[count] = val;
  if (CloseFile (handle) < 0) {
     lec9450_err = 316;
     return lec9450_err;
  LinEv1D (wvfm, *acq_pts, vert_gain, -vert_offset, wvfm);
i*
The ASCII file is written from the array.
*/
  output = OpenFile (output_file, 2, 0, 1);
  for (i = 0; i < num_of_pts; i++) {
     FmtFile (output, "%s<%f[w15] \t \n", wvfm[i]);
  CloseFile (output);
  return lec9450_err;
}
/* This function checks an integer to see if it lies between a minimum
/* and maximum value. If the value is out of range, set the global error */
/* variable to the value err code. The return value is equal 0 for
/* success and -1 for error.
                                                            */
int lec9450 invalid integer range (val, min, max, err code)
int val:
int min;
int max:
int err code;
  if (val < min || val > max) {
     lec94xx err = err code;
     return -1;
```

A.3.2 Include File Called by the File Format Conversion Program

```
This program defines the response to buttons
used by the TOF/TOF instument control program.
________
/* ------ LabWindows Generated Code: Mon Aug 10 21:27:11 1992 ------ */
/* = Lecroy 9410/14/20/9424/30/9450 DSO's Include File
*
/* = GLOBAL FUNCTION DECLARATIONS
int lec94xx init (int, int);
int lec94xx config vert (int, double, int, double);
int lec94xx config horiz (int, int, int);
int lec94xx config probe (int. int):
int lec94xx auto setup (void);
int lec94xx_config_stand_trig (int, int, int, int, double, double);
int lec94xx config smart trig (int, int, int, double, int, int, int, int);
int lec94xx read wvfm arr (int, int, long, double [8192], double *, int *);
int lec94xx_read_wvfm_to_file (int, char *, int, long, long);
int lec94xx_write_wvfm_to_inst (int, char *);
int lec94xx_read_wvfm_inst_mem (int, int);
int lec94xx parse wvfm header (char *, int, char *);
int lec94xx_read_wvfm_file_arr (char *, int, double [8192], double *, int *);
int lec94xx trig (void);
int lec94xx_read_stat (int *, int *, int *, int *, int *, int *, int *);
int lec94xx save load setup file (char *, int, int);
int lec94xx save load setup inst (int, int);
int lec94xx_hard_copy_setup (int, int, int, int, int, int);
int lec94xx hard copy (int);
int lec94xx close (void):
/* = GLOBAL VARIABLE DECLARATIONS
/* Global error variable for the instrument module */
int lec94xx err:
```